Biocatalytic oxidative conversion of valencene to nootkatone mediated by lipoxygenase and cytochrome P450

By

Christopher Raboya

(1618713)

A dissertation submitted to the Faculty of Science at the University of the Witwatersrand, Johannesburg, in fulfilment of the requirements for the degree of Master of Science.

Supervisor: Prof. Dean Brady

Co-supervisor: Dr Kennedy Ngwira

Date: March 2024

DECLARATION

I declare that the dissertation is hereby submitted for the Degree of Master of Science in Chemistry at the University of the Witwatersrand, Johannesburg has not previously been submitted for any degree or examination. And that this is my work in design and execution and all material contained herein has been duly acknowledged.

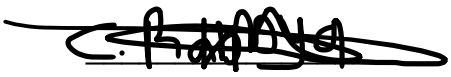

Christopher Raboya On __11_ July _2024__at Johannesburg_.

DEDICATION

I would like to dedicate this work to:

- My late father, Matome William Raboya
- My lovely and caring mother, Modjadji Elsie Raboya
- My siblings: Solomon Ntele Raboya, Grace Sello Raboya, Sam Raboya, Oscar Raboya and Ntai Raboya

ACKNOWLEDGEMENTS

My sincerest gratitude goes to my supervisor, Prof Dean Brady, and Co-supervisor, Dr Kennedy Ngwira for their support, guidance, and unrivaled patience during this work. I would further like to extend many thanks to the following individuals for all their assistance during this academic journey, without whom successful completion would have been near impossible:

- The School of Chemistry at The University of the Witwatersrand for allowing me to pursue my master's degree in their institution.
- Applied Protein Biotechnologies (APBIO) and THRIP for financial support and APBIO group: Stephanus Marais, Lindelo Mguni, and Deidre Davids for introducing me to biocatalysis and providing me with some technical skills and support.
- Dr. Mudzuli Maphupha and the Organic group for your contribution to my work.
- My lab mates and academic family: Otisha Govender (Nana), Kabelo Dilebo (Warrikzo), Khanya Jaceni (Warikiriki), Josephine Maboya, and Lebo Tefu for academic and social support.
- The mass spec team: Eric Morifi, Refilwe Moepya, and Thapelo Mbhele for helping with GC and equipping me with your expertise in running the instruments throughout.
- My friends, Selumi Juda Mawasha (Kota mohwelere!!) and Minah Maphakela Mohopa for all the advice and encouragement.
- My family for their prayers, support, and encouragement.
- Lastly and most of all, the almighty God for the strength and endurance to complete this degree.

Kea leboga bafethu!!!

ABSTRACT

Nootkatone (NK) is an oxygen-containing sesquiterpene with a significant grapefruit aroma and plays an important role in the flavour and fragrance industry. The natural production of NK through extraction produces trace amounts and is therefore not a viable option to meet industrial needs. The chemical synthesis often utilises reagents harmful to the environment. The purpose of this research was to explore the use of crude lipoxygenase (LOX) enzyme extracted from soya beans, commercial mutants of CYP450 as well as laccase enzymes for the conversion of valencene (VL), the aroma components of citrus fruits to NK. For the LOX reactions, a conversion of 28.79 % (mol/mol) was obtained when the reactions were performed with LOX only. The best conversion of 74.46 % was realised when $FeSO_4.7H_2O$ and $MnSO_4$ were added to the reaction. In the temperature studies, 70 ˚C was shown to be the optimal temperature for the conversion. In addition, we observed that vegetable oils provided sufficient unsaturated fatty acids to facilitate the conversion of VL to NK with sunflower oil being the best. In exploring the potential of LOX to oxidise other organic molecules, caryophyllene was oxidised to novel caryophyllene oxide, and styrene was oxidised to benzoic acid, 1-phenylethane-1,2-diol, and 2-hydroxyl-2-phenylethyl benzoate. This is the first time that such oxidations are reported, and this underlines the potential of LOX in biotransformation and organic synthesis. For CYP450 reactions, the best conversion of 16.70 % was obtained using a variant sourced from Prozomix. Evaluation of parameters such as temperature, pH (7.0 to 7.5), using buffer solutions should be explored to optimise the activity of the enzyme. Laccase from *Novoprime Base 268* showed no activity for the conversion of VL to NK despite making use of mediators. Therefore, we should explore changing the reaction conditions, varying the pH of the reaction, buffer strength or mediator and laccases from other sources such as *Cerrena unicolor* and *Trametes versicolor,* as *well* as *a* fresh batch of laccase from Trichoderma (Merck) should be assessed in the conversion of VL to NK.

TABLE OF CONTENTS

DECLARATION i
DEDICATION ii
ACKNOWLEDGEMENTS iii
ABSTRACT iv
LIST OF FIGURES viii
LIST OF SCHEMES xi
LIST OF TABLES xii
LIST OF ABBREVIATIONS xiv
CHAPTER 1 1
INTRODUCTION 1
1.1 Background 1
1.2 Green Chemistry 1
1.3 Biocatalysis 3
1.4 Enzymes 4
1.4.1 Lipoxygenases (LOX) 4
1.4.2 Cytochrome P450 (CYP450) 6
1.4.3 Laccase 10
1.5 Terpenes and their Origin 10
1.5.1 Sesquiterpenes 12
1.5.1.1 Valencene (VL) 13
1.5.1.2 Nootkatone (NK) 14
1.6 Chemical conversion of VL to NK 15
1.7 Biocatalytic conversion of VL to NK 16
1.8 Previous Work performed 21
1.9 Aim and Objectives 21
1.9.1 Aims 21
1.9 .2 Objectives 21
CHAPTER 2 22
RESULTS AND DISCUSSION 22
2.1 The Starting Material 22
2.2 Extraction of Lipoxygenase (LOX) 23
2.3 The crude LOX enzyme activity 25

2.4 Isolation and Characterisation of NK 27
2.5 Factors affecting LOX activity. 35
2.5.1 Influence of metal ions on nootkatone synthesis 35
2.5.2 Temperature study 40
2.5.3 Impact of fatty acid mediators 44
2.5.4 Impact of enzyme source from ground or defatted soya beans (GSB or MDS) 46
2.5.5 The influence of the enzyme extraction period. 49
2.6 Oxidation of other terpenes and related organic compounds. 50
2.6.1 Other terpenes 50
2.6.2 Styrene 52
2.7 Cytochrome P450 (CYP450) 54
2.7.1 PRO-HT-P450-40x plate (Sourced from Prozomix) 54
2.7.2 CoE-P450P plate (Codexis) 56
2.7.3 Fatty acid study (acts as a substrate) 57
2.8 Laccase Enzyme Activity 58
2.8.1 Variation of mediators 59
2.8.2 Amounts of the buffer or enzyme 59
2.8.3 Variation of terminal temperature 59
CHAPTER 3 61
CONCLUSIONS AND RECOMMENDATIONS 61
Recommendation 63
CHAPTER 4 65
METHODS AND MATERIALS 65
4.1 GENERAL PROCEDURES 65
4.2 CHEMICALS 65
4.3. SPECTROSCOPY AND PHYSICAL DATA 65
4.3.1. Nuclear Magnetic Resonance (NMR) 65
4.4 CHROMATOGRAPHY 66
4.4.1 Gas chromatography (GC) 66
4.5 SAMPLE PREPARATION 67
4.5.1 NMR 67
4.5.2 GC-MS 67
4.6 Enzyme extraction method 67
4.7 Biocatalytic reaction procedures 67

4.7.1 LOX enzyme activity 67
4.7.2 Cytochrome P450 enzyme..... 71
4.7.3 Laccase 72
REFERENCES..... 74
APPENDIX..... 85

LIST OF FIGURES

Figure 1: The mechanism of enzymatic activity in the synthesis of substrate to product (17). 4

Figure 2: A labelled structure of CYP102A1 (P450 BM3) from Bacillus megaterium (25). 7

Figure 3: Applications and some shortcomings of CYP450 monooxygenases. Areas that are already been used or have the potential to be applied are presented on a blue background and the properties of CYP450 that need improvements are displayed on an orange background (29). 9

Figure 4: Classification of linear terpenes (38). 11

Figure 5: Structures representing valencene, aristolochene and nootkatone. 14

Figure 6: Types of unsaturated fatty acids suitable as LOX oxidation mediators. 17

Figure 7: A chromatogram obtained from the gas chromatography (GC) analysis of the commercial valencene 22

Figure 8: The crude MDS and GSB extracts of LOX. 24

Figure 9: Phase separation. The emulsion was caused by a mixture of two or more immiscible liquids in the presence of natural emulsifiers from the biomass, with reduced emulsification occurring where the defatted biomass was added. The organic and aqueous phases separated using ethyl acetate through extraction. 25

Figure 10: GC chromatogram of the crude NK product obtained from the LOX reaction. 26

Figure 11: TLC plate showing spots of isolated product and standards for VL and NK run on mobile phase of 20% ethyl acetate/80% hexane viewed under UV at 254 nm. 27

Figure 12: ^{1}H NMR spectrum of nootkatone. 28

Figure 13: ^{1}H NMR spectrum of valencene. 29

Figure 14: ^{13}C NMR spectrum of nootkatone. 31

Figure 15 : DEPT135 NMR spectrum of nootkatone. 32

Figure 16a: GC chromatogram for nootkatone. 34

Figure 17: Assessing ion combinations showing a positive effect on MDS after 7 days of reaction. 38

Figure 18: The average conversion per day using concentration of 2.64 mM of $FeSO_4.7H_2O$ and $MnSO_4$ on MDS LOX. 39

Figure 19: The mol % of NK formed with the addition of $FeSO_4.7H_2O$ and $MnSO_4$ using a concentration of 2.64 mM respectively on MDS LOX. 40

Figure 20: Effects of various temperatures on MDS LOX crude enzyme after a two-day reaction. 40

Figure 21: Kinetics of average conversion at 60 and 70 ˚C over 9 days. 42

Figure 22: The standard deviation versus mean for the three runs (triplicates) at 60 ˚C and 70 ˚C. 43

Figure 23: The structure of unsaturated fatty acids. 44

Figure 24: The VL conversion function of biocatalyst preparation (GSB and MDS) and time. 49

Figure 25: The oxidation of caryophyllene. 51

Figure 26: GC chromatogram of caryophyllene oxide (CPO). 51

Figure 27: GC chromatogram for the styrene oxidation. 53

Figure 28: GC chromatogram for crude product of NK using CYP450 as catalyst. . 55

Figure 29: GC chromatogram of a reaction in the conversion of VL to NK using oleic acid on CYP450. 58

Figure 30: GC chromatogram for a reaction in the conversion of VL to NK using laccase. 60

Figure 31: ^{13}C NMR spectrrum of valencene. 85

Figure 32: DEPT135 NMR spectrum of valencene. 86

Figure 33: HPLC spectra for NK isolated from a crude mixture resulted from the conversion of VL. The peak at 219.1749 represents NK while at 437.3409 represents its dimerisation 87

Figure 34: Calibration curve of NK... 88

LIST OF SCHEMES

Scheme 1: The oxygenation mechanisms of unsaturated fatty acids (24). 6

Scheme 2: The catalytic cycle of the $CYP450_{cam}$ reaction mechanism (31). 8

Scheme 3: The biosynthesis pathway of farnesyl pyrophosphate (FPP) and geranyl (GPP) via the coupling of isoprene units (40). 12

Scheme 4: The formation of valencene and aristolochene from farnesyl pyrophosphate (41). 13

Scheme 5: The chemical synthesis of nootkatone from valencene (49). 15

Scheme 6: Chemical synthesis of nootkatone via hydroperoxide intermediate (50). 16

Scheme 7: Proposed mechanisms for the biocatalytic oxidative conversion of valencene to nootkatone by lipoxygenase from soya beans through an hydroperoxide intermediate formed from oleic acid (55). 18

Scheme 8: A multi-step conversion of triglyceride fatty acid to fatty acid peroxide (56). 19

Scheme 9: The oxidation of valencene to nootkatone and other numerous products by mutant $CYP450_{BM-3}$ (58). 20

Scheme 10: The biotechnological conversion of valencene to nootkatone via laccase with conversion efficiency ranging from 14.43 to 58.28%. or cytochrome P450 with 7.7% yield **(46).** 21

Scheme 11: Proposed biosynthetic pathway of the intermediates made from styrene with a-f representing different steps of the reaction. 53

LIST OF TABLES

Table 1: The application of enzymes in biocatalytic reactions (16). 3

Table 2: The key signals of ^{1}H NMR accounting for NK structure. 30

Table 3: The key signals of ^{13}C NMR accounting for NK structure. 33

Table 4: Effects of metal ions from different mole ratios and equal grams of different salts on MDS LOX after 7 days of reaction. 36

Table 5: Effects of different salts with each concentration of 2.64 mM*. 37

Table 6: Reaction kinetics at temperatures 60 and 70 ˚C with the addition of $FeSO_4.7H_2O$ and $MnSO_4$ using a concentration of 2.64 mM respectively.for 9 days on MDS LOX. 42

Table 7: Fatty acid composition of vegetable oils. 44

Table 8: Evaluation of fatty acids and vegetable oils on LOX crude enzyme in the conversion of VL to NK with the addition of $FeSO_4.7H_2O$ and $MnSO_4$ at 60 ˚C..... 46

Table 9: The reactions using crude LOX enzyme extracted from MDS and GSB per number of days at 60 ˚C. 47

Table 10 : The two different runs and their average per day as results of GSB and MDS at 60 ˚C with the addition of $FeSO_4.7H_2O$ and $MnSO_4$ using a concentration of 2.64 mM respectively 48

Table 11: Effects of enzyme soaking duration on conversion..... 50

Table 12: The intermediates resulting from the oxidation of styrene as determined by gas chromatography. 52

Table 13: Evaluation of mutants of CYP450 from PRO-HT-P450-40x plate in the conversion of VL to NK. 55

Table 14: Various mutants of CYP450 from PRO-HT-P450-40x plate in the conversion of VL to NK from different wells ran for 2 days. 56

Table 15: Evaluation of different mutants of CYP450 from CoE-P450P plate in the conversion of VL to NK ran for 2 days. 57

Table 16: The mol % of NK formed with the addition of $FeSO_4.7H_2O$ and $MnSO_4$ using a concentration of 2.64 mM respectively on MDS LOX. 89

Table 17: All the runs and average conversions of salts in 1:1 mole ratio 90

LIST OF ABBREVIATIONS

VL	Valencene
NK	Nootkatone
LOX	Lipoxygenase
PUFA	Polyunsaturated fatty acids
MUFA	Monounsaturated fatty acids
HPODE	Hydroperoxides
GSB	Ground soya beans
MDS	Milled defatted soya beans
CYP450	Cytochrome P450
NADPH	Nicotinamide adenine dinucleotide phosphate
NADH	Nicotinamide adenine dinucleotide hydrogen
H_2O	Water
Cam	Camphor
BM	*Bacillus megaterium*
IPP	Isopentenyl pyrophosphate
DMAPP	Dimethylallyl pyrophosphate
GPP	Geranyl pyrophosphate
FPP	Farnesyl pyrophosphate
FDA	Food and Drug Administration
GRAS	Generally recognized as safe
NIST	National Institute of Standards Technology
DCM	Dichloromethane
$CDCl_3$	Deuterated chloroform
TOF	Time of flight
CP	Caryophyllene
CPO	Caryophyllene oxide
EtOAc	Ethyl acetate
RF	Retention factor

GC	Gas chromatography
MS	Mass Spectrometry

CHAPTER 1

INTRODUCTION

1.1 Background

Flavours and fragrances have been used for over 5,000 years, mainly for medical reasons or for pleasure (1–3). It is believed that the ancient Egyptians incorporated perfume into their culture by using perfume balms for their religious ceremonies and romantic liaisons. They also used myrrh, opopanax, and frankincense for fragrance, while in Mesopotamia they used cedar, cypress, frankincense, and myrrh. People became interested in essential oils because of their aroma. The scents which are found in essential oils are mainly extracted from various parts of a plant such as barks, flowers, buds, peels, seeds, and leaves. The flavour and fragrance world started to industrialise because of the increase in demand for these compounds which occurred around the year 1850 with the manufacture of cinnamic aldehyde, vanillin, benzaldehyde, and methyl salicylate through chemical synthesis (2). One such compound that has attracted a lot of interest because of its versatility in commercial products is nootkatone.

In the 20th century, with increased demand outstripping availability and an expanding market for cheaper products, synthetic chemistry was applied to the production of artificial flavours and fragrances. In the 1980s, a shift of production of flavours and fragrances back towards natural products arose due to consumer preferences. However, a compound is only regarded as natural if it is extracted from microorganisms, animals, or plants, and/or results from the transformation of enzymatic processes or whole cells (2). The production of natural products requires green chemistry, to minimise the use of hazardous substances.

1.2 Green Chemistry

Green chemistry is an area of chemistry that aims to minimise waste production and improve the sustainability of chemical products and process, as well as decreasing the generation of hazardous substances (4). In the 1990s, green chemistry was

conceptualized by John Warmer and Paul Anastas to capture the growing awareness of environmental issues in chemistry (4,5). Green chemistry is now broadly applied in technological development, government policy, industrial management, and educational practice all over the world. The main aim of the green chemistry community is to develop greener and more sustainable technologies that are harmless to human wellbeing and the climate by basing their research on 12 principles (6–8).

The 12 principles of green chemistry are (9,10):

1. Waste prevention

2. Designing Safer Chemicals

3. Atom Economy

4. Design for Energy Efficiency

5. Less Hazardous Chemical Syntheses

6. Safer Solvents and Auxiliaries

7. Reduce Derivatives

8. Real-time Analysis for Pollution Prevention

9. Use of Renewable Feedstocks

10. Catalysis (including biocatalysis)

11. Inherently Safer Chemistry for Accident Prevention

12. Design for Degradation

These principles aim to minimise the generation of dangerous substances, resource consumption, and risks when manufacturing, applying, and designing chemical substances (11). The use of these principles has led to the development of guidelines for the pharmaceutical industries, starting from drug discovery to industrial production (12). Whenever scientific challenges arise from an increase in structural complexities and/or synthetic steps, they could be solved using modern chemically selective methods (10). One of the key principles of green chemistry is catalysis, including biocatalysis, the significance of which will be discussed in more detail below.

1.3 Biocatalysis

Biocatalysis refers to the use of a biological catalyst such as enzymes that are used to catalyse chemical reactions. The process of biocatalysis starts with (i) identifying the target reaction, (ii) discovering the biocatalyst, (iii) characterisation, (iv) protein engineering, and (v) process modelling. Moreover, there are key drivers of biocatalysis, which are process specifications, market needs, safety, risk management, health, environment, robustness, biocompatibility, industrial process improvement, product quality, molecular economy and specificity (13). Recently, there have been advances which help to elaborate the functional activities and structure of enzymes and have led to an increase in the substrate specificity, activity, and stability of enzymes (14).

Biocatalysis (enzyme facilitated catalysis) empowers all forms of life starting from the microorganism to humans (15). Which we are increasingly applying to industrial processes. In comparison, other kinds of catalysts are often used in industry such as heterogeneous catalysts whereby catalytically active centres bonds with solid carriers (metal oxides or zeolites) and homogeneous catalysts whereby ligands are responsible for reaction specificity. However, enzymes usually exhibit better selectivity as shown in **Table 1** and this is not an exhaustive list of advantages and disadvantages since there are many more depending on how the enzyme is applied and the associated bioprocess being employed.

Table 1*:* The application of enzymes in biocatalytic reactions (16).

Advantages	**Disadvantages**
Very high enantioselectivity	Long development times for new enzymes
Very high regioselectivity	Instability at extremes of pH and temperature
Transformation under mild conditions	Availability for selected reactions only
Solvent often water	However, in some cases, the substrates are only soluble in organic solvents, and not all enzymes can function in the presence of organic solvents

1.4 Enzymes

Enzymes are biological catalysts that speed up a biochemical reaction without themselves being destroyed or absorbed in the reaction. The description of enzyme action involves catalysing the conversion of substrate molecules to the desired target products (17). **Figure 1** shows the mechanism of enzymatic activity, the example being provided below is that of an enzyme involved in the synthesis of substrates to products revealing how enzyme structure and substrate binding play an important role in this kind of reaction whereby the charge properties and shape of the active site empower the binding of a single type of substrate molecule. Moreover, certain enzymes illustrate considerable specificity toward catalytic activities.

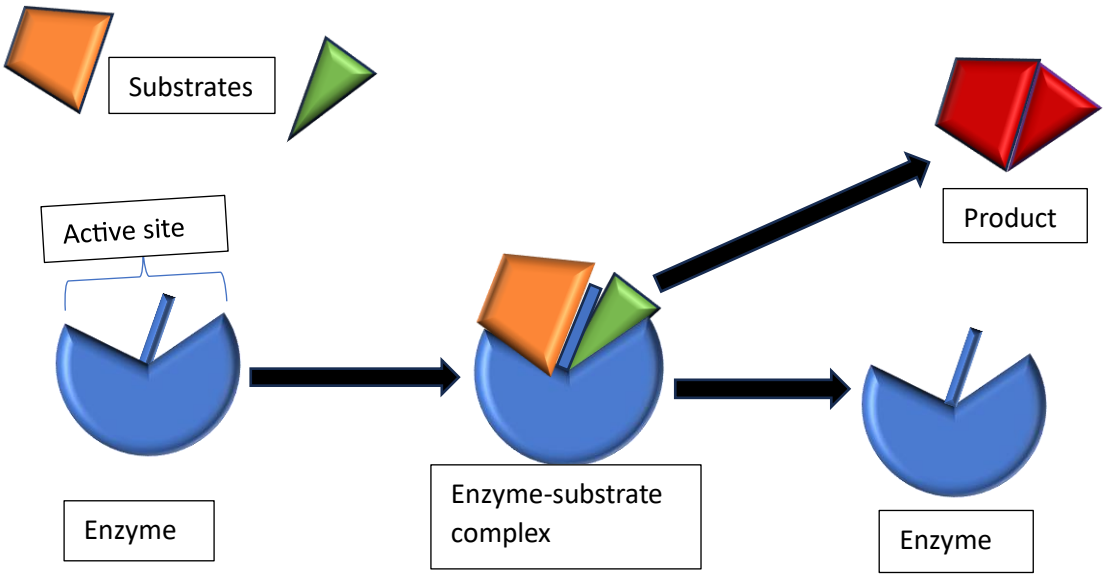

Figure 1: The mechanism of enzymatic activity in the synthesis of substrate to product (17).

Three enzymes that have been used in the biocatalytic conversion of valencene to nootkatone are lipoxygenases, cytochrome p450s and laccase

1.4.1 Lipoxygenases (LOX)

Lipoxygenases (LOX) are a group of non-haem, non-sulfur iron, or manganese containing dioxygenases that are broadly distributed in animals (usually found in more

than 60 species) and plants where they perform physiological functions, including initiating inflammation and other stress responses. LOX is a type of oxidoreductase responsible for the catalytic oxygenation of polyunsaturated (PUFA) and monounsaturated fatty acids (MUFA) which result in the formation of hydroperoxides (HPODE). Moreover, the formation of hydroperoxide takes place on the 9 or 12 position of the fatty acids through an insertion of oxygen to generate a 9 or 13-HPODE. Lipoxygenases are usually found in various biological tissues and organs, but mostly in potato tubers and grain legume (pulses) seeds (peas and beans) (18,19).

The regio- and stereo-specificity of LOX results from the depth of the active site, oxygen channels, different head-to-tail orientations, and residue position of the hydrogen for abstraction (20). The HPODE can be involved in subsequent oxidative reactions. Lipoxygenase extracted from soya bean seed is regarded as the best characterised plant LOX, even though its physiological role is yet to be identified. Plant LOX enzymes are multifunctional enzymes that catalyse reactions by (i) the formation of epoxy leukotrienes, (ii) the deoxygenation of lipid substrates, and (iii) the secondary conversion of hydroperoxyl lipids (19,21).

All lipoxygenases come from the same gene family, which is characterised by sequence homology of their catalytic domains and conserved metal irons (22,23). Although most of LOX are Fe-based, some are Mn based. The Mn-LOX are only found in ascomycete fungi whereby they form their distinctive subfamily (20). **Scheme 1** illustrates a proposed mechanism for the oxygenation of linoleic acid as catalysed by LOX. This mechanism is initiated when the LOX abstracts hydrogen (pro-S) from C-11 of the fatty acids resulting in a linoleoyl radical, which is reversibly oxygenated to produce (11*S*)-peroxy radical leading to (11*S*)-HPODE. The oxygen that is incorporated into the reaction attacks the linoleoyl radical at C-13 position to form (13*R*)-HPODE (24). However, (13*R*)-HPODE predominates in the Fe-LOX reactions as it is primarily produced from linoleic acid while Mn-LOX show variability in the formation of (11*S*)- and (13*R*)-HPODE products (24).

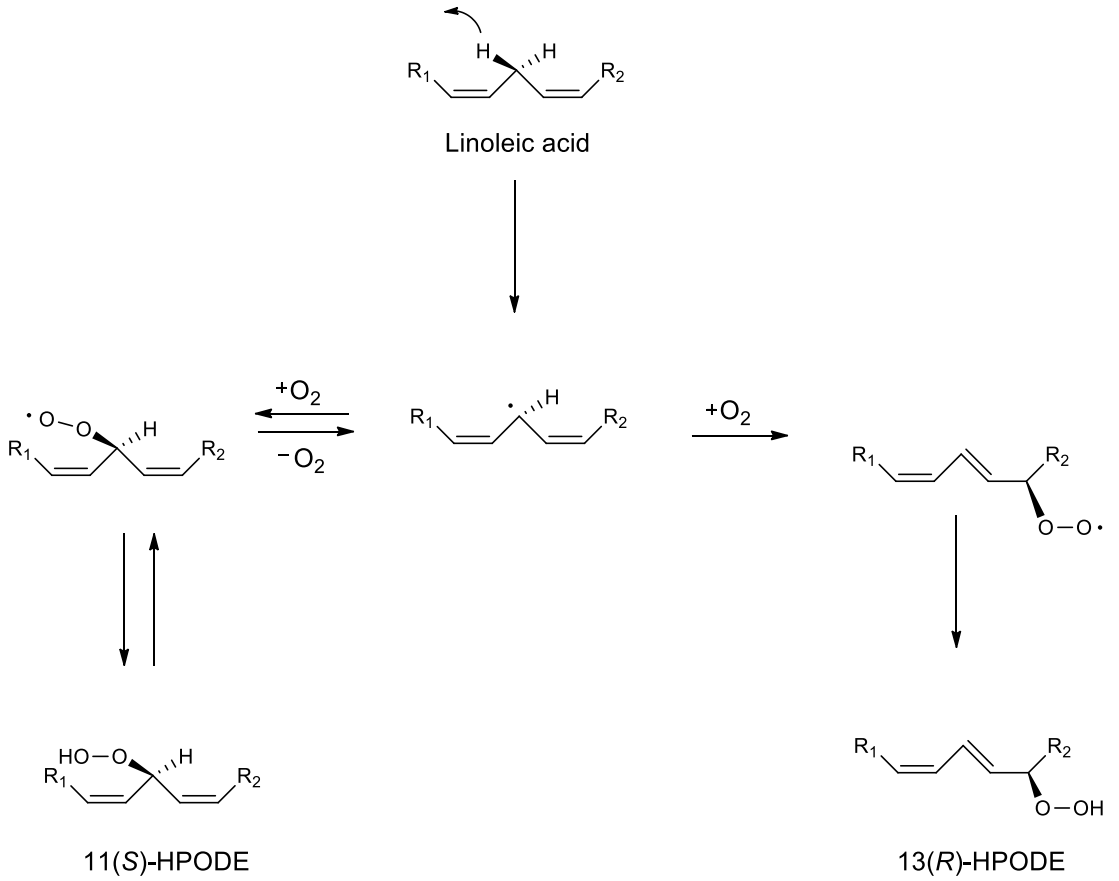

Scheme 1*:* The oxygenation mechanisms of unsaturated fatty acids (24)*.*

1.4.2 Cytochrome P450 (CYP450)

Cytochrome P450 is a haem-thiolate protein where the haem's prosthetic group is connected to apoprotein through an axial conserved cysteine (**Figure 2**). Hence, it belongs to the superfamily of cysteine thiolate-ligated haem-containing monooxygenase enzymes which are responsible for many of the physiological functions of different kinds of organisms (25–27). There are different types of CYP450 varying in substrate selectivity (28,29). They are responsible for about 70% of therapeutic drug metabolism. In humans, they are normally found in the liver and play an important role in the catalysis of different types of regio- and stereo-selective mono-oxygenation and detoxification processes. These enzymes range in molecular weight between 45 to 60 kDa and have a broad range of versatility in a diverse number of reactions that contribute effectively toward synthetic biology, biotechnological and pharmaceutical applications for investigations of newly synthesised drugs (25).

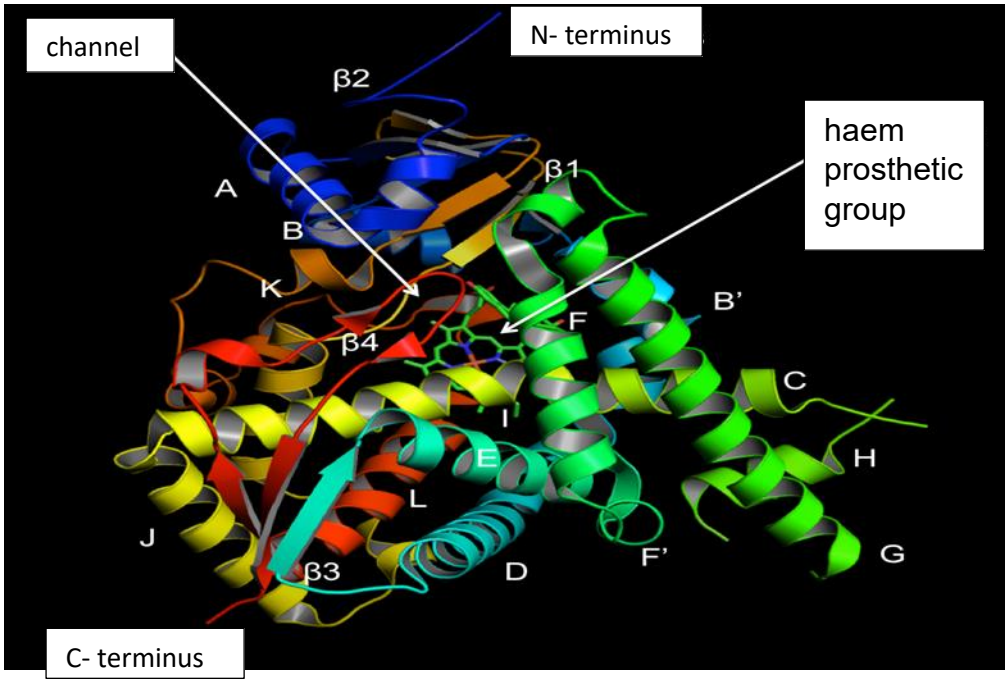

Figure 2*:* A labelled structure of CYP102A1 (P450 BM3) from *Bacillus megaterium* (25).

CYP450s are responsible for catalysing oxygen atom transfer from molecular oxygen into a broad range of biological substrates, where the second oxygen atom is reduced by two hydrogens to form a water molecule. The monooxygenase can engage in the biotransformation of products that occur naturally during the drug and oxidative metabolism of xenobiotics. Hydroxylation, heteroatom dealkylation, epoxidation, and heteroatom oxidation are reactions that are most often facilitated by the enzyme CYP450 (27,30).

Monooxygenase requires redox cofactor such as NADPH and NADH. **Scheme 2** shows a summarised catalytic cycle where a generalised substrate RH is used (31). The first step is substrate-binding where hydrogen transfer has been favoured due to redox cofactor (NADPH or NADH). Afterward the spin state of the haem iron changes at the active site, and this process results in a conformational change of the enzyme which activates the interaction with the redox components. The second step is the first reduction reaction where the Fe^{3+} ion is reduced by transferring an electron from NADH or NADPH through an electron transfer chain (31,32). The third step is oxygen-binding where the O_2 molecule forms the Fe^{2+}-O_2 complex by binding quickly with Fe^{2+}

and it is proven that this complex then goes through a slow conversion resulting in a more stable complex (Fe^{3+} -O_2).

The fourth, rate determining, step is where the second reduction reaction occurs. Fifth step, O_2 cleavage where the O-O bond from O_2^{2-} breaks when reacting with two protons from the surrounding solvents to form water and leaves the $(Fe\text{-}O)^{3+}$ complex. The sixth step is product formation where there is a transfer of Fe-ligated O atoms to the substrate to form a hydroxylated form of the substrate. The seventh and last step is where the active site of the enzyme releases the product, thereby returning to its initial state (25).

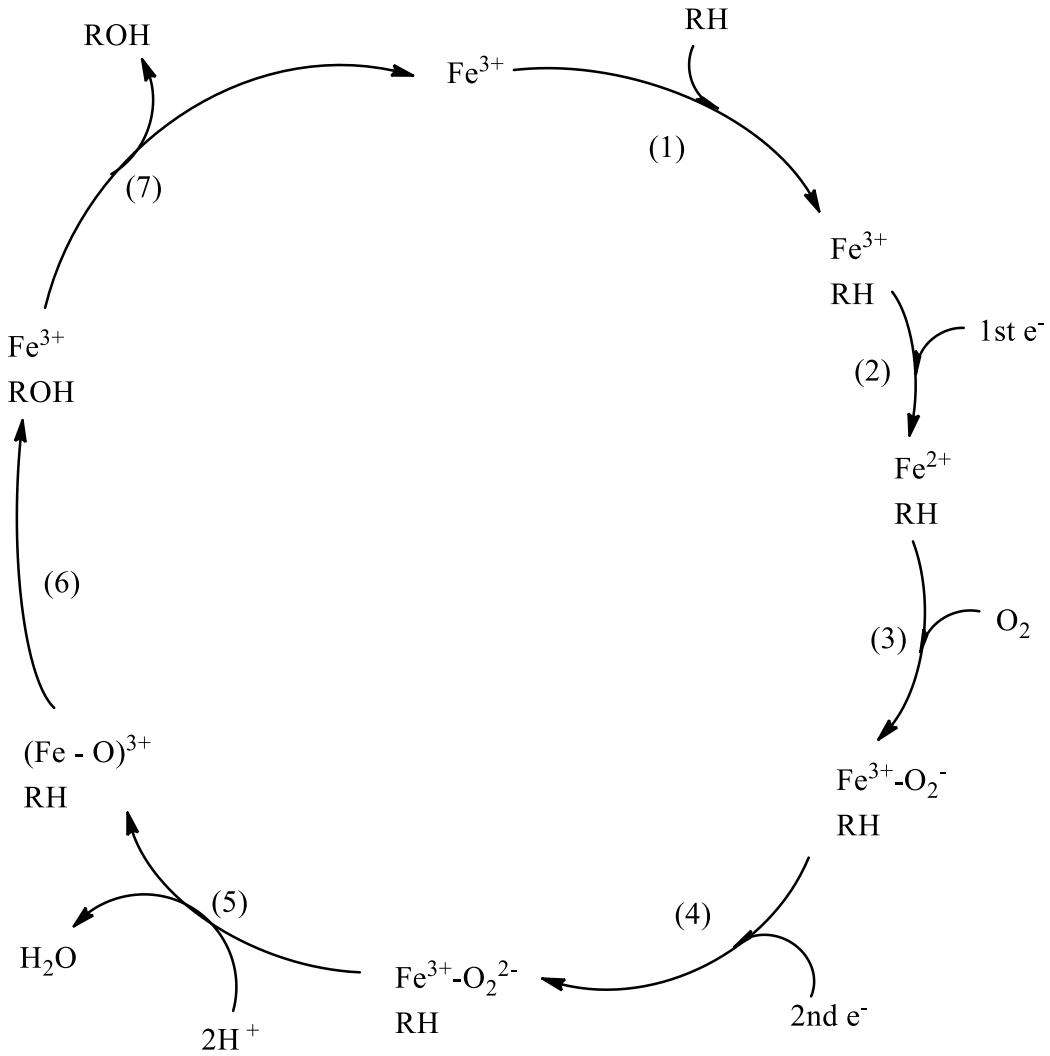

Scheme 2*:* The catalytic cycle of the $CYP450_{cam}$ reaction mechanism (31).

In recent years, studies on protein engineering of CYP450 have been conducted to rationally help in redesigning the active site of the CYP450 enzyme, through directed evolution or random mutagenesis, or by a combination of these two approaches (31). For example, two new variants $CYP450_{cam}$ and $CYP450_{BM-3}$ engineered and successfully used in biocatalytic oxidative reactions, while the wild-type CYP450 enzymes evaluated showed no oxidation activity due to the enzyme active site being unable to accommodate larger and/or more hydrophobic molecules. However, the protein engineering challenges differ depending on each type of CYP450 enzyme (29). **Figure 3** shows some applications and operational challenges of CYP450 monooxygenases (29).

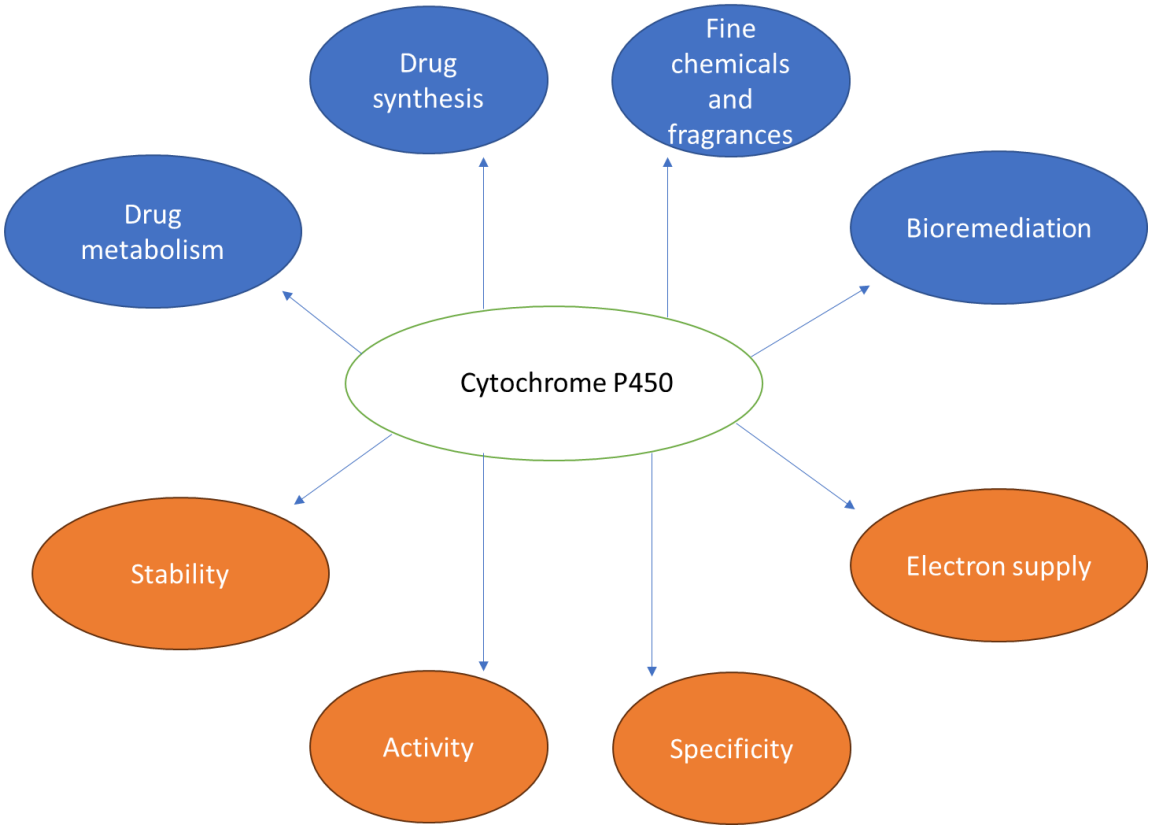

Figure 3: Applications and some shortcomings of CYP450 monooxygenases. Areas that are already been used or have the potential to be applied are presented on a blue background and the properties of CYP450 that need improvements are displayed on an orange background (29).

1.4.3 Laccase

Laccase is a versatile and monomeric or multimeric part of a larger copper-containing family of proteins referred to as multicopper oxidases that can catalyse a wide spectrum of substrates such as aromatic amines, phenol-like compounds (mono-, di-, and polyphenols, methoxy phenols, and amino phenols), and organic compounds which use molecular oxygen as an electron acceptor (33). It is a large blue, white or yellow copper protein and ligninolytic enzyme which is mainly found both in woody plants that are capable of synthesising lignin as well as organisms that degrade wood. Intensive studies of laccase explored its ability to reduce molecular oxygen resulting in water formation and oxidising the phenolic compounds (34,35).

Laccases are extraordinarily non-specific in their products, partly due to various substrates having multiple oxidation pathways. The oxidation of the substrate results from the loss of a single electron and a free radical formation (33,36). Additionally, the radical is found to be unstable and may undergo a further catalysed laccase oxidation. Moreover, the inclusion of reaction mediator compounds such as salicylic acid, ferulic acid, benzoic acid, sodium benzoate in laccase reactions enhances the oxidation capability to a very broad range of substrates. Laccase can be extracted from either a microbial source such as *Cerrena unicolor*, *Trametes versicolor* or a host of recombinant DNA. Some laccases are purchased from commercial vendors (33).

The three oxidative enzymes described above, lipoxygenase, CYP450, and laccase, can be utilised in the biocatalytic conversion of terpenes

1.5 Terpenes and their Origin

In nature, terpenes are the most diverse class of substances that are derived from isoprene units (from its carbon backbone) which is achieved through tail-to-tail and head-to-tail polymerisation of the activated building blocks (37). They are also secondary metabolites since their formation is caused by enzymatic reactions of primary metabolites (vitamins, amino acids, sugar, and others) and they have the ability to create fragrances and other compounds for plants to serve as a protection from infectious germs and animal predation. There are various different types of linear

terpenes, which are hemiterpenes, monoterpenes, sesquiterpenes, diterpenes, sesterpenes, triterpenes, sesquarterpene, and tetraterpene depending on their carbon units (38). **Figure 4** shows the classification of linear terpenes whereby the bonds coloured in red indicate separate isoprene units which makes it easier to count the number of isoprene units per terpene. We focus on sesquiterpene as this is the precursor of valencene.

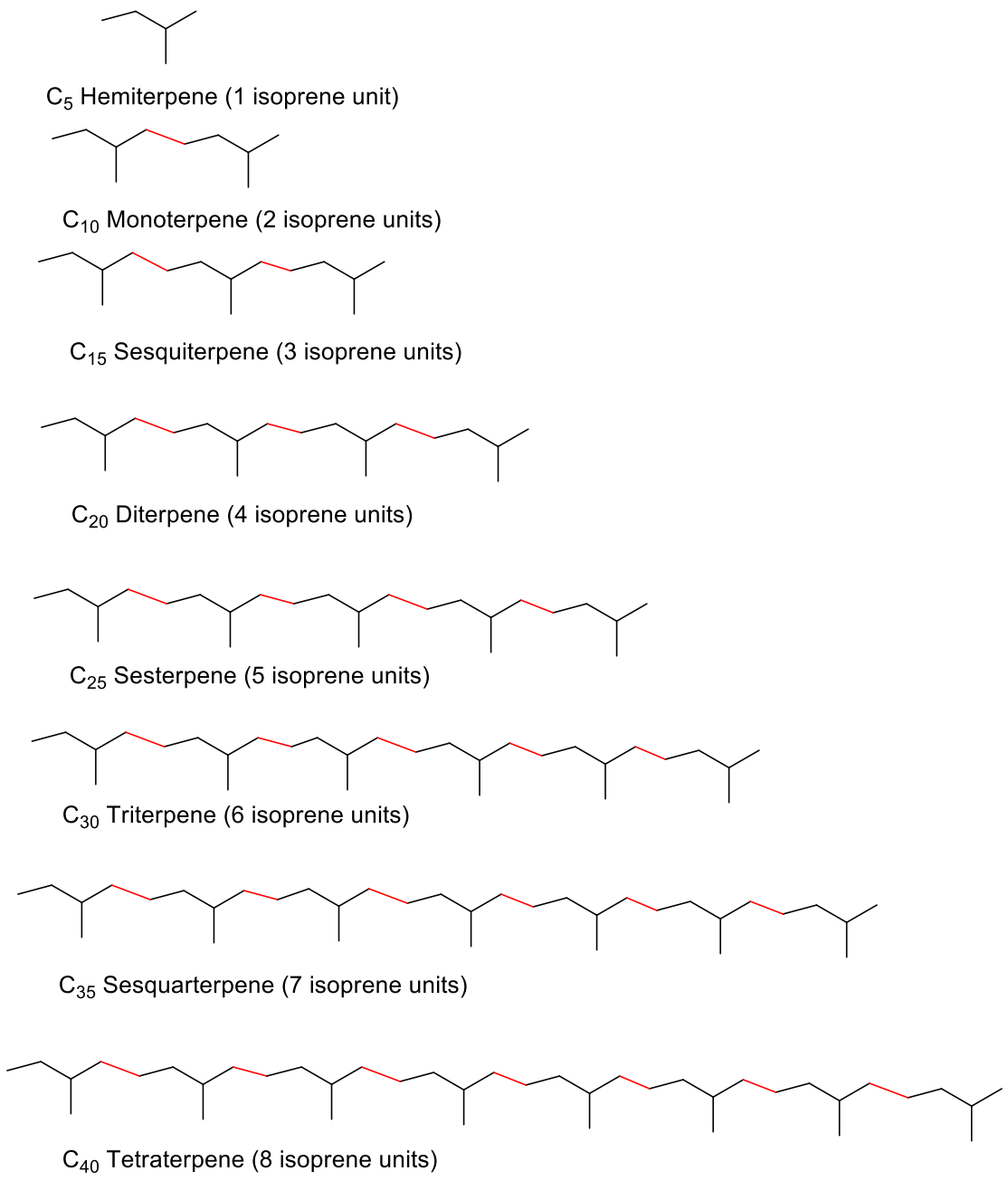

Figure 4*:* Classification of linear terpenes (38)*.*

1.5.1 Sesquiterpenes

Sesquiterpenes are a class of secondary metabolites that are made up of three isoprene units. They can be linear, branched, or cyclic (monocyclic, bicyclic, and tricyclic) (38). **Scheme 3** shows the biosynthesis of geranyl (GPP) and farnesyl pyrophosphate (FPP) via the coupling of isoprene units (39).

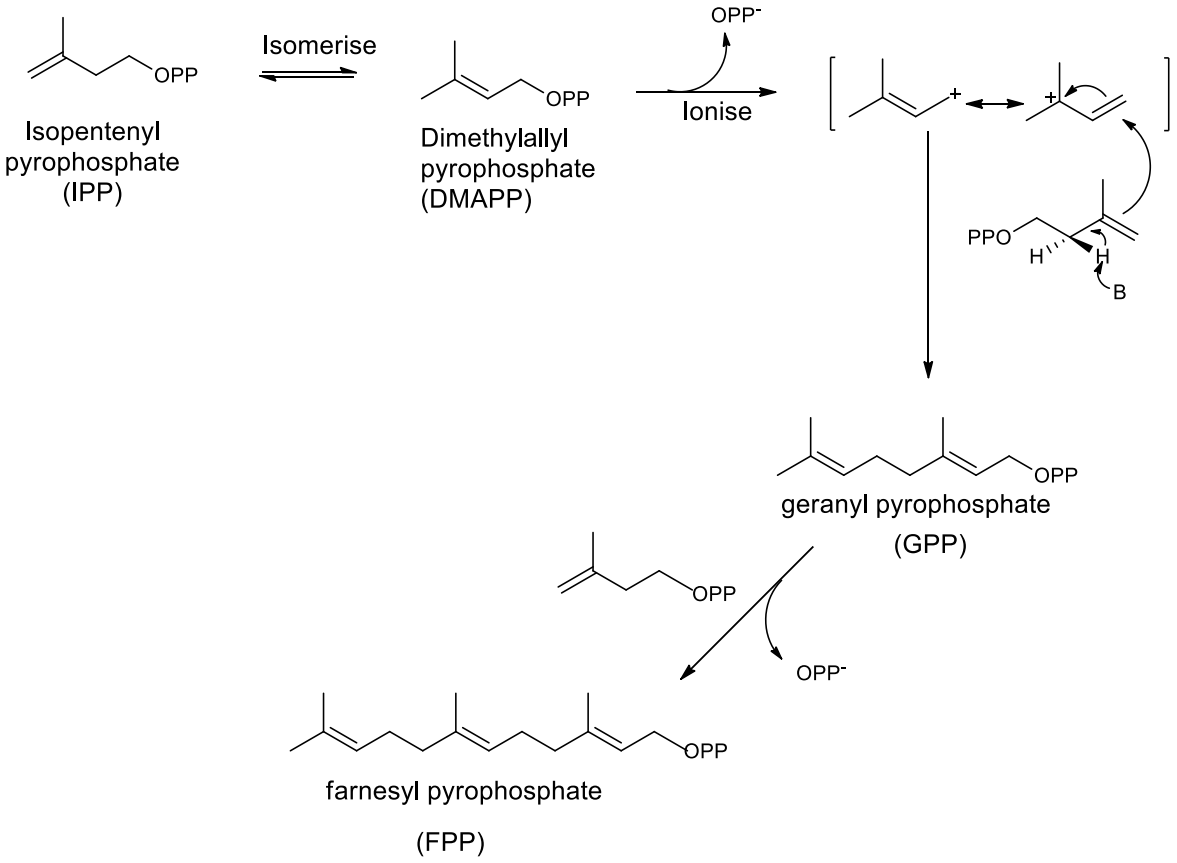

Scheme 3*:* The biosynthesis pathway of farnesyl pyrophosphate (FPP) and geranyl (GPP) via the coupling of isoprene units (40).

Faraldos *et al.* reported the formation of aristolochene and valencene from FPP, which was mediated by aristolochene synthase from *Penicillium roqueforti,* which is a sesquiterpene cyclase that catalyses the Mg^{2+} dependant conversion of FPP via germacrene intermediate, as displayed in **Scheme 4** (41).

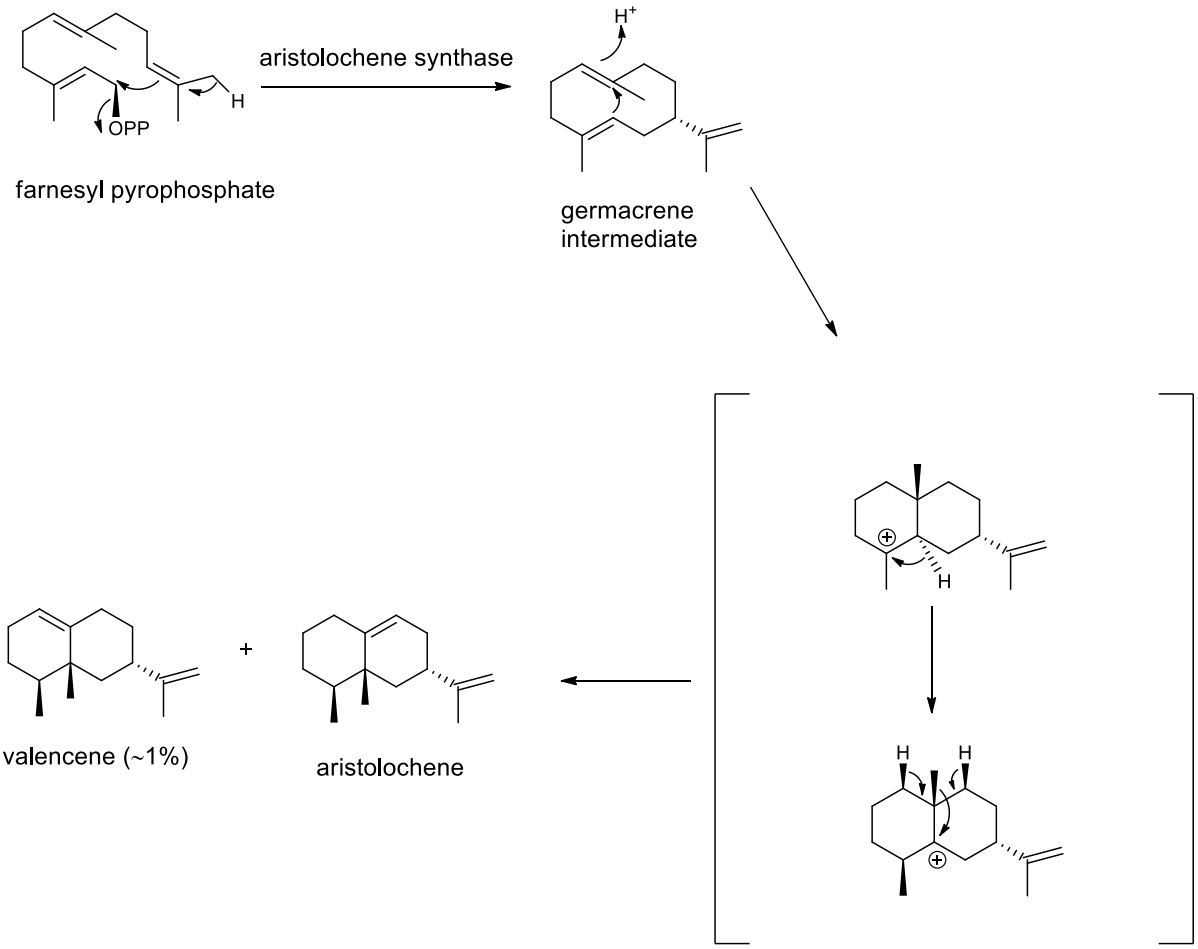

Scheme 4: The formation of valencene and aristolochene from farnesyl pyrophosphate (41).

1.5.1.1 Valencene (VL)

Valencene is a member of the sesquiterpenes found in many citrus fruits such as Valencia oranges, tangerines, mangoes, grapefruit, and nectarines (37,42). It is known to be a potent insecticide and is mostly used as a cleaning product, a mosquito repellent, and other pest control products. It is also used in the manufacturing of beauty products and orange-scented personal care products (43). Sometimes, it can be infused with food ingredients and olive oils for an extra layer of flavour (44). Additionally, valencene has shown to be useful in treating and preventing different kinds of cancers and can also function as a skin protectant by reducing itching, increasing skin barrier protection, and soothing inflammatory responses (37). *Ambrož et al.* reported that the efficacy of the anthracycline antibiotic Doxorubicin was increased by valencene: Doxorubicin is the drug that is used against cancer resistant

cells in chemotherapy (45). Literature has not shown any side effects nor potential risks to people whenever they are using or consuming valencene. However, it is toxic to insects, which makes it an effective bug-repellent. **Figure 5** shows structures representing valencene and its isomer aristolochene. These two sesquiterpenes can be oxidised using enzymes to form nootkatone. **Figure 5** shows structures of valencene, its isomer aristolochene and nootkatone.

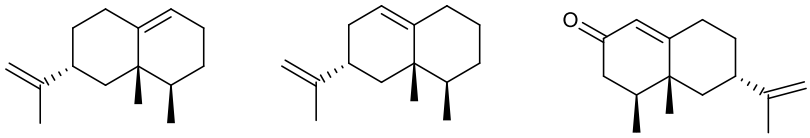

Valencene Aristolochene Nootkatone

Figure 5*:* Structures representing valencene, aristolochene and nootkatone.

1.5.1.2 Nootkatone (NK)

Nootkatone is a ketone derivative of a valencene that was originally found in Alaska Cedar (2,5). It has a distinctive grapefruit aroma with a very low threshold of 1 µg/L and its organoleptic properties makes it highly valuable in the flavour and fragrance industry (5). Moreover, its significant flavour component of grapefruit makes it a useful ingredient in soft drinks, perfumery, and other beverages leading to their distinctive flavour and fragrance. Nootkatone also serves as an insecticidal, anti-tumour, anti-bacterial, anti-inflammatory and, anti-oxidative, as well as exhibiting other pharmacological properties (46). The FDA (Food and Drug Administration) considers nootkatone as a GRAS (Generally Recognised As Safe) substance which means that the product is safe for humans and other mammals (6). Hence, it is broadly used in cosmetics, agriculture, food, pharmaceutical, and other fields. Annually, 10 tonnes of valencene are produced and about half (5 tonnes) of the amount happens to be used in the production of nootkatone for flavour and fragrance. The formation of NK from the oxidation of VL, using chemical synthesis or enzymes, will be explained in more detail below.

1.6 Chemical conversion of VL to NK

Naturally nootkatone, is present in citrus, grapefruit, and other peel oils in only small amounts (47). Due to limited quantities of NK derived from plant sources, chemical synthesis was considered because of its ability to meet industrial demands. However, the chemical synthetic route to produce nootkatone from valencene was undertaken using toxic reagents such as potassium dichromate, amphiphilic molybdenum catalysts, tert-butyl peracetate and tert-butyl hydroperoxide, which are harmful to the environment (48). **Scheme 5** illustrates a three-step chemical synthesis process where VL **(A)** was oxidised using tert-butyl peracetate with cuprous bromide (CuBr) to obtain an ester **(B)**, which was then reduced to nootkatol **(C)** utilising $LiAlH_4$ in THF. The alcohol **(C)** was then oxidised with potassium dichromate ($K_2Cr_2O_7$) in aqueous H_2SO_4 to produce the desired NK **(D).**

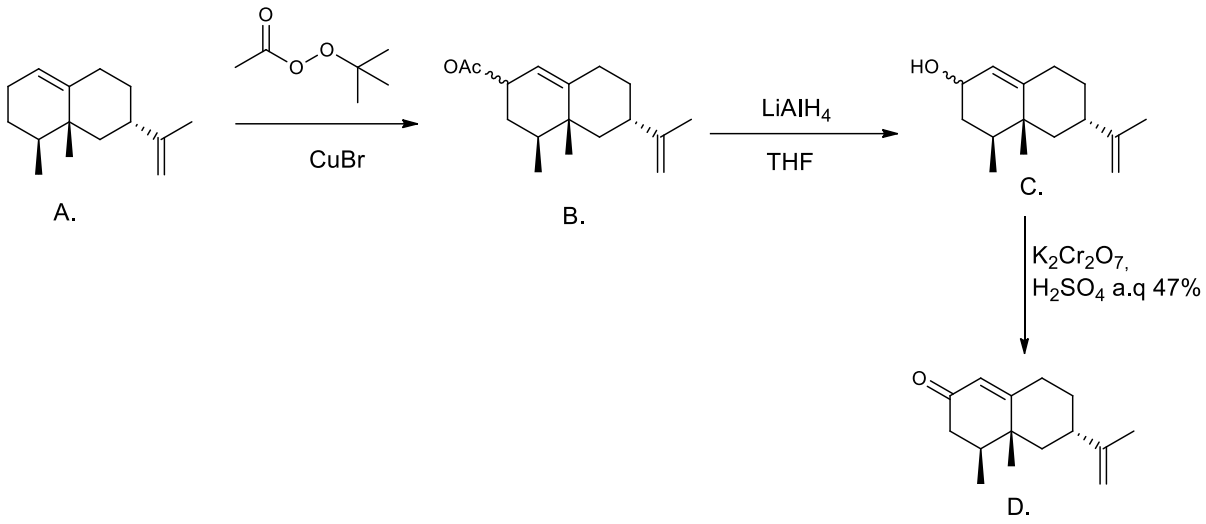

Scheme 5*:* The chemical synthesis of nootkatone from valencene (49).

Hong et al. also reported chemical synthesis of NK in **Scheme 6**, starting by photooxidation of VL **(A)** using light rose Bengal in methanol (MeOH) to obtain hydroperoxide **(E)** with 71% and **(F)** with 17% yield. Hydroperoxide **(E)** selectivity was accounted for by steric effect, as a result it was rearranged into **(G)** using toluene at 40 ºC. Followed by the conversion of **(G)** into desired NK **(D)** using amphiphilic molybdate ions in the presence of toluene (50). Although this was accomplished, the nootkatone produced from such processes might not be considered to be a natural

product and consequently, the product does not satisfy the high natural aromatic demands (2).

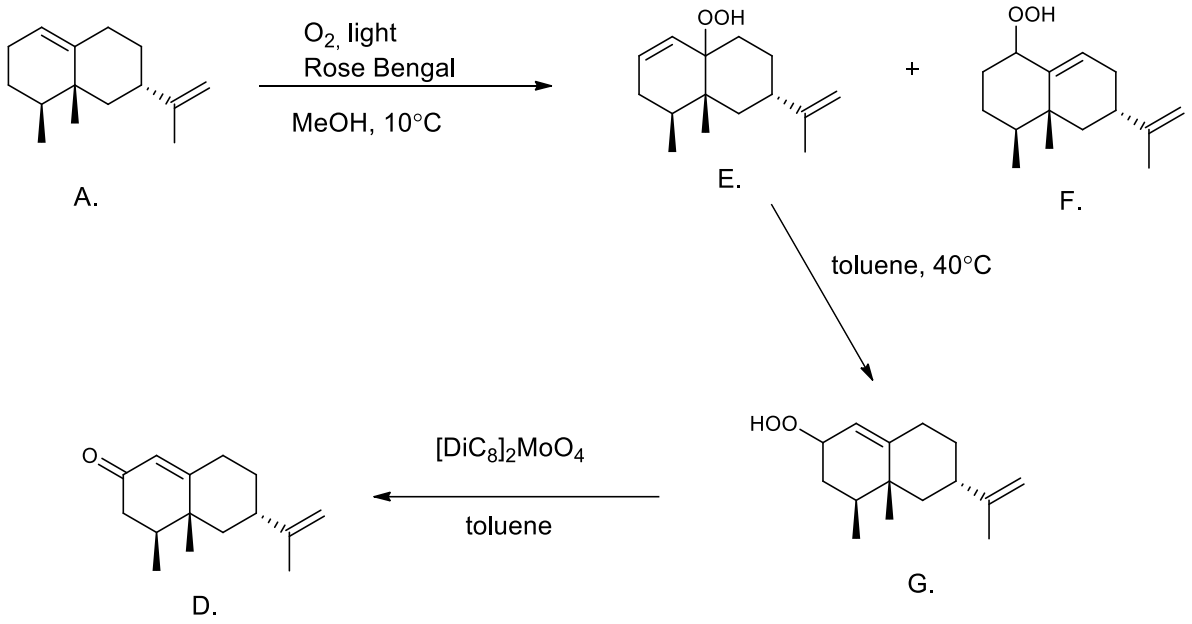

Scheme 6: Chemical synthesis of nootkatone via hydroperoxide intermediate (50).

To circumvent the drawback of chemical synthesis, attempts have been made through biotechnological processes using either plants, fungi, or bacteria involving enzymes such as lipoxygenases (dioxygenases), cytochrome p450 (monooxygenases), laccase (oxidoreductases) (51). This biosynthetic route was documented by regioselective allylic hydroxylation where the oxygen group is introduced into the allylic carbon group followed by the oxidation to nootkatone (2).

1.7 Biocatalytic conversion of VL to NK

The biological conversion of VL to NK was first achieved in the 1970s (46). This biotransformation is possible using various types of biological materials, such as plant cells, micro-organisms, related enzymes, edible mushrooms, microalgae, and others. The benefit of using enzymes is that the compounds produced will no longer depend on the quantity of the plant material (1) but are perceived as nature identical. However, at the same time there are shortcomings to surmount, such as: (i) the cost of VL is

comparatively high; (ii) the bioconversion process is not optimal due to substrate and product inhibition; (iii) interfacial mass transport limitations negatively affect the performance of the process for biomass based biotransformations, while the alternative of using purified enzymes is prohibitively expensive (52).

LOX enzymes are incapable of direct oxidation of VL to NK, they therefore depend upon a fatty acid as a mediator. There are various kinds of unsaturated fatty acids that may be used and are shown in **Figure 6** (53,54).

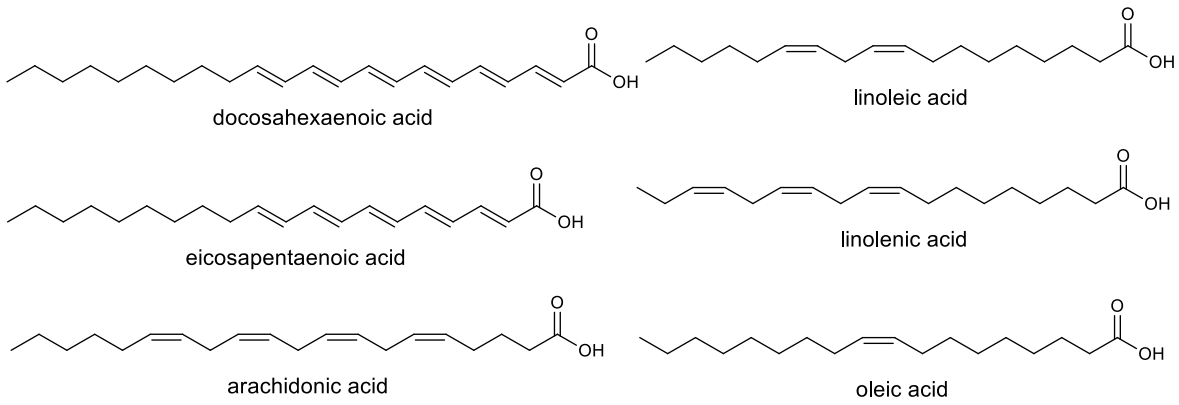

Figure 6: Types of unsaturated fatty acids suitable as LOX oxidation mediators.

Scheme 7 illustrates the proposed mechanism, where oleic acid is used as a mediator. Oleic acid is oxidised using a radical mechanism that involves the LOX enzyme reacting with oleic acid to form an unstable hydroperoxide intermediate which oxidises the valencene at allylic carbon (C2) position and route (a) nootkatone was formed directly while route (b) starts by forming nootkatol which is then converted to nootkatone. The conversion of NK from LOX was 77% GC peak area within 48 h and the optimum pH conditions were in the range of 3-6 when the LOX extraction in sodium borate buffer had a pH of 8.1 and 7.5 (55).

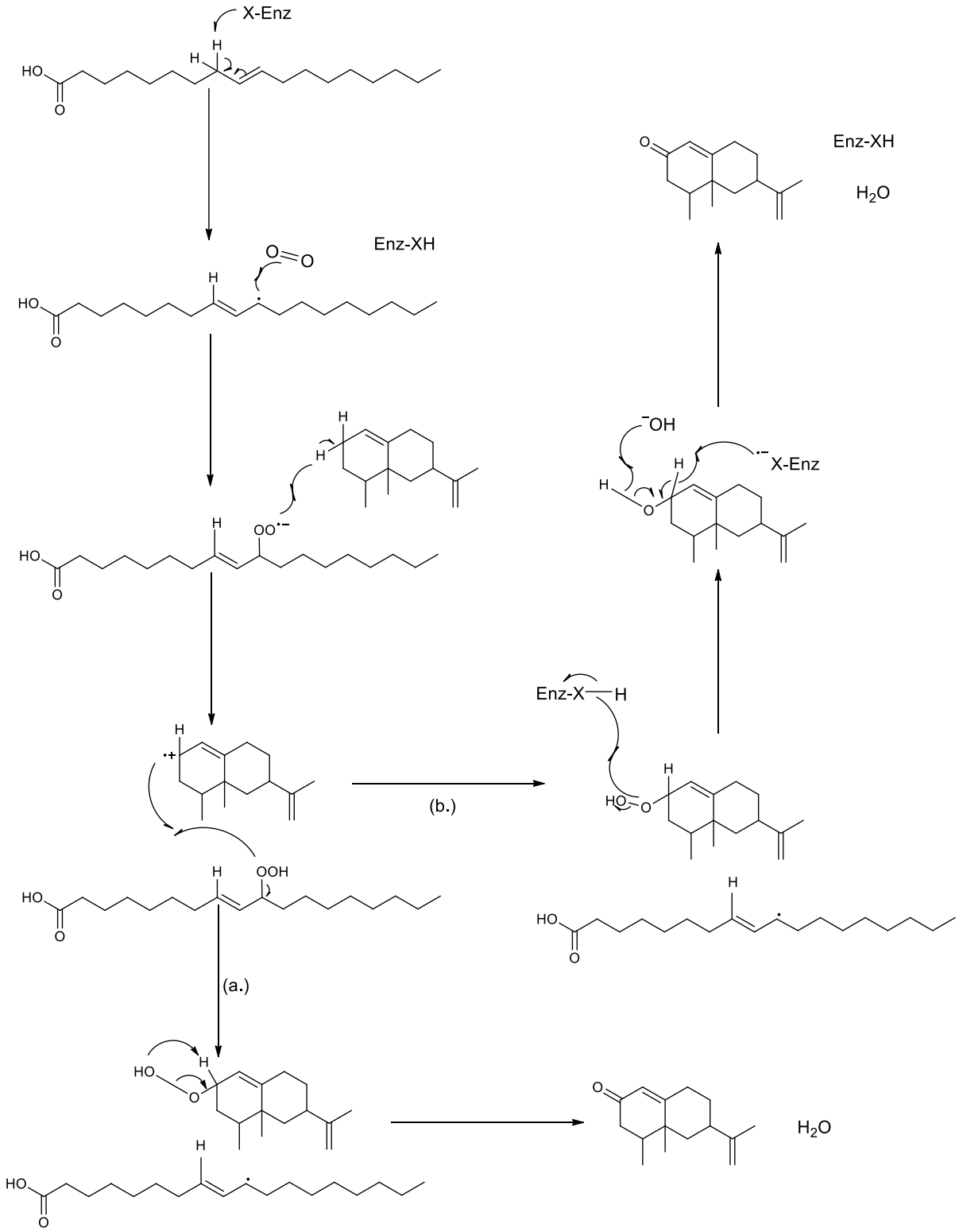

Scheme 7: Proposed mechanisms for the biocatalytic oxidative conversion of valencene to nootkatone by lipoxygenase from soya beans through an hydroperoxide intermediate formed from oleic acid (55).

Additionally, fatty acids from vegetable oils, for example, canola oil, olive oil and sunflower oil, can be used after hydrolysis from the glycerol of the triacylglyceride. This hydrolysis can be catalysed by lipase (56). **Scheme 8** shows a reaction where sunflower oil was used, and a combination of lipase and LOX was applied to liberate the fatty acid and form the hydroperoxide (HPODE). Lipases from *Candida rugosa* and *Pseudomonas fluorescens* were able to hydrolyse sunflower oil to >75% within 5 h at a pH of 8.0 and HPODE was produced in a yield of 70 g/L within 7 h using LOX from soya bean extract (56,57).

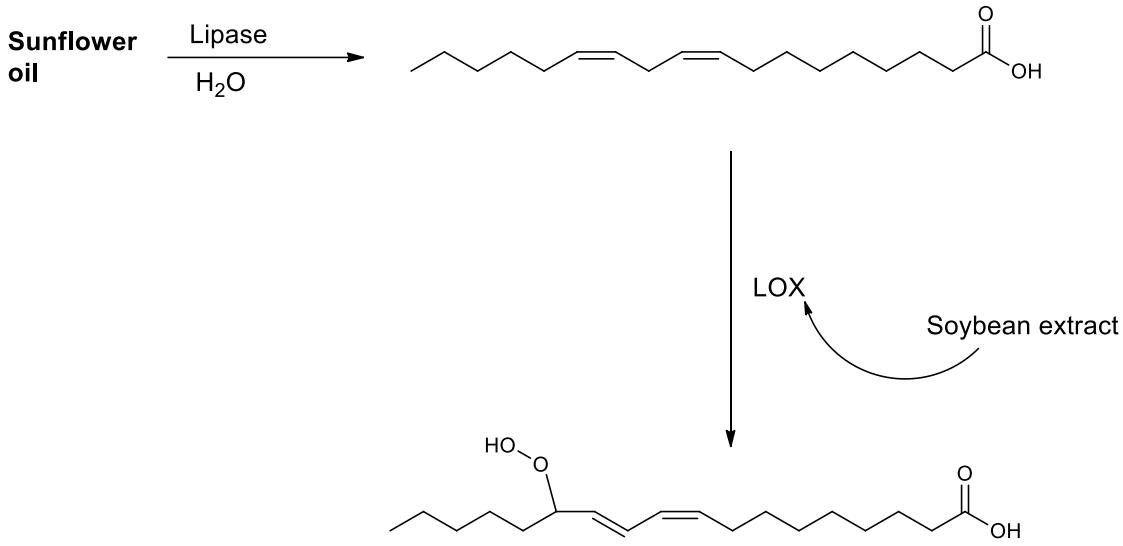

Scheme 8*:* A multi-step conversion of triglyceride fatty acid to fatty acid peroxide (56).

An alternative oxidative biocatalytic reaction is the direct oxidation of VL to NK using wild-type and mutant of $CYP450_{BM-3}$ sourced from *Bacillus megaterium* in a mixture with NADPH and sodium phosphate buffer (pH 7.4, 0.1 M) at 30 for 2 min, however, resulted in numerous side products, due to low regioselectivity as displayed in **Scheme 9** and the yield for NK was 7.7% (58)**.**

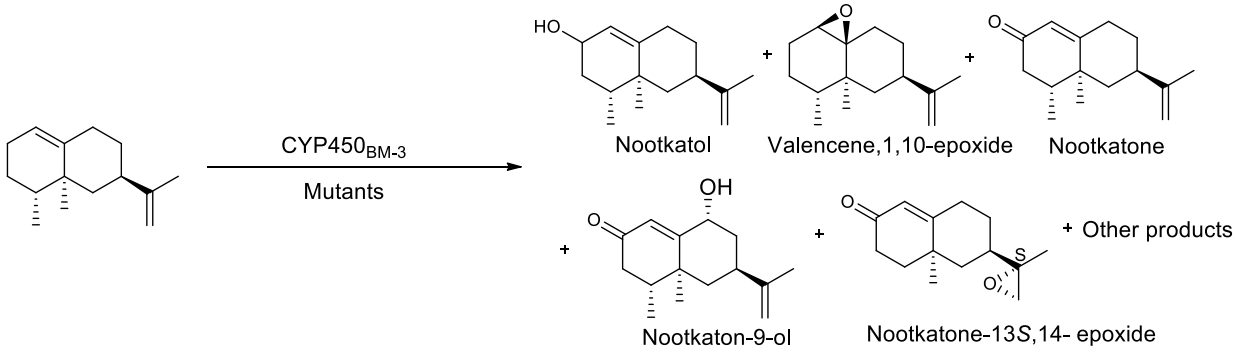

Scheme 9*:* The oxidation of valencene to nootkatone and other numerous products by mutant CYP450$_{BM-3}$ (58).

Biocatalytic oxidation can also be catalysed by laccases. *Huang et al.* reported that the oxidation of VL to NK using laccases from *Botrytis cinerea* and *Trametes versicolor*, mediator, emulsifier, and 0.1 M citrate buffer with pH ranging from 3 to 7 in the presence of an oxygen source usually forms valencene hydroperoxide, which is subsequently degraded to nootkatone (59). The degradation of the hydroperoxide required heating or the use of a catalyst. **Scheme 10** below shows the oxidation of VL to NK mediated by route (a.) CYP450 via nootkatol intermediate and route (b.) laccase via valencene hydroperoxide intermediate which both were then further oxidised to NK and the conversion efficiency ranging from 14.43 to 58.28%.

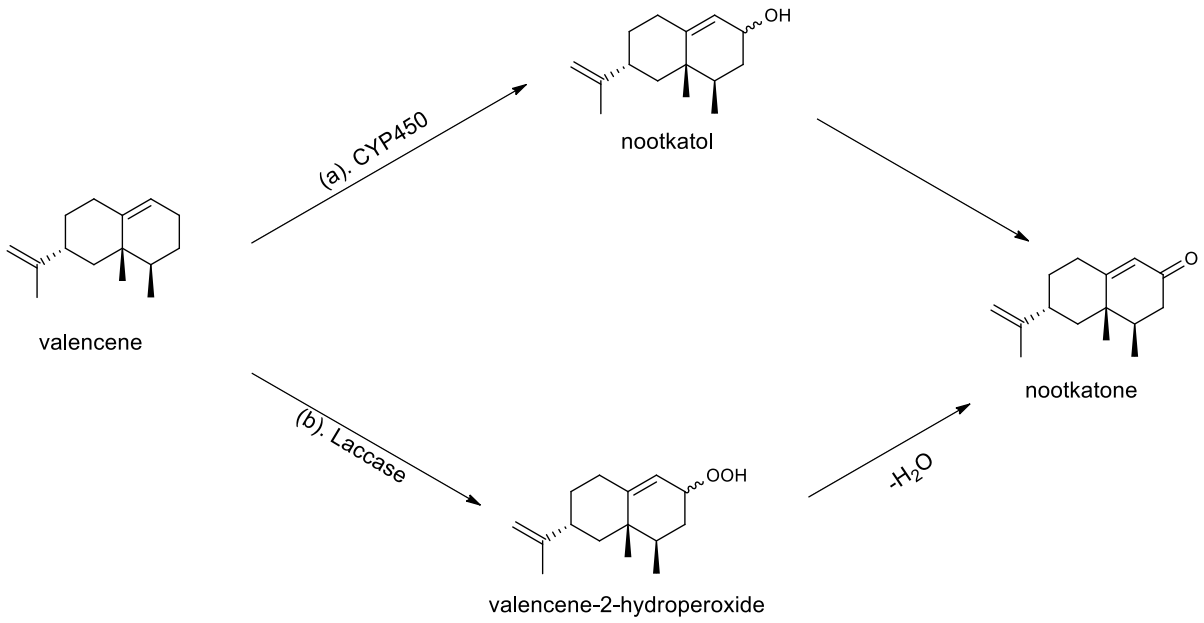

Scheme 10*:* The biotechnological conversion of valencene to nootkatone via laccase with conversion efficiency ranging from 14.43 to 58.28%. or cytochrome P450 with 7.7% yield (46).

1.8 Previous Work performed

Our group has successfully converted VL to NK using LOX isolated from soya beans. Although the conversion was high with a 77 % GC peak area, the isolated yield of NK was very low at 25 %. In addition, other factors that could impact this oxidation were not evaluated. In this research, we planned to modify the previously reported reaction conditions for LOX mediated oxidation of VL to NK. We also envisaged to expand this previous work by employing alternative enzymes for the conversion of VL to NK.

1.9 Aim and Objectives

1.9.1 Aims

- This project aims to evaluate the use of LOX from soya beans, CYP450 from Codexis and Prozomix, and laccase from *Novoprime Base 268* for the conversion of Valencene (VL) to Nootkatone (NK).

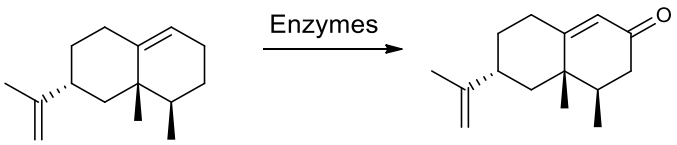

1.9 .2 Objectives

- Evaluate and compare LOX (extracted from Soya beans), commercial CYP450 and laccase enzymes for the biocatalytic conversion of VL to NK.
- Develop and optimise a method for the isolation of NK using column chromatography.
- Identify high-performance mutants of CYP450 from Codexis and Prozomix.
- Develop and optimise conditions for the conversion of VL to NK using the identified enzymes.

CHAPTER 2

RESULTS AND DISCUSSION

In this chapter, we address the biocatalytic conversion of valencene (VL) to nootkatone (NK) by evaluating the use of oxidative enzymes such as lipoxygenase, cytochrome P450 and laccase through exploration of factors affecting enzymes' activities. This could assist in the development of optimum reaction conditions leading to high products yields. The progress towards achieving the conversion of VL to NK is comprehensively elucidated in distinct sections, offering a detailed exploration of this study.

2.1 The Starting Material

We began by characterising the quality of valencene (VL). This preliminary assessment was crucial, as the subsequent determination of % conversion relied on the concentration of VL. The sample was, therefore, run on GCMS to assess its purity. Consequently, we established that the GC purity for valencene was 54.04%, which was supported by the product specification provided by Evolva and **Figure 7** shows the GC chromatogram with VL eluted at 03:49.0 (min: sec).

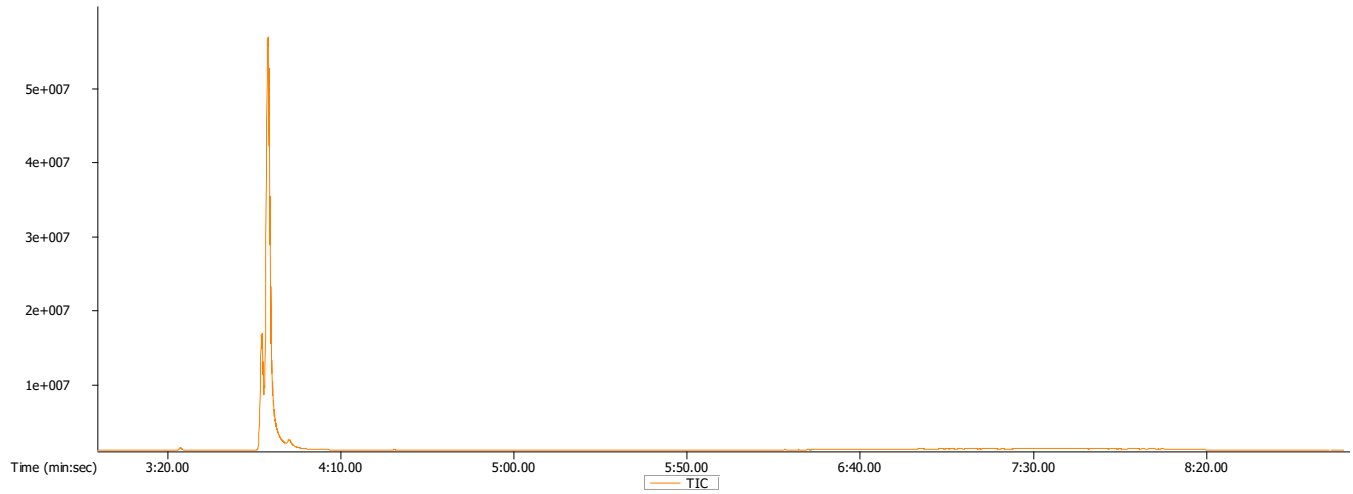

Figure 7*:* A chromatogram obtained from the gas chromatography (GC) analysis of the commercial valencene

2.2 Extraction of Lipoxygenase (LOX)

Lipoxygenase (LOX)

To convert the valencene to nootkatone we required lipoxygenase as a catalyst. Soya beans, similar to all seeds, contain enzymes primarily intended for the germination process. Among these enzymes, Lipoxygenase (LOX) is the most prevalent in soya beans (60,61). Moreover, LOX plays an important role in catalysing the oxidation of unsaturated fatty acids through molecular oxygenation. Consequently, we opted for soya bean as the source of the crude LOX in the oxidation of VL to NK, leveraging their natural enzymatic content for our intended purposes.

Soya beans are naturally hard, this serves as an advantage to the beans by delaying seed germination, providing resistance against seed coat pathogens, and protecting from spoilage (62). In previous work performed in our group, mortar and pestle were used to crush the ground soya beans into a coarse meal. However, this technique required intensive labour and it was time-consuming, leading to the introduction of a more efficient coffee grinder. The coffee grinder is efficient and grinds the soya beans with ease.

In order to access the LOX enzyme, we used two preparations of soya beans, namely ground soya beans (GSB) and milled defatted soya beans (MDS). The GSB was ground into fine flour using a coffee grinder while the milled MDS was supplied by a commercial producer in a defatted coarse meal texture.

The milling process disrupts the soya bean cell wall, improving enzyme extraction. In order to extract the enzyme, the ground flour (MDS and/or GSB) was then placed in a sodium borate buffer (pH 8.5, 100 mM) and left overnight in a refrigerator at 4 ˚C. **Figure 8** shows MDS and GSB crude extracts. Previously, in our group, this extraction was performed using three different buffers which were sodium borate buffer, tris buffer, and potassium phosphate buffer (pH 7.4 and 8.5, 100 Mm) and it was

established that the borate buffer showed best activity amongst the three buffers hence we opted for borate buffer in this study (55).

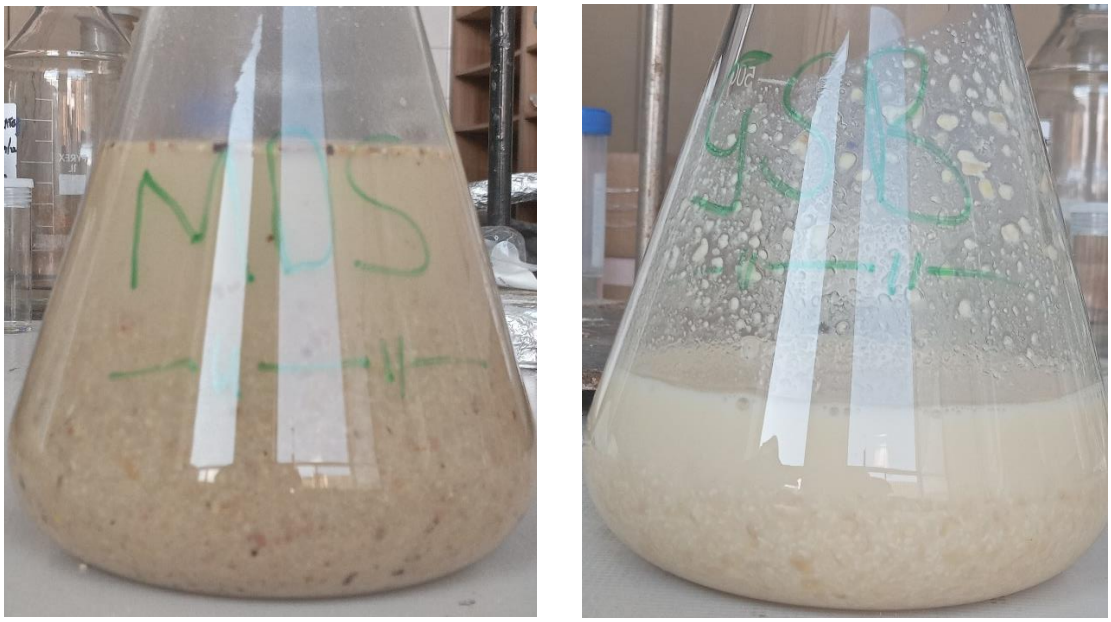

a. Milled defatted soya bean (MDS). b. Ground soya bean (GSB).

Figure 8*:* The crude MDS and GSB extracts of LOX.

The extraction process from GSB yielded a more viscous and emulsified cream, posing a significant challenge in workup procedures as opposed to the MDS. **Figure 9A** illustrate an emulsion from GSB reactions. Established methods to breakdown emulsions include letting the sample to stand for some time, acidifying the sample, adding table salt (NaCl) or, other more effective salts such as potassium pyrophosphate, filtering through sodium sulphate, centrifugation, and/or ultrasonic bath (63)**.** However, the implementation of some of these techniques on a large-scale reaction poses a challenge. Therefore, we focused on extracting the LOX enzyme from MDS, where phase separation occurred without any effort. **Figure 9B** illustrates MDS extraction where the emulsion broke down naturally by letting the sample stand. The extraction of LOX crude enzyme was achieved through a filtration method using cheesecloth to trap the biomass from the soya bean allowing the enzyme to pass through the cloth to a suitable container. This proved to be easy and efficient method

by eliminating the need for a Buchner funnel. Additionally, there were no blockages or problems encountered using this method.

a. GSB b. MDS

Figure 9*:* Phase separation. The emulsion was caused by a mixture of two or more immiscible liquids in the presence of natural emulsifiers from the biomass, with reduced emulsification occurring where the defatted biomass was added. The organic and aqueous phases separated using ethyl acetate through extraction.

2.3 The crude LOX enzyme activity

Satisfied that we extracted the enzyme, the next critical step was to evaluate the use of the crude enzyme in the oxidation of VL to NK. *Muller et. al.,* performed this reaction using purified lipoxygenase. They reported its advantages, particularly in addressing issues related to viscosity. The mixture contained sodium phosphate buffer (pH 8.5, 100 mM) to maintain pH, 10 % (w/v) aqueous NaOH solution for pH control, and linoleic acid (4 g, 14.263 mmol) as a mediator to facilitate the formation of hydroperoxide, and an oxygen inlet to create an oxygen-rich environment, which is a crucial aspect in oxidation reactions. The reaction proceeded for 2 days (48 hrs) at 60 ˚C, followed by extraction with ethyl acetate, washing with 10 % (w/v) of NaOH

solution, and neutralisation with brine, and concentration. They achieved 41.7 % conversion (mol/mol) of NK (64).

Inspired by this approach, we adopted a similar procedure with a modification of using a sodium borate buffer (pH 8.5, 100mM), as reported by *Makhubela* to be more effective than phosphate and tris buffer (55). The same reaction conditions were applied in our conversion of VL to NK reaction using crude LOX rather than purified LOX.

In our preliminary results, we observed a 2.63 % conversion (mol/mol) of VL to NK when oleic acid (1 g, 3.54 mmol) was used and a 6.29 % conversion (mol/mol) when linoleic acid (1 g, 3.57 mmol) was used, and both reactions were run for 2 days. However, we opted to use oleic acid (1 kg for $7.00) going forward rather than linoleic acid (1 kg for $25.00) due to its cost effectiveness. When we left the reaction to run for 5 days, 8.9 % conversion was obtained and when this was further extended to 7 days the conversion rose to 29.87 %. **Figure 10** shows GC chromatogram that displays the elution of VL and NK on a crude sample catalysed by LOX.

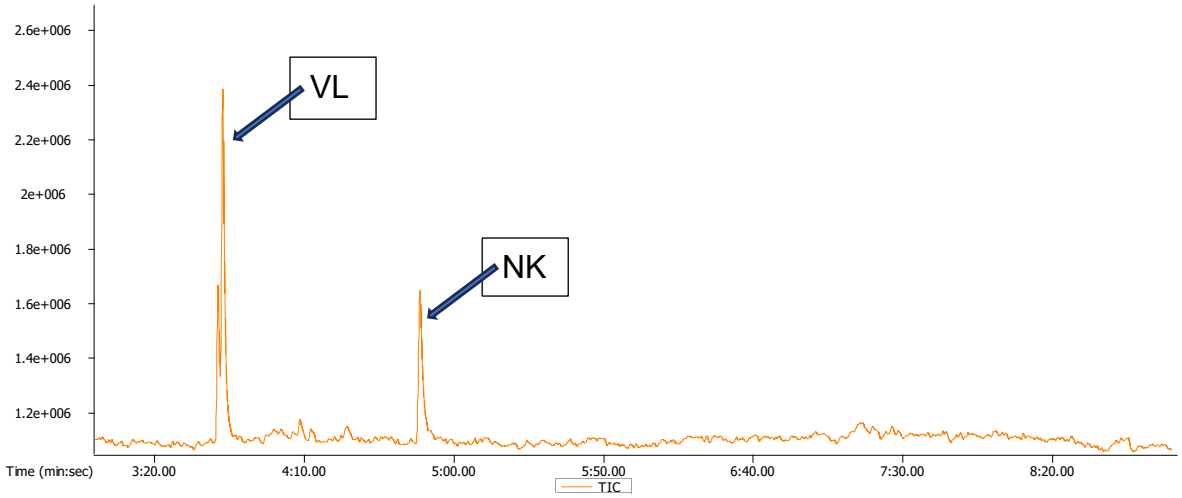

Figure 10*:* GC chromatogram of the crude NK product obtained from the LOX reaction.

2.4 Isolation and Characterisation of NK

With the conversion achieved in the biotransformation of valencene (VL) to nootkatone (NK), our focus shifted to the isolation and characterization of NK. The product isolation was accomplished through column chromatography, and subsequent characterization involved NMR, HPLC, and GC-MS analyses. The column chromatography contained silica gel as the stationary phase and a mobile phase composed of distilled ethyl acetate (20%) and hexane (80%). Fractions were systematically collected and monitored via silica thin layer chromatography (TLC), using the same mobile phase (20% ethyl acetate/80% hexane). The spots were visualised under a UV lamp, **Figure 11** displays the fractions of the isolated product alongside standards for VL and NK which were co-spotted on the TLC plate. TLC confirmed the successful synthesis of NK, evident from identical Rf values (0.432 and 0.459) for the synthesised and standard NK, while the Rf value for standard VL was 0.757. The absence of a VL spot in the isolated product further affirmed its purity and supported the higher conversion we reported. Additionally, NK exhibited a lower Rf value than VL due to its comparatively higher polarity. Since a carbonyl functional group is introduced in NK, the oxygen of the carbonyl interacts via hydrogen bonding with the hydroxy group on the stationary phase silica gel.

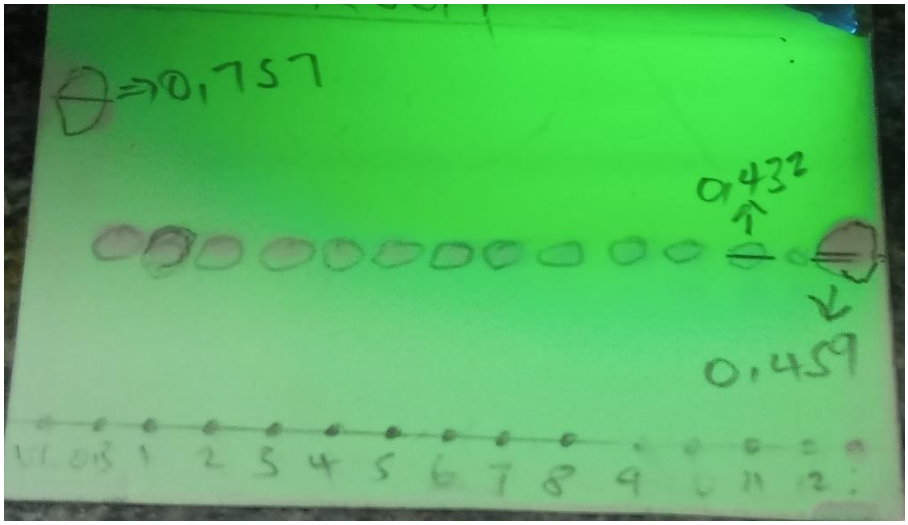

Figure 11*:* TLC plate showing spots of isolated product and standards for VL and NK run on mobile phase of 20% ethyl acetate/80% hexane viewed under UV at 254 nm.

Following the confirmation of purity through TLC analysis for selected fractions, the pure fractions were combined, dried, and concentrated under vacuum using a rotary evaporator. Analysis of the ^{1}H NMR spectra revealed two distinct signals for NK in **Figure 12**. A singlet, appearing downfield at 5.77 ppm, integrating for one proton and was attributed to the cyclic vinyl proton, H1. This proton deshielded compared to the corresponding proton in VL as displayed in **Figure 13**, which was observed at 5.33 ppm. Similarly, the doublet signal at 4.74 ppm in NK, integrating for two protons in **Figure 12**, was slightly downfield compared to the doublet at 4.70 ppm in VL as displayed in **Figure 13**. The downfield shifting of protons in NK, relative to VL, resulted from the influence of the introduced oxygen, leading to the deshielding of carbons and protons within its vicinity.

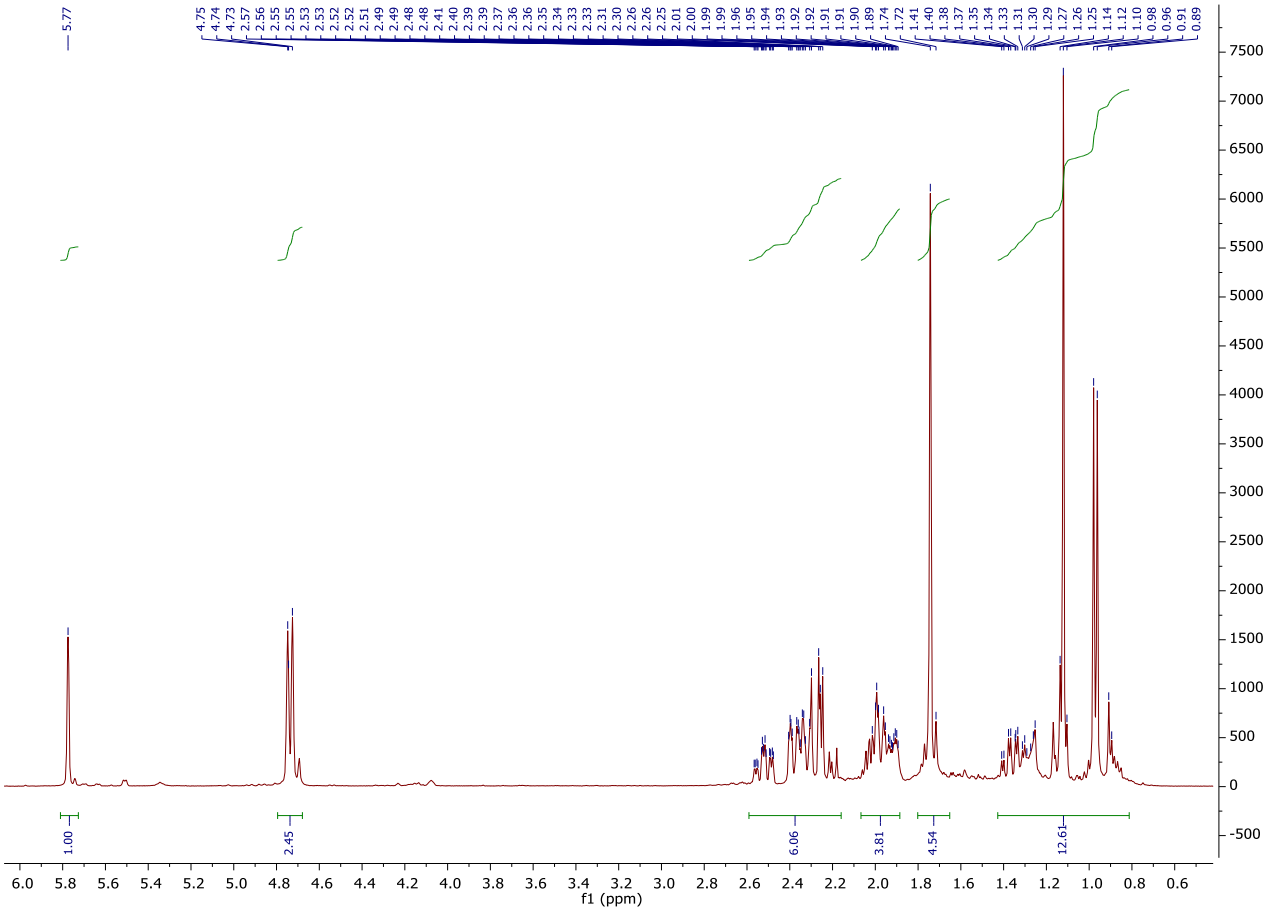

Figure 12: ^{1}H NMR spectrum of nootkatone.

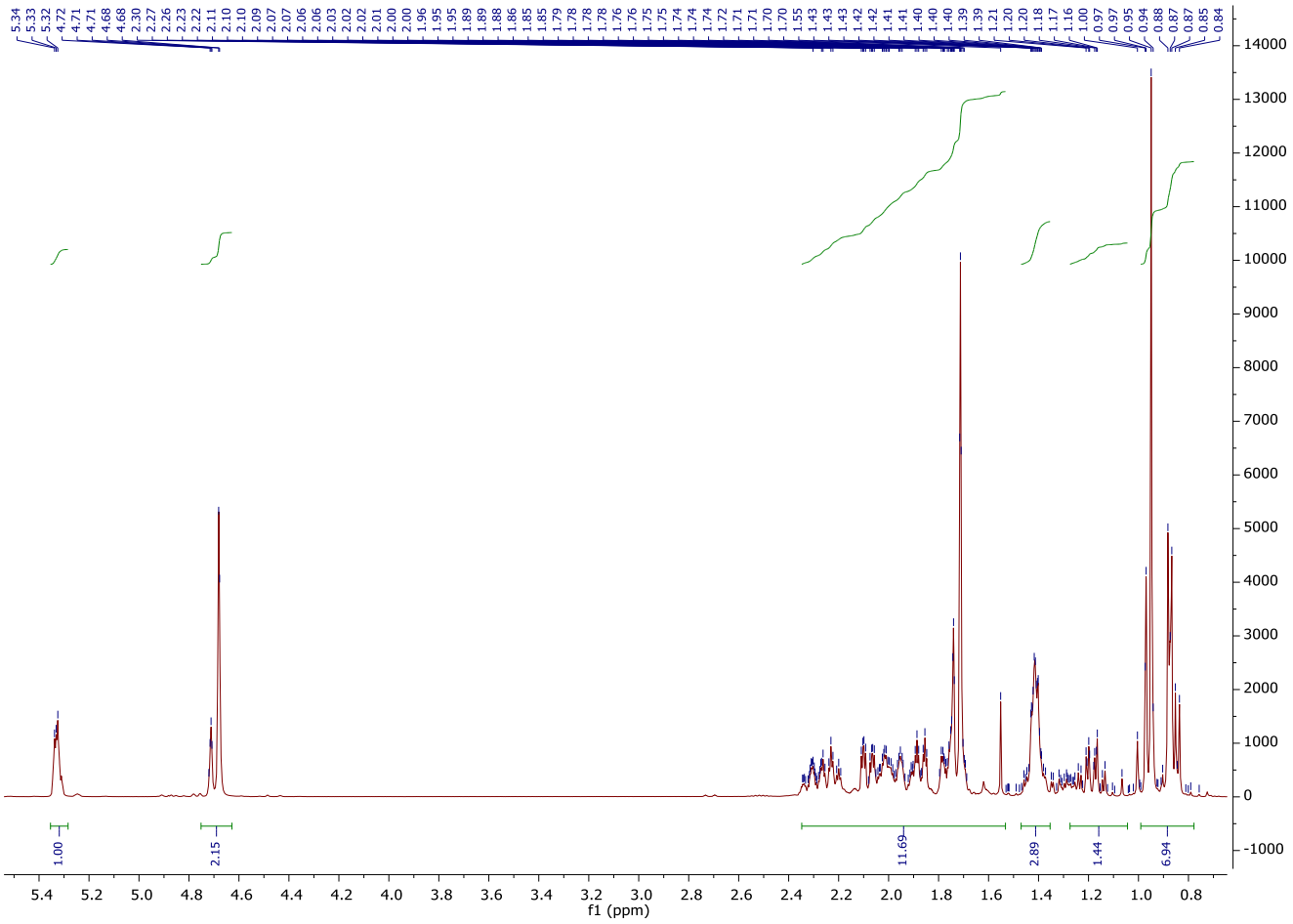

Figure 13*:* ^{1}H NMR spectrum of valencene.

Table 2 presents the ^{1}H NMR data, signals associated with two double bonds and three methyl groups. This data aligns well with findings by *Xie et al.* and *Zhang et al.* reinforcing the credibility of our ^{1}H NMR spectrum results (65,66). The nomenclature of carbons from 1 to 15 in the NK structure followed the IUPAC name (4S,4aR,6S)-4,4a-dimethyl-6-(prop-1-en-2-yl)-4,4a,5,6,7,8-hexahydronaphthalen-2(3H)-one, which was confirmed by *Fan et al.* (49).

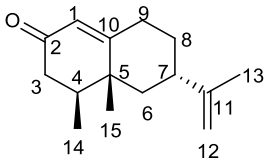

Table 2*:* The key signals of ^{1}H NMR accounting for NK structure.

Protons	Purified NK Signals (ppm)	*Xie et al.*(65) Signals (ppm)	*Zhang et al.*(66) Signals (ppm)
1H, s, H-1	5.77	5.80	5.64
2H, m, H-12	4.74	4.78	4.67
3H, m, H-13	1.90	1.77	1.66
3H, m, H-15	1.25	1.15	1.04
3H, m, H-14	0.96	0.99	0.87

The confirmation of NK isolation was further substantiated through the utilisation of the ^{13}C NMR spectrum in **Figure 14**. The spectrum revealed distinctive carbon signals, including a carbonyl carbon signal (C2) at 199.66 ppm. The presence of five CH_2 (methylene) protons in the NK structure was confirmed through DEPT135 analysis in **Figure 15**. Notably, the olefinic group's carbon (C12) was observed at 109.26 ppm, while other CH_2 carbons were identified at C6 (43.94 ppm), C3 (42.09 ppm), C9 (42.09 ppm), and C8 (31.64 ppm).

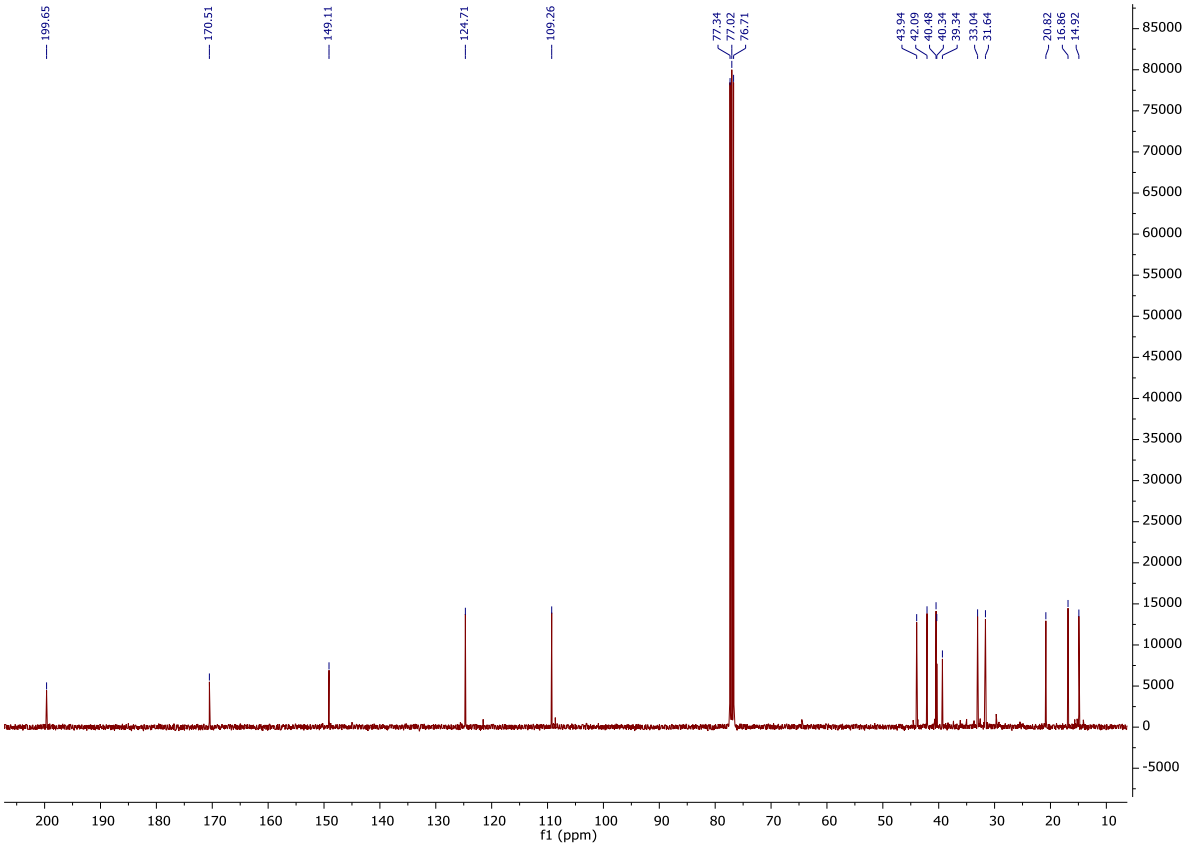

Figure 14: ^{13}C NMR spectrum of nootkatone.

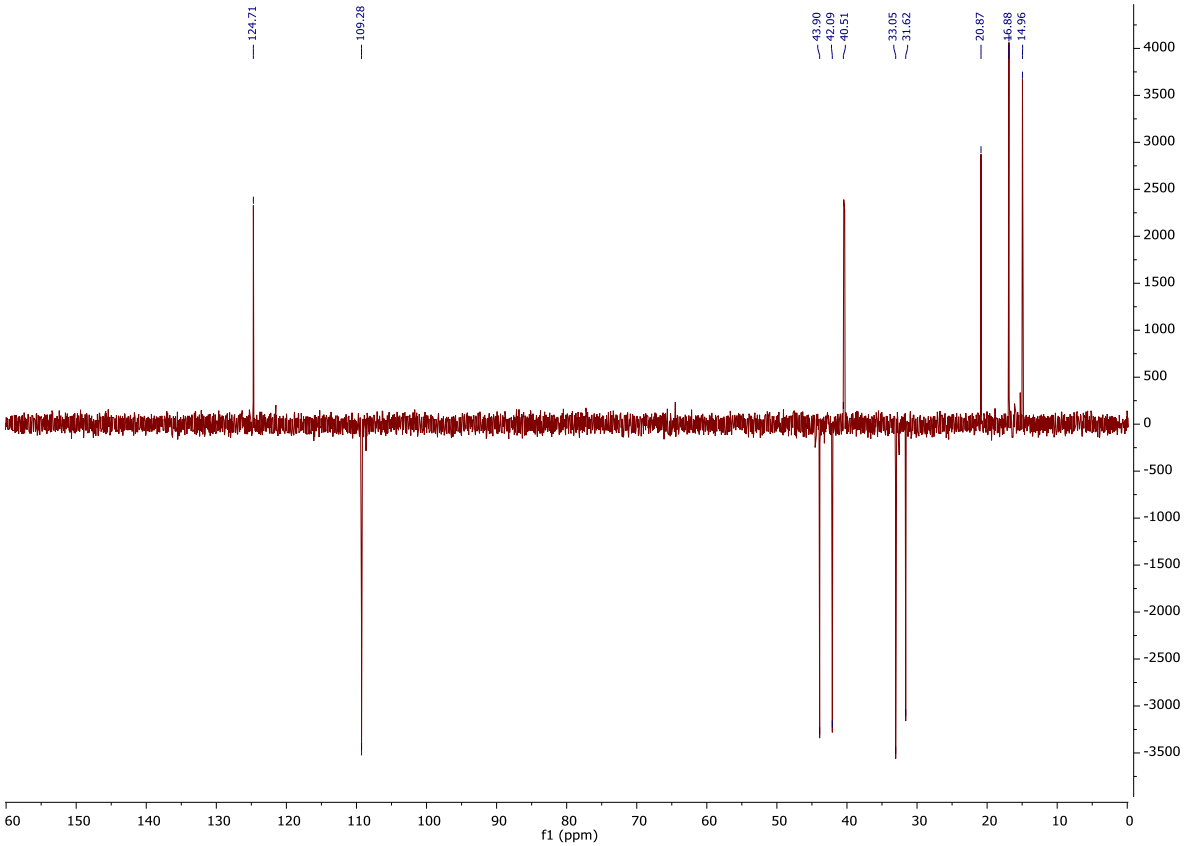

Figure 15 *:* DEPT135 NMR spectrum of nootkatone.

Further details on additional carbon signals can be found in **Table 3**. The agreement of these carbon signals with those reported by *Zhang et al.* support the validity of our ^{13}C NMR spectrum analysis (66).

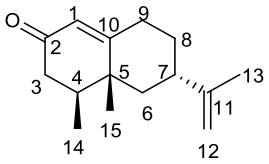

Table 3: The key signals of ^{13}C NMR accounting for NK structure.

Carbons	Purified NK Signals (ppm)	*Zhang et al.* (66) Signals (ppm)
C2	199.66	198.6
C10	170.51	170.1
C11	149.11	149.5
C1	124.71	124.5
C12	109.26	109.7
C6	43.94	43.8
C3	42.09	42.1
C7	40.48	40.5
C5	40.34	40.4
C4	39.34	39.9
C9	33.04	32.6
C8	31.64	31.7
C13	20.82	21.2
C15	16.86	17.0
C14	14.42	15.2

The confirmation of NK isolation was further substantiated through GCMS and HPLC analyses. In **Figure 16**, the GC chromatogram displays the elution of NK at 5:50.00 (min: sec) and the MS spectra using the isolated NK, this confirms its purity and also provides additional validation.

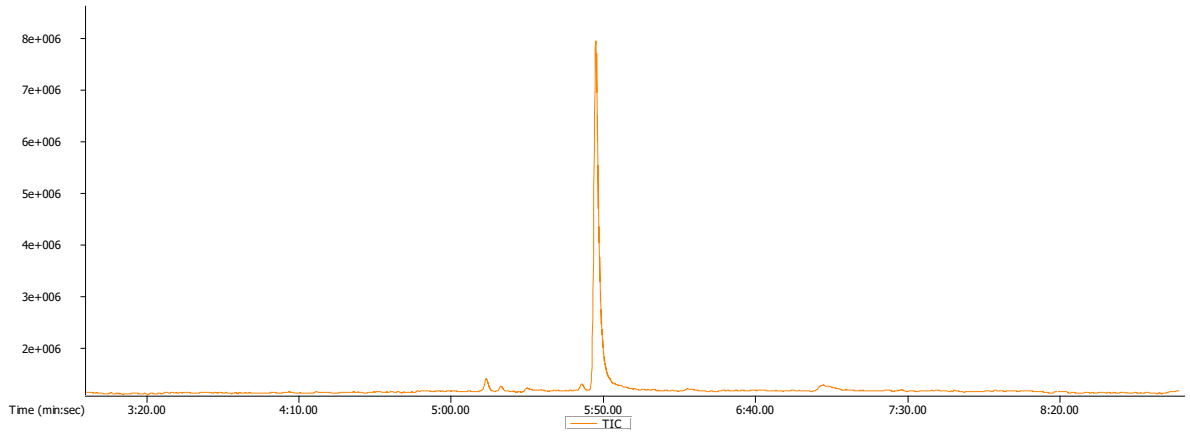

Figure 16a*:* GC chromatogram for nootkatone.

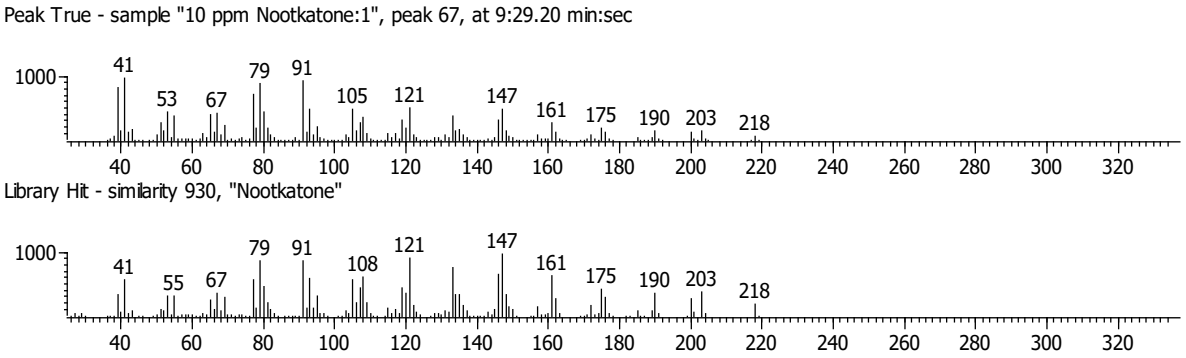

Figure 16b: MS spectra for nootkatone.

Additionally, HPLC (**Appendix, Figure 33**) was employed, detecting the mass of NK at [M + H] = 219.1749, precisely matching the expected mass of NK (218.1749). Another detected mass at [2M + H] = 437.3409 indicates dimerisation, where the mass of NK was added twice, along with a proton. With this comprehensive information, the successful isolation of NK was confirmed as outlined above.

2.5 Factors affecting LOX activity.

Given the low % conversion of our preliminary results, we recognised the need for modification to enhance the % conversion. Therefore, the evaluation of potential factors which could affect LOX activity was followed. The factors included metal ions, temperature, type of unsaturated fatty acid, type of enzyme source (MDS or GSB extraction), and enzyme soaking period. In the subsequent sections, we reported on the results of evaluating each of the factors.

2.5.1 Influence of metal ions on nootkatone synthesis

The activity of crude LOX enzyme can be influenced by metal ions, acting either as activators, enhancers, or inhibitors. *Koch et el.* reported that Ca^{2+} and Mn^{2+} acted as activators while Fe^{2+} and Cu^{2+} acted as competitive inhibitors for navy bean lipoxygenase (67). Additionally, the presence of Ca^{2+} is known to promote the interaction between the enzyme and the fatty acids, although the precise molecular mechanism of Ca^{2+} is not yet known (68). A wide spread of salts such as $FeSO_4.7H_2O$, $FeSO_4$, $MnSO_4$, $MnCl_2.4H_2O$, $CuSO_4.5H_2O$, $CuCl_2.2H_2O$, and $CaCl_2.2H_2O$ were prepared as sources of Fe^{2+} and Cu^{2+}, $Ca^{2+,}$ or Mn^{2+} each at a mass of 0.05 g.

In our preliminary results, the 7-day reaction demonstrated a higher % conversion compared to the 2- and 5 -day reactions as mentioned above. As a result, all subsequent reactions were undertaken for 7 days, and the results are reported in **Table 4**. The results indicate both negative and positive impacts depending on a specific metal ion used in each reaction*. Mohammed et al.* reported data showing that some metal ions both enhanced and inhibited purified LOX activity, while some ions had no significant effect (69).

From the data in **Table 4**, we could not identify a clear pattern regarding the effects of the metal salts on the crude LOX activity. The combination between $FeSO_4.7H_2O$ and $MnSO_4$ (entry 3) showed the best conversion of 59.60%, surpassing the control (entry 1), which had a conversion of 29.87%. Conversely, $FeSO_4.7H_2O$ alone (entry 2) and

combined with $MnCl_2.4H_2O$ (entry 4) or $CuSO_4.5H_2O$ (entry 6) or $CuCl_2.2H_2O$ (entry 5) or $CaCl_2.2H_2O$ (entry 8) and $FeSO_4$ combined with $MnSO_4$ (entry 7) all displayed conversions lower than the control, showing inhibitory effect on crude LOX enzyme activity. The inhibitory effect of metal ions is suspected to be through competitive reduction of ferric ions, crucial for LOX activity. Therefore, the reduction of ferric ions on crude LOX led to enzyme inactivation (70).

Table 4: Effects of metal ions from different mole ratios and equal grams of different salts on MDS LOX after 7 days of reaction.

Salts	% Conversion
1. Control	29.87
2. $FeSO_4.7H_2O$	1.30
3. $FeSO_4.7H_2O$ and $MnSO_4$	59.60
4. $FeSO_4$ and $MnSO_4$	5.22
5. $FeSO_4.7H_2O$ and $MnCl_2.4H_2O$	7.55
6. $FeSO_4.7H_2O$ and $CuCl_2.2H_2O$	1.30
7. $FeSO_4.7H_2O$ and $CuSO_4.5H_2O$	0.00
8. $FeSO_4.H_2O$ and $CaCl_2.2H_2O$	4.85

Based on the literature we had anticipated a clear impact of metal ion addition on conversion, but this was not so. An obvious complication of the experiment was that we had added salts by mass and not by mole, making it difficult to ascertain the precise impact of these metal salts. Additionally, the poor reproducibility of these reactions further complicated the interpretation of our results **(Table 4)**. To address these shortcomings, the reactions were repeated in duplicates using identical mole ratios of the metal salts (**Table 5)**. These reactions were monitored daily, however we focused on the 6^{th} day, as it clearly emphasises the effect of metal ions. The % conversion of VL to NK when $MnSO_4$ (entry 2) was used was 11.50% and this was lower than the control (entry 1) with a conversion of 22.07%, whilst with $FeSO_4.7H_2O$ (entry 3) a conversion of 26.26% was realised which was higher than the control. These results are consistent with findings by *Marvian-Hosseini et al.* who reported that $FeCl_2$ had a more significant effect than $MnCl_2$ on purified lipoxygenase from sesame seeds (70).

Table 5*:* Effects of different salts with each concentration of 2.64 mM*.

Days	% Conversion						
	Control	$MnSO_4$	$FeSO_4.7H_2O$	$FeSO_4.7H_2O$ and $MnSO_4$	$FeSO_4$ and $MnSO_4$	$FeSO_4.7H_2O$ and $MnCl_2.4H_2O$	$FeSO_4.7H_2O$ and $CaCl_2.2H_2O$
0	0	0	0	0	0	0	0
1	7.11	4.67	10.70	6.18	10.30	16.93	16.45
2	8.43	6.22	16.14	11.09	20.39	22.06	21.02
3	12.51	7.73	17.16	18.46	25.77	23.27	24.65
4	15.60	9.92	18.65	21.60	30.26	23.86	32.42
5	14.62	11.35	20.33	27.08	35.60	25.64	38.04
6	**22.07**	**11.50**	**26.26**	**34.40**	**40.03**	**26.19**	**39.02**
7	27.03	12.42	26.65	42.88	46.17	27.67	40.59

*0.331 mmol in a 125 ml reaction volume

Moreover, the combination of $FeSO_4.7H_2O$ with $MnSO_4$ (entry 4) or $MnCl_2.4H_2O$ (entry 6) or $CaCl_2.2H_2O$ (entry 7) and $FeSO_4$ with $MnSO_4$ (entry 5) were assessed to enhance the % conversion of NK and all these combinations showed better conversions. In search of a clear pattern for effective combinations, **Figure 17** was constructed to assess the effect of ion combinations. It is evident that within the first 2 days (Fe+ Mn+ Cl_2) proved superior, while (Fe+ Ca+ Cl_2) surpassed from the 3rd to the 5th day. This aligns with findings by *Marvian-Hosseini et al.* who reported that $CaCl_2$ had more significant effect than $MnCl_2$ on purified lipoxygenase from sesame seeds (70). Ultimately, in the last 2 days (Fe+ Mn+ SO_4) outperformed the two combinations. As a result, (Fe+ Mn+ SO_4) combination emerged as an effective combination for crude LOX from MDS with high % conversion of NK.

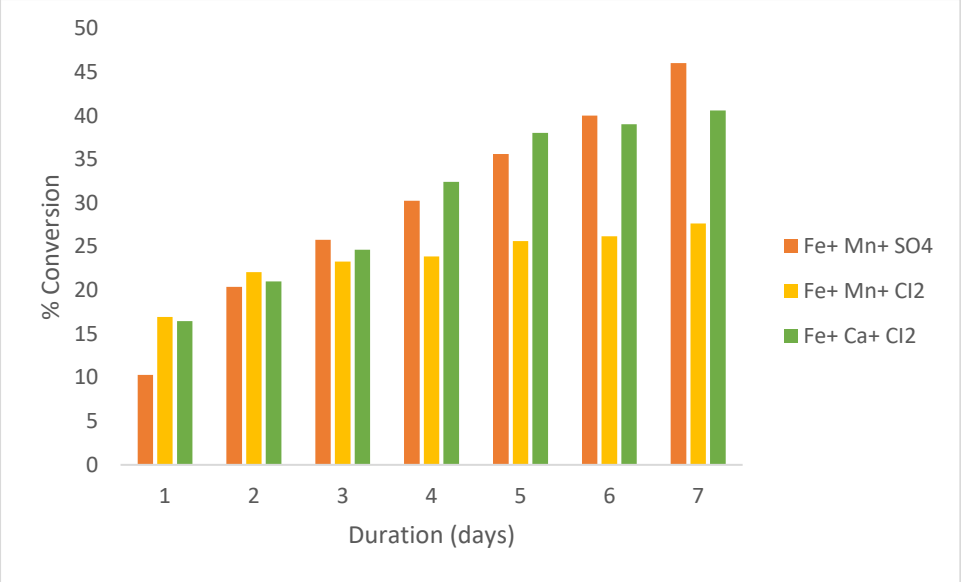

Figure 17*:* Assessing ion combinations showing a positive effect on MDS after 7 days of reaction.

Studying the impact of metal ions on crude LOX has revealed that metal ions have the capability to speed up the enzyme's catalysis in the conversion of VL to NK. Additionally, another trend emerged, indicating that the % conversion rises with an increase in the number of days. Based on the replicated results, the combination of $FeSO_4.7H_2O$ and $MnSO_4$ emerged as the most effective addictive. **Figure 18** illustrates a linear trend, with the % conversion consistently increasing over an extended period. Moreover, the replicates demonstrate good accuracy of sampling and assay, while having a linear kinetics with a high R squared indicating that this model is a good fit by highlighting a strong correlation between duration and % conversion. This shows the importance of allowing the crude LOX to proceed for an extended duration, as it leads to a continuous enhancement in the % conversion of NK.

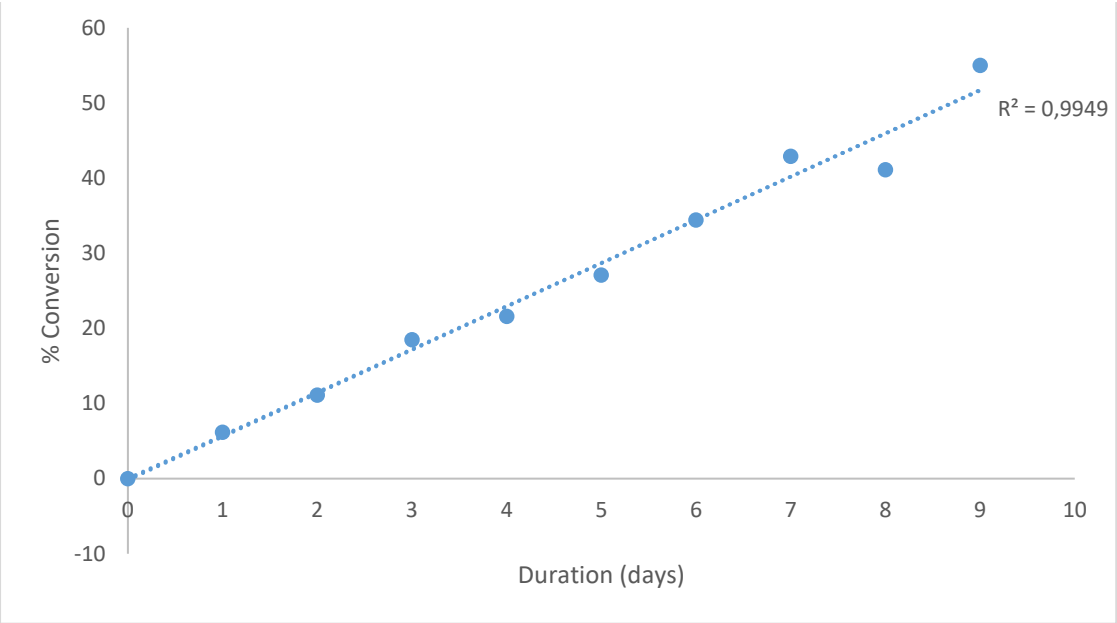

Figure 18: The average conversion per day using concentration of 2.64 mM of $FeSO_4.7H_2O$ and $MnSO_4$ on MDS LOX.

Due to consistency of the results in **Figure 18**, we were eager to assess the mole balance of NK formed as the reaction proceeded for 9 days. **Figure 19** displays a linearity between duration of the reaction and the amount of NK formed with a high value of R squared, which confirms the correlation between the two variables. This data was generated from **Appendix, Table 16.**

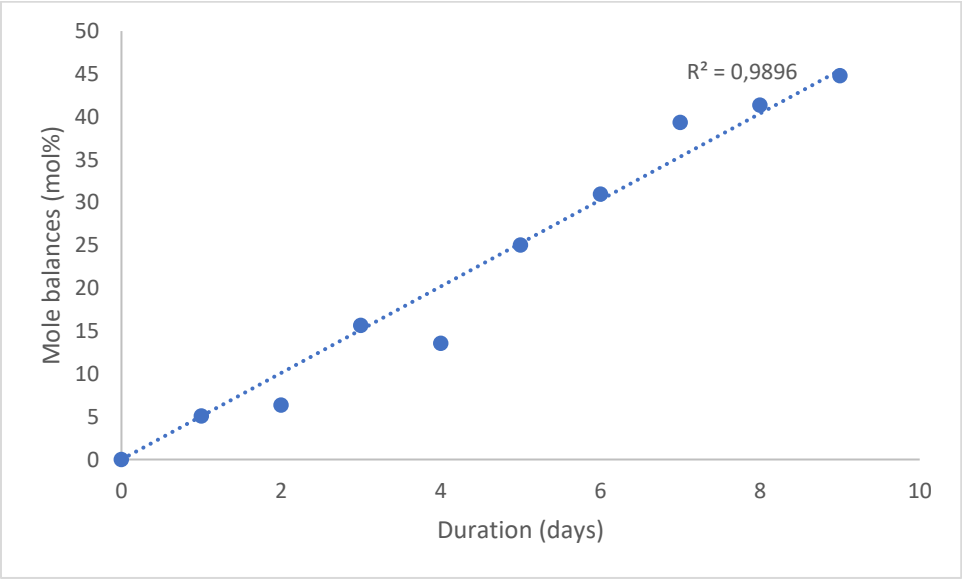

Figure 19*:* The mol % of NK formed with the addition of $FeSO_4.7H_2O$ and $MnSO_4$ using a concentration of 2.64 mM respectively on MDS LOX.

2.5.2 Temperature study

The thermal stability of an enzyme is an important factor, as it determines whether the enzyme is active, inactive, or denatured. Enzymes typically differ in thermal stability properties when exposed to lower and higher temperatures. *Muller et al.* reported that LOX works effectively within a broad temperature range (20 to 80 ˚C), with temperatures above 50 ˚C demonstrating enhanced conversion of VL to NK in a 24 hour and 48 hour reactions (64). Inspired by this finding, our study adopted a similar procedure and conducted reactions at varied temperatures (60, 70, 80, and 90 ˚C) over 2 days (48 hours). The MDS LOX crude enzyme exhibited maximum activity at 70 ˚C with a 10.69% conversion, followed by reaction at 60 ˚C with a 2.63% conversion, showing a better enzyme activity compared to reactions undertaken at 80 ˚C and 90 ˚C, as depicted in **Figure 20**. The decline in enzyme activity at high temperatures (80 ˚C and 90 ˚C) could have been because of enzyme denaturation, where enzyme loses its structure. Some reports indicate that LOX extracted from various sources remained active within a temperature range of 30 ˚C to 50 ˚C (70).

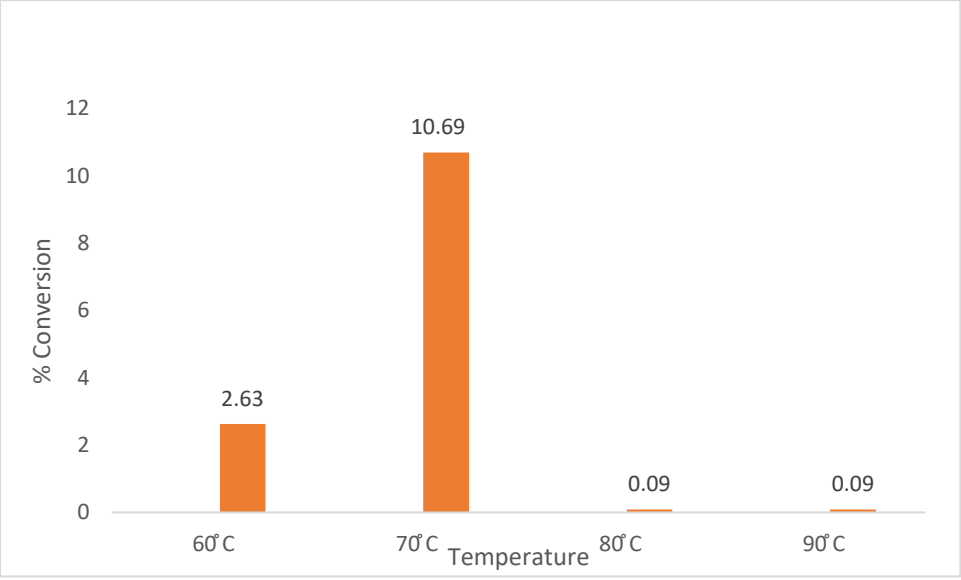

Figure 20*:* Effects of various temperatures on MDS LOX crude enzyme after a two-day reaction.

Having established that 60 and 70 ˚C represented the optimal temperatures for the conversion of VL to NK, we then decided to carry out prolonged reactions at these temperatures. This involved the addition of $FeSO_4.7H_2O$ and $MnSO_4$ combination, with the results highlighted in **Table 6**. Notably, the reactions maintained at 70 ˚C showed enhanced kinetic activity compared to the ones maintained at 60 ˚C, as the conversion at 70 ˚C consistently surpassed the conversion at 60 ˚C from 1st day to the 8th day. However, on the 9th day the 60 ˚C reaction exceed that of 70 ˚C. The plot of the data shows that the reaction at 70 ˚C slows with time, possibly due to thermal denaturation of the LOX **(Figure 21)** and suggests that the optimal reaction temperature for maximum conversion may be 65 ˚C. This trend is also in agreement with findings reported by *Muller et al.* in studies involving purified LOX, where % conversion of VL to NK was 21,25% at 70 ˚C, surpassing the 18.75% at 60 ˚C after 24 hour reaction (64). **Figure 21** clearly represents the consistency of our results concerning kinetic activity of MDS LOX crude enzyme, as the reaction was monitored daily. However, **Table 6** shows variations between experiments, which might be due to variations in stirring between reactions or other technical errors.

Table 6: Reaction kinetics at temperatures 60 and 70 ˚C with the addition of $FeSO_4.7H_2O$ and $MnSO_4$ using a concentration of 2.64 mM respectively for 9 days on MDS LOX.

Days	% Conversion							
	60 ˚C $FeSO_4.7H_2O$ and $MnSO_4$				70 ˚ C $FeSO_4.7H_2O$ and $MnSO_4$			
	1st run	2nd run	3rd run	**Average**	1st run	2nd run	3rd run	**Average**
0	0	0	0	**0**	0	0	0	**0**
1	1.91	6.30	10.33	**6.18**	5.22	9.45	18.52	**11.06**
2	1.78	13.05	18.45	**11.09**	18.58	18.66	27.91	**21.72**
3	16.28	14.06	25.04	**18.46**	35.70	23.52	31.02	**30.08**
4	19.32	15.39	30.10	**21.60**	44.67	28.00	32.54	**35.07**
5	29.09	19.57	32.59	**27.08**	49.29	32.95	34.09	**38.78**
6	43.67	22.58	36.95	**34.40**	60.56	35.32	38.40	**44.76**
7	59.60	22.88	46.16	**42.88**	65.56	38.21	39.84	**47.87**
8	54.66	27.14	41.48	**41.09**	67.08	45.26	49.26	**54.00**
9	75.46	30.29	59.25	**55.00**	------	40.17	49.17	**44.67**

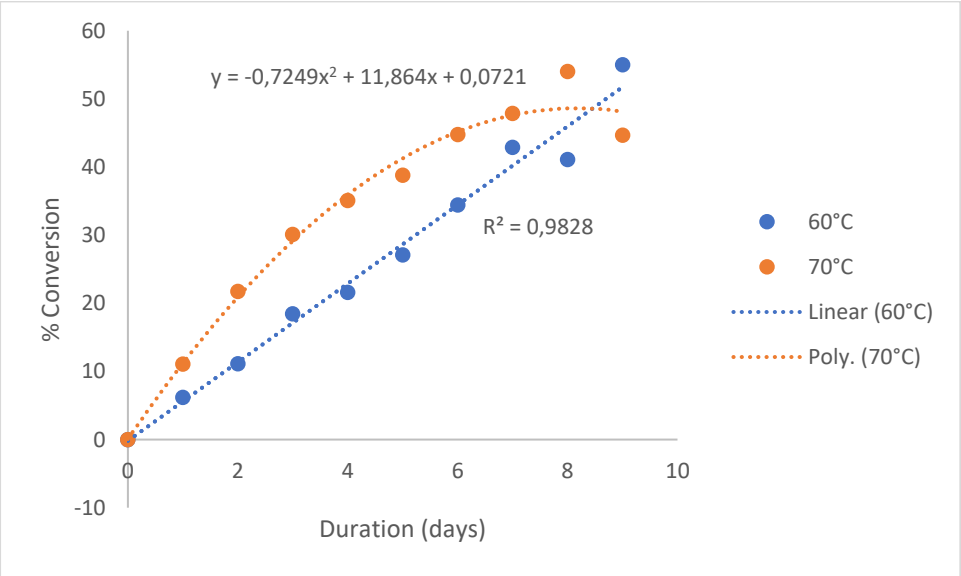

Figure 21: Kinetics of average conversion at 60 and 70 ˚C over 9 days.

Following the positive outcome in the study of temperature, we decided to evaluate the correlation of standard deviation and mean using our results. *Andrade* explored the relationship between standard deviation (Std dev) and mean, with mean representing the average value and Std dev indicating the spread of values around the sample mean (71). To evaluate the variation between Std dev and mean in our results, we calculated and plotted their graph using % conversion of the triplicates. **Figure 22** exhibit a direct proportionality, revealing that as the mean increases, Std dev also tends to rise for most data points. This implies that Std dev values closely align with the mean across the three runs, resulting in less scattered values and also showing consistency in the % conversion of NK.

$$\text{Std dev} = \frac{\sqrt{\sum(X-\mu)^2}}{n-1}$$

μ= sample average

X= individual values in a sample

n= the total number of individual values in a sample

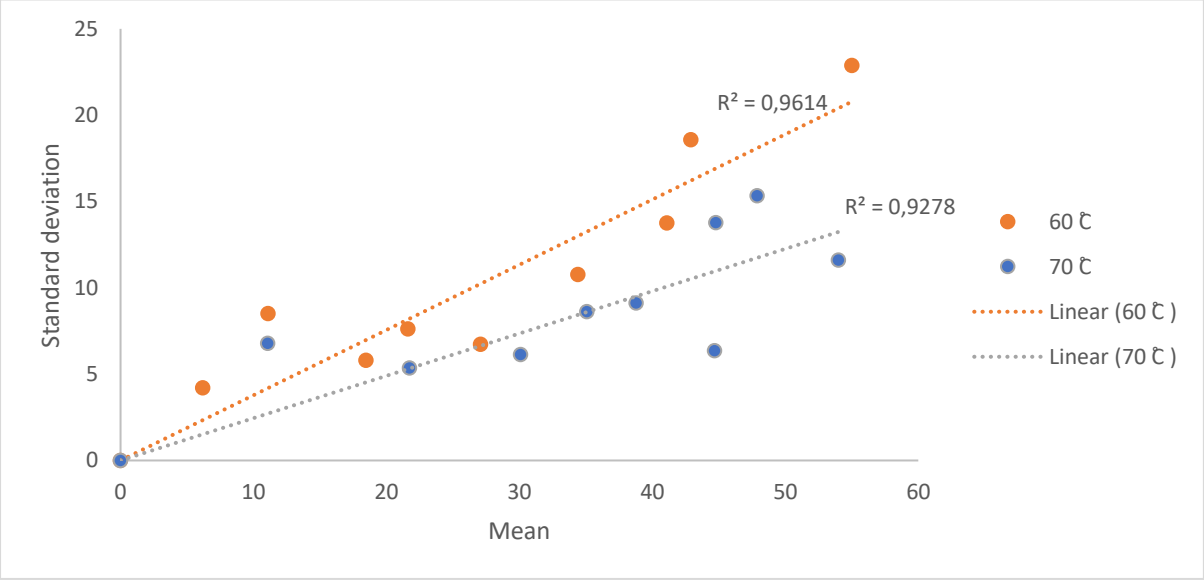

Figure 22*:* The standard deviation versus mean for the three runs (triplicates) at 60 ˚C and 70 ˚*C.*

2.5.3 Impact of fatty acid mediators

All lipoxygenase enzymes require a fatty acid as a substrate for hydroperoxide (HPODE) formation, which acts as an intermediate in the conversion of VL to NK. *Marti et al.* observed the formation of hydroperoxides in the presence of LOX enzyme using sunflower oil (56). In this study, we conducted the oxidation reactions using unsaturated fatty acids such as sunflower oil, canola oil, olive oil, linoleic acid, and anarcadic acids. **Figure 23** illustrates the structures of various unsaturated fatty acids which were assessed in this reaction.

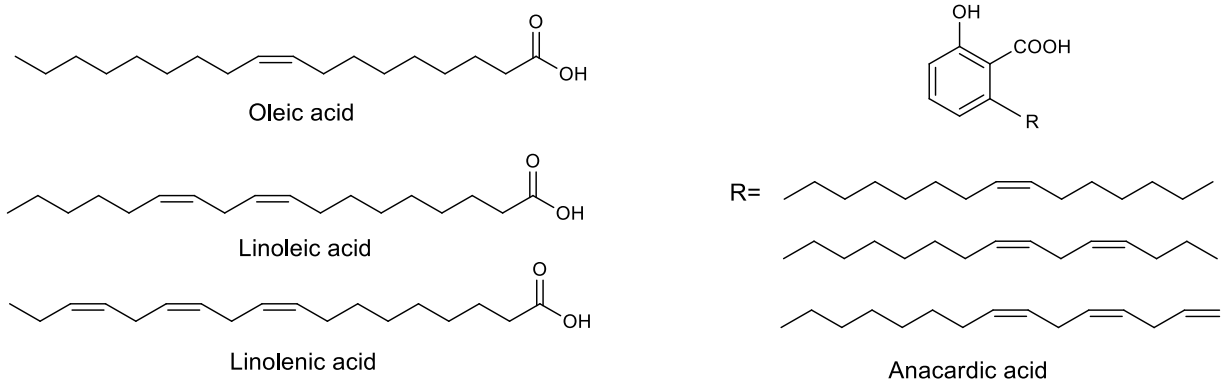

Figure 23*:* The structure of unsaturated fatty acids.

Table 7 outlines the amounts of fatty acids bound to glycerol and the composition of fatty acids in each of the oils. We envisioned that for the oils to promote the formation of hydroperoxides, the fatty acids needed to be hydrolysed from the glycerol. The hydrolysis process is typically catalysed by the lipase enzyme (56).

Table 7*:* Fatty acid composition of vegetable oils.

Fatty acid	Sunflower oil (72)	Canola oil (73)	Olive oil (74)
Oleic acid	14-43%	65.39%	55-83%
Linoleic acid	44-75%	16.32%	3-21%
Linolenic acid	------	7.54%	<1%

Rigo et al. successfully produced lipases with high activity from soybeans (75). Therefore, the MDS crude enzyme extract contains enzymes, lipases and LOX. The combination of lipase and LOX contained in MDS could liberate the fatty acid and form

hydroperoxide (HPODE) for the conversion of VL to NK. *Prabakaran et al.* reported that soya beans contribute fatty acids such as oleic acid, linoleic acid, and linolenic acid which play an important role in the oxidation of VL to NK (76).

Pignitter et al. reported that the oxidation of vegetable oils is more constrained compared to free fatty acids, attributing this limitation to the hydrolysis of triglycerides, which might slow down the hydroperoxide formation due to solubility (77). As a result, the data in **Table 8** indicates that oleic acid exhibited a higher conversion of VL to NK when compared to vegetable oils, linoleic acid, and anacardic acid. The 7^{th} day as highlighted in **Table 8** demonstrated a remarkable 59.60% conversion using oleic acid, which is double the conversions observed for other fatty acids with addition of $FeSO_4.7H_2O$ and $MnSO_4$ at 60 ˚C.

The reactions using linoleic acid (polyunsaturated fatty acid), characterized by higher degree of unsaturation compared to oleic acid (monounsaturated fatty acid), were anticipated to yield a greater formation of hydroperoxide (HPODE) and subsequently increase in the conversion of VL to NK (78). However, the reactions using linoleic acid exhibited lower conversion compared to oleic acid, as depicted in **Table 8**. This would contradict the understanding that monounsaturated fatty acids are less readily oxidized than polyunsaturated fatty acids (77,78).

On the other hand, the comparison between the vegetable oils represented by data in **Table 8**, reveals that sunflower oil outperformed both canola and olive oil in the conversion of VL to NK from 1^{st} day to the 7^{th} day. This suggests that sunflower oil is the preferred vegetable oil for achieving a greater HPODE formation compared to the other two vegetable oils. Notably sunflower oil is comparatively rich in linoleic acid and deficient in oleic acid (**Table 7**). These findings aligns with the reports by *Pignitter et al.* who noted that sunflower oil exhibited a greater HPODE formation compared to canola oil after 7 days (77). Additionally, *Halvorsen et al.* reported that olive oil exhibited lower HPODE formation and secondary oxidation products (ketones and aldehydes) compared to sunflower oil (78). This implies that there is a complicating factor in these experiments, such as oxidation of the linoleic acid during storage.

Lastly, the reaction performed using anacardic acid (fatty acid), did not proceed (no GC peak detected for NK) as indicated in **Table 8.** *Kubo et al.* reported that anacardic acid acts as an inhibitor towards LOX enzyme by chelating the iron in the active site or by reducing the active ferric iron (Fe^{3+}) form to the inactive ferrous iron (Fe^{2+}) form of the enzyme (79). Moreover, the hydrophilic head portion of anacardic acid (a salicylic acid moiety), first binds to the active site of the enzyme, followed by the hydrophobic tail which interacts with the C-terminal domain where the iron is located (80). Anacardic acid normally acts as an antioxidant in numerous ways including inhibition of different pro-oxidant enzymes that are included in the production of the reactive oxygen species. Moreover, they can chelate transition metal ions, yet do not quench the reactive oxygen species. So, whenever the appropriate head portion is selected, scavenging activity could take place therefore the head portion appears to be the determining feature(79–81). As a result, the conversion of VL to NK did not occur.

Table 8: Evaluation of fatty acids and vegetable oils on LOX crude enzyme in the conversion of VL to NK with the addition of $FeSO_4.7H_2O$ and $MnSO_4$ at 60 ˚C.

Days	% Conversion					
	Oleic acid	Sunflower oil	Canola oil	Olive oil	Linoleic acid	Anacardic acid
0	0	0	0	0	0	0
1	1.91	1.30	0.00	0.00	2.36	0.00
2	1.78	6.97	3.33	4.57	3.44	0.00
3	16.28	11.47	9.32	6.32	3.73	0.00
4	19.32	15.75	9.23	9.17	-----	0.00
5	29.09	18.25	13.68	13.63	9.48	0.00
6	**43.67**	**22.15**	**15.85**	**18.53**	**10.36**	**0.00**
7	59.60	27.13	16.45	17.71	11.82	0.00

2.5.4 Impact of enzyme source from ground or defatted soya beans (GSB or MDS)

The LOX crude enzyme used in this study was sourced from soya beans and two types of distinct extracts were employed. The primary extract milled defatted soya

bean (MDS) which was crushed between two rollers was the predominant extract for assessing crude LOX activity throughout the study due to its advantages outlined in **section 2.3.** The secondary extract, ground soya bean (GSB) which was ground into flour by coffee grinder was only used for comparison with MDS due to its disadvantages outlined in **section 2.3**. The results presented in **Table 9** indicated that the conversions obtained from MDS for 2 days and 7 days were higher than the ones from GSB. Surprisingly, for a 5-day reaction GSB had a higher conversion than MDS. This observation suggested that the optimal reaction period for GSB might be 5 days since beyond this timeframe led to a decrease in the conversion of NK. On the other hand, MDS required more days for the reaction to give a higher conversion. As a result, more reactions and their replicates were required to justify the assumption made.

Table 9: The reactions using crude LOX enzyme extracted from MDS and GSB per number of days at 60 ˚C.

Days	%Conversion	
	GSB	MDS
2	1.79	2.6
5	14.06	8.90
7	1.65	29.87

Following the preliminary results shown in **Table 9**, we then conducted more comparative reactions for both GSB and MDS where both cases, $FeSO_4.7H_2O$ and $MnSO_4$ were added to enhance the enzyme activity. These results are displayed in **Table 10** where the % conversion of both the individual runs as well as average runs are reported. GSB had a higher average % conversion than MDS from the 1^{st} day to the 5^{th} day. However, on the 6^{th} and 7^{th} day MDS displayed a higher conversion than GSB. This trend was consistent in both the 1^{st} and 2^{nd} run together with their average conversions, confirming that after 5 days in GSB reactions, produced NK underwent over-oxidation to form nootkatone-11,12 epoxide. This was confirmed by GCMS analysis where nootkatone-11,12 epoxide peak was observed, and corresponding mass was obtained.

Table 10 *:* The two different runs and their average per day as results of GSB and MDS at 60 ˚C with the addition of $FeSO_4.7H_2O$ and $MnSO_4$ using a concentration of 2.64 mM respectively

Days	% Conversion in the presence of $FeSO_4.7H_2O$ and $MnSO_4$					
	GSB			MDS		
	1st run	2nd run	**Average**	1st run	2nd run	**Average**
0	0	0	**0**	0	0	**0**
1	11.29	10.72	**11.00**	1.91	10.33	**6.12**
2	20.33	22.24	**21.29**	1.78	18.45	**10.12**
3	26.38	25.67	**26.03**	16.28	25.04	**20.66**
4	30.77	27.42	**29.10**	19.32	30.10	**24.71**
5	33.50	43.35	**38.43**	29.09	32.59	**30.84**
6	32.35	44.96	**38.66**	43.67	36.95	**40.31**
7	27.86	47.48	**37.67**	59.60	46.16	**52.88**

Figure 24 displayed a direct linearity of the MDS reaction as percentage conversion increased with an increase in the number of days, while that using GSB halts after 5 days.

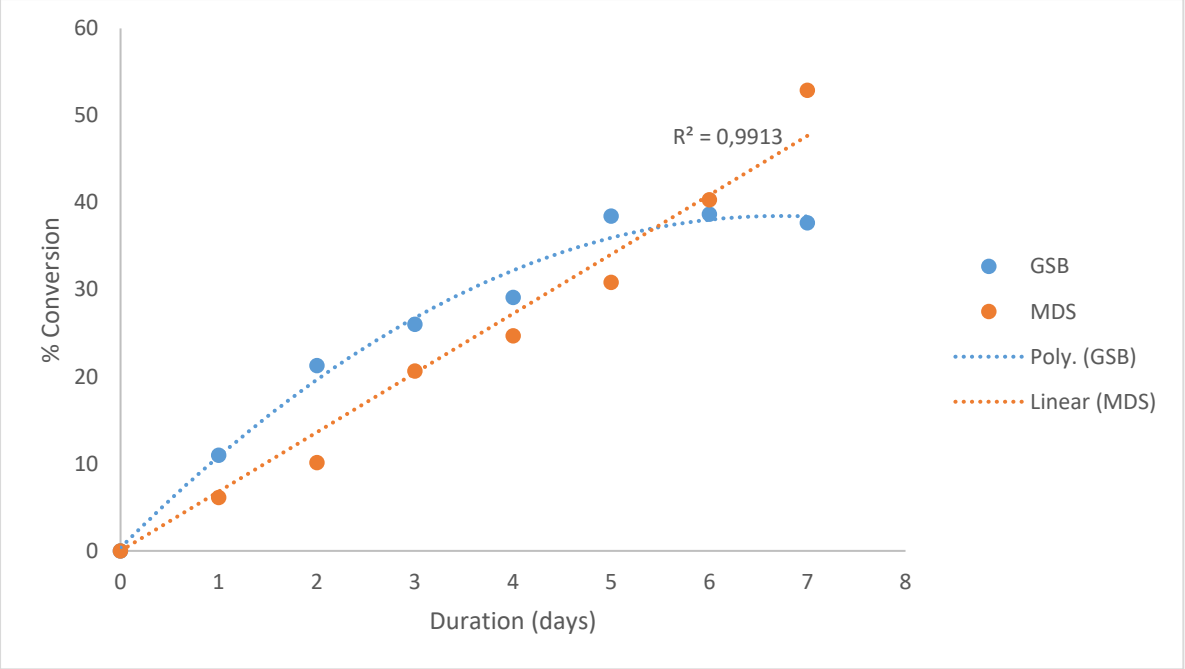

Figure 24*:* The VL conversion function of biocatalyst preparation (GSB and MDS) and time.

Mazumder et al. reported that defatting soya beans reduces the fat content since soya beans contain high protein and fat content (82). This observation agrees with studies conducted by *Khetarpaul et al.* (83). As a result, we suspect that the overoxidation of NK in GSB might be attributed to the high protein and fat content, resulting in the % conversion of NK decreasing with an increase in the number of days compared to MDS.

2.5.5 The influence of the enzyme extraction period.

The ground flour as outlined in **section 2.3** was typically left in a buffer for 18 hours (overnight) in a refrigerator at 4 ˚C. However, for comparison purposes, the flour was also soaked in a buffer for 60 hours (over the weekend). The main reason was to assess the effect of the duration of the flour soaking period on the activity of LOX crude enzyme. The data illustrated in **Table 11** presents the results conducted for 5 days for both MDS and GSB and 7 days for MDS. The LOX crude enzyme soaked for 18 hours (overnight) had a higher conversion compared to the one soaked for 60 hours (over the weekend) for both MDS & GSB reactions.

These results were confirmed by *Mazumder et al.* who reported the effect of soaking on the LOX activity for soya beans over 120 minutes. The reactions were monitored for 30, 60, 90 and 120 minutes and the results revealed that LOX was inhibited more after 120 minutes of soaking (120 > 90 > 60 > 30) than other time intervals (82). Additionally, *Makhubela* reported that buffers experience limitations such as a decrease in buffering capacity, formation of polyvalent cations, and/or the buffer acting as an inhibitor (55). As a result, the enzyme soaked for an extended period exhibited a lower conversion, which might be caused by the above-mentioned limitations.

Table 11*:* Effects of enzyme soaking duration on conversion.

Days	%Conversion	
	18 hours	60 hours
5 days (GSB)	14.06	7.16
5 days (MDS)	8.90	8.18
7 days (MDS)	29.87	15.17

2.6 Oxidation of other terpenes and related organic compounds.

Following the conversion of VL to NK, it became evident that other classes of compounds could potentially be oxidised under the same conditions used throughout in this study. As a result, we opted to investigate the oxidation of various terpenes present in the starting material containing VL and styrene.

2.6.1 Other terpenes

The starting material contained VL and other terpenes, which could also be involved in oxidation reactions. Among the observed terpenes on the GCMS, caryophyllene caught our attention. As a result, we sought to determine whether caryophyllene (CP) could undergo oxidation to form caryophyllene oxide (CPO) (**Figure 25)** under the same conditions used in the conversion of VL to NK. To our delight, the oxidation occurred, and this aligns with the work of *Fidyt et al.* who reported that caryophyllene oxide is an oxidation derivative of caryophyllene, which occurs naturally in various plants (84). Moreover, caryophyllene oxide is a sesquiterpene similar to VL and it is

capable of altering numerous important pathways of cancer development (45,84). Additionally, it has pharmacological potentials such as anti-cholinesterase, analgesic, local anaesthetic, anti-inflammatory, anti-fungal activities and can be used as a natural insect repellent (85,86). Caryophyllene oxide is well-known as preservative in cosmetics, food, and drugs, which has been tested in vitro as an antifungal against dermatophytes (87). This oxygenated terpenoids can also be found in cloves, lemon balm, basil, hops, black pepper, oregano, and rosemary (86). The oxidation of caryophyllene-to-caryophyllene oxide had a remarkable 56.98% conversion at 60 ˚C with the addition of $FeSO_4.7H_2O$ and $MnSO_4$. This observation has not been previously reported in the literature, resulting in a novel reaction.

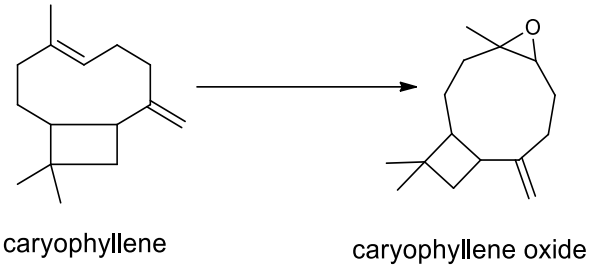

Figure 25*:* The oxidation of caryophyllene.

Figure 26 shows GC chromatogram which displays the elution of VL, CPO and NK on a crude sample mediated by LOX.

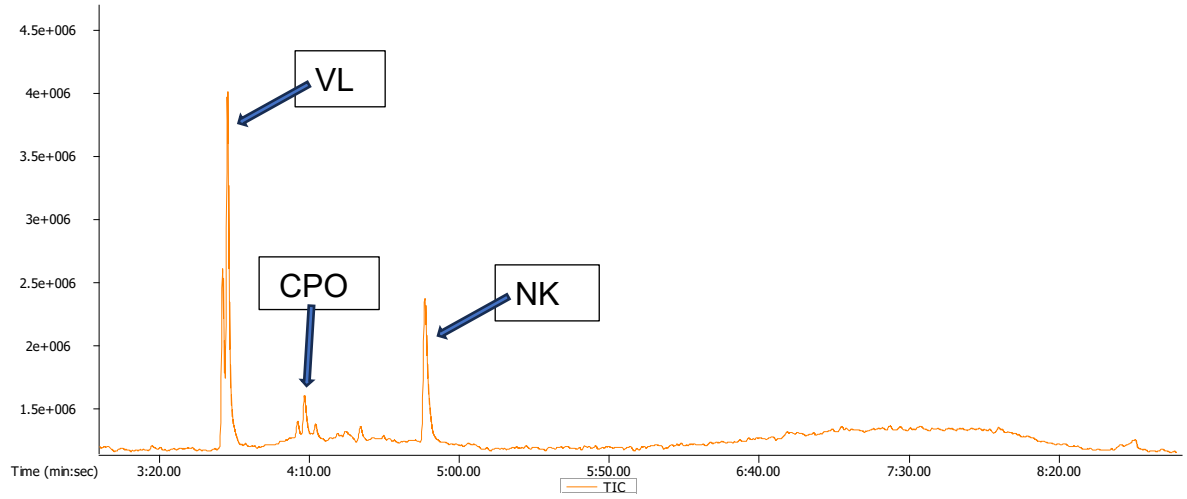

Figure 26*:* GC chromatogram of caryophyllene oxide (CPO).

2.6.2 Styrene

After being contented with the formation of caryophyllene oxide from the oxidation of caryophyllene as a consequence of using LOX in the NK reaction, we studied the potential conversion of styrene into its ketone, aldehyde, carboxylic acid, or ester products through an oxidation reaction, thereby evaluating the application of LOX in organic synthesis. Previous study by *Nickerson et al.* used $CYP450_{cam}$ mutant for styrene oxidation, resulting in benzaldehyde and styrene oxide, which serves as intermediates for several products (88). However, most of studies report the use of catalysts such as cobalt acetate, hydrogen peroxide, tery-butyl hydroperoxide and others (89,90).

The oxidation of styrene under the same conditions as VL in **Section 2.4** was carried out, and we anticipated the formation of benzaldehyde and styrene oxide similar to the study of styrene reported. However, the reaction resulted in the formation of benzoic acid, 1-phenylethane-1,2-diol, and 2-hydroxy-2-phenylethyl benzoate rather than the desired benzaldehyde and styrene oxide, as shown in **Table 12**. *Gazu et al.* reported that over-oxidation of styrene oxide and benzaldehyde using metal catalysts such as nickel and copper resulted in compounds such as 1-phenylethane-1,2-diol, phenylacetaldehyde, benzoic acid, and acetophenone (91). As a result, we assume that in our reaction, the formation of styrene oxide resulted into 1-phenylethane-1,2-diol via epoxide ring opening and that the benzaldehyde was readily converted to benzoic acid.

Table 12: The intermediates resulting from the oxidation of styrene as determined by gas chromatography.

	% Conversion	
Compounds	2^{nd} day	5^{th} day
Benzoic acid	6.38	12.34
1-phenylethane-1,2-diol	2.40	------
2-hydroxy-2-phenylethyl benzoate	-----	6.43

The proposed biosynthetic pathway is indicated in **Scheme 11**. Moreover, the combination of 1-phenylethane-1,2-diol and benzoic acid underwent esterification, resulting in the formation of 2-hydroxy-2-phenylethyl benzoate and water. This ester formation from styrene oxidation has not been previously reported, providing a novel enzymatic reaction.

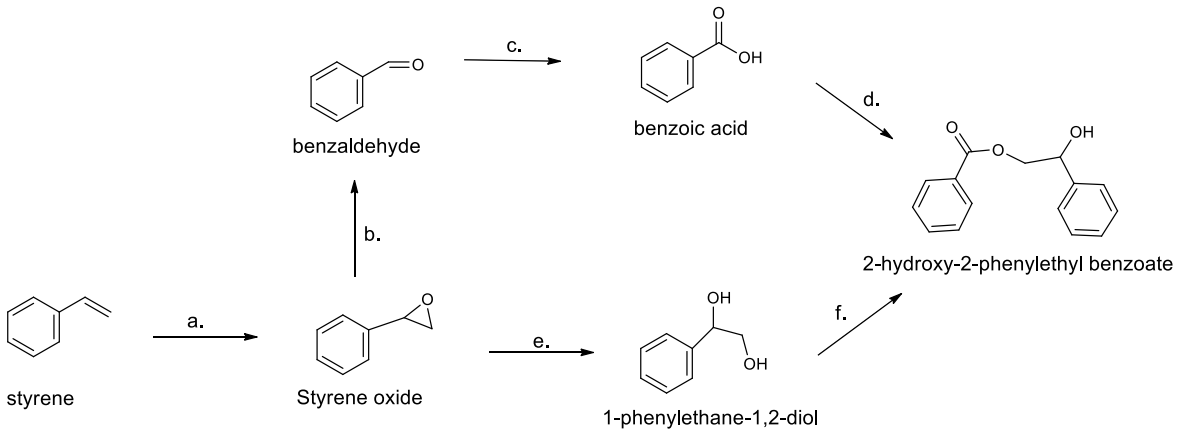

Scheme 11*:* Proposed biosynthetic pathway of the intermediates made from styrene with a-f representing different steps of the reaction.

Figure 27 shows GC chromatogram which displays the elution of benzoic acid, 1-phenylethane-1,2-diol, and 2-hydroxy-2-phenylethyl benzoate on a crude sample mediated by LOX.

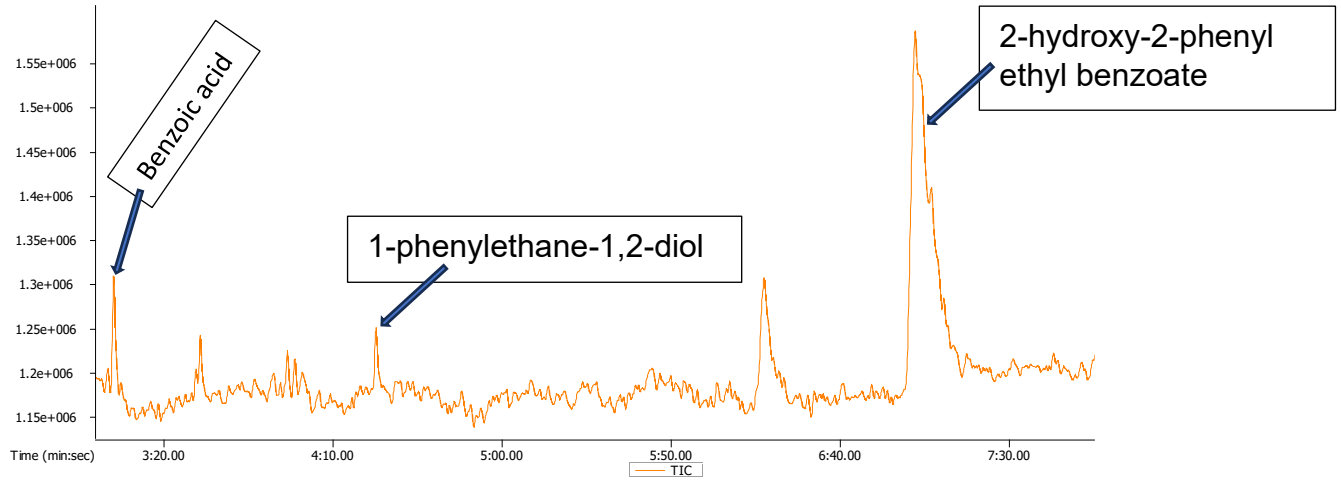

Figure 27*:* GC chromatogram for the styrene oxidation.

2.7 Cytochrome P450 (CYP450)

Satisfied with our results on LOX mediated conversion of VL to NK, we now turned our attention to explore other oxidative enzymes that may perform the same conversion, in particular Cytochrome P450. The conversion of VL to NK using wild-type CYP450 enzyme sourced from *Pseudomonas putida*, and *Bacillus megaterium,* has previously been demonstrated but has shown some inhibitory effects, given that NK is known to inhibit CYP450 (92). As a result, CYP450 enzymes are normally subjected to engineering via site-directed mutagenesis to facilitate the oxidation of VL to NK. This approach was adopted because it is unlikely for NK to inhibit all engineered CYP450 variants (92). In this study, we used two distinct 18-well plates containing unique enzymes, namely PRO-HT-P450-40x (Prozomix) and CoE-P450P (Codexis) to assess, develop, optimise, and identify the high-performance mutants for the efficient oxidation of VL to NK. Each well in these plates contained a unique type of mutant for the CYP450 enzyme.

2.7.1 PRO-HT-P450-40x plate (Sourced from Prozomix)

In literature, the oxidation of VL to NK using various CYP450 mutants has successfully been performed (40,93,94). In this study, we adopted the reaction conditions using CYP450 sourced from Prozomix. The reaction mixture contained NADPH (26 mg, 0.0349 mmol) as a redox cofactor, initiating the reaction by facilitating the transfer of an electron to molecular oxygen. Potassium phosphate buffer (pH 7.2, 100 mM) was incorporated to establish an aqueous phase and maintain the pH for the reaction. The reaction was kept at 37 ˚C with an oxygen inlet to create an oxygen environment, as this plays an important role given the oxidation nature of the reaction. This reaction proceeded for 5 days, followed by extraction with ethyl acetate and the solvent was removed in *vacuo*.

Subsequent reactions were performed using various mutants of the CYP450 enzyme from the above-mentioned plate. Each well contained a different mutant, generating data showing their effect on the conversion of VL to NK. **Table 13** reveals that for all three mutants, the 2nd day exhibited higher conversion compared to the 1st and 5th day,

suggesting that the optimal period for CYP450 enzyme might be 2 days. Additionally, wells D1 and A2 had no activity on the 1st day and well D2 showed no activity on the 5th day. These results showed how CYP450 fluctuated in a short period, influencing the reaction positively or negatively depending on how the progress of these reactions was monitored.

Table 13*:* Evaluation of mutants of CYP450 from PRO-HT-P450-40x plate in the conversion of VL to NK*.*

Days	%Conversion		
	Well D1	Well A2	Well D2
1	0.00	0.00	7.54
2	16.70	1.87	16.33
5	0.031	0.025	0.00

Figure 28 shows a GC chromatogram that displays the elution of VL and NK on a crude sample mediated by CYP450.

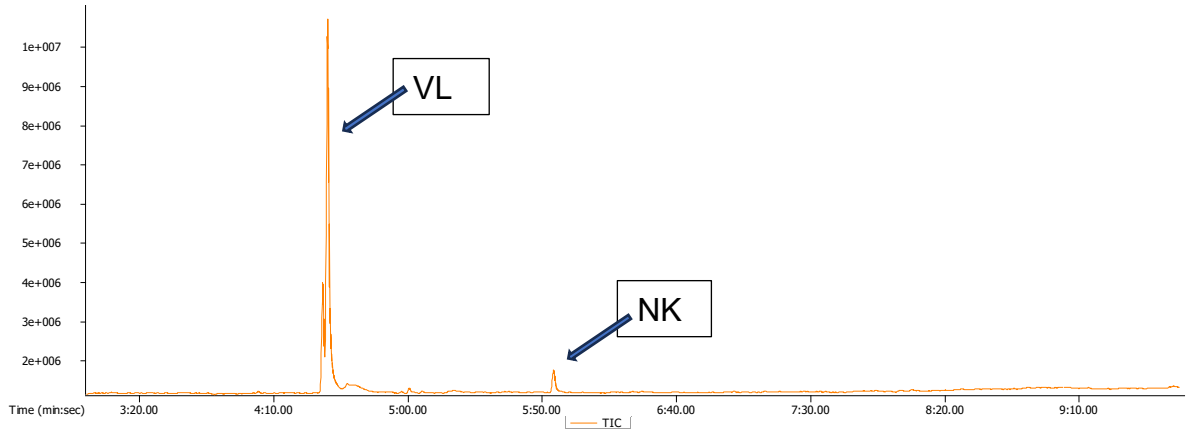

Figure 28*:* GC chromatogram for crude product of NK using CYP450 as catalyst.

Based on the observations made from **Table 13**, we decided to proceed with CYP450 reactions for 2 days, aiming to identify the mutants with higher activity compared to others and optimise the CYP450 enzyme. The data presented in **Table 14** outlines that mutants from wells D1 and D2 had the highest conversions of 16.70% and 16.33% respectively, surpassing other mutants in different wells. On the other hand, mutants from wells A1 and B2 showed no enzymatic activity. Some studies suggests that the

reason for the absence of VL oxidation activity might be due to the enzyme's active site's inability to accommodate the substrate, particularly larger or more hydrophobic molecules (92).

Table 14*:* Various mutants of CYP450 from PRO-HT-P450-40x plate in the conversion of VL to NK from different wells ran for 2 days.

Enzyme variant	%Conversion			
	1	2	3	4
A	0.0	1.87	0.81	0.72
B	0.41	0.0	----	0.77
C	0.34	3.78	1.02	0.81
D	16.70	16.33	0.55	0.67

2.7.2 CoE-P450P plate (Codexis)

The successful conversion of VL to NK using CYP450 from Prozomix, as evident from the data in **Table 14**, prompted us to use CYP450 from Codexis with the same reaction conditions. The main reason was to assess the activity of various mutants from different CYP450 enzymes in attempt to enhance the conversion of VL to NK. The reactions were conducted for 2 days, however the wells contained 2 mg of CYP450 in each well. The data from **Table 15** indicates that the mutants from well B3 had the highest conversion of 3.60%, outperforming mutants from other wells. On the other hand, the mutants that had the lowest conversion was from well C1 with 0.48%. The difference in the conversion which determines the enzyme's activity of the mutants is within the same range in most enzyme variants depicted in **Table 15**, which is between 0.78 -1.93 % and such results are expected as the mutants are from the same enzyme engineered differently. In this study, a notable limitation was that we could not identify the specific enzyme in each well, despite repetitively inquiring for clarification to suppliers.

Sowden et al. reported the conversion of VL to NK mediated by engineered $CYP450_{cam}$ and $CYP450_{BM-3,}$ achieving the highest conversion of 47% and 7.7% for NK respectively, showing a significant difference in % conversion between the two mutants (40). These two CYP450 were from two different sources, namely *Pseudomonas putida*, and *Bacillus megaterium,* which resulted in different activities and regioselectivities hence their difference in % conversion. Similarly, the CYP450 enzyme used in our study, sourced from Prozomix and Codexis achieved highest conversion of 16.70% and 3.60% respectively. This variance in CYP450 sources might explain the differences in their % conversion similar to CYP450cam and $CYP450_{BM3}$. The low conversion of VL to NK has previously been reported with CYP450 from various sources, showing a high activity with low regioselectivity leading to multiple products, where nootkatol was dominant over nootkatone (51,93,95). Additionally, *Wriessnegger et al.* have identified and overexpressed endogenous alcohol dehydrogenase, which has the capacity to overcome this shortcoming by enhancing the formation of NK from nootkatol (96). However, the results in our study did not detect the GC peak for nootkatol.

Table 15*:* Evaluation of different mutants of CYP450 from CoE-P450P plate in the conversion of VL to NK ran for 2 days.

Enzyme variant	%Conversion		
	1	2	3
A	0.78	1.35	1.21
B	1.00	0.84	3.60
C	0.48	1.14	-----
D	-----	1.23	1.93

2.7.3 Fatty acid study (acts as a substrate)

The CYP450 enzymes are known to be involved in the hydroxylation reaction of unsaturated fatty acids, exhibiting both α- and β-hydroxylation capabilities (97,98).

Additionally, these enzymes participates in the biosynthesis of secondary metabolites such as terpenoids through fatty acids (98). Therefore, we expected the fatty acids to be converted and participate in the oxidation of VL to NK. As a result, we conducted three reactions using CYP450 from Prozomix, similar to the ones displayed in **Table 14.** These reactions involved three different mutants, to explore the impact of fatty acids on CYP450 enzyme activity hence unsaturated fatty acid (oleic acid) was added. Unfortunately, the conversion of VL to NK was unsuccessful, as NK was not detected by TLC, GCMS, and H^1NMR. **Figure 29** shows GC chromatogram which displays the elution of VL with the absence of NK elution from a crude sample using unsaturated fatty acid (oleic acid) and CYP450. Moreover, due to limited plates of CYP450 mutants, we could not proceed with CYP450 research.

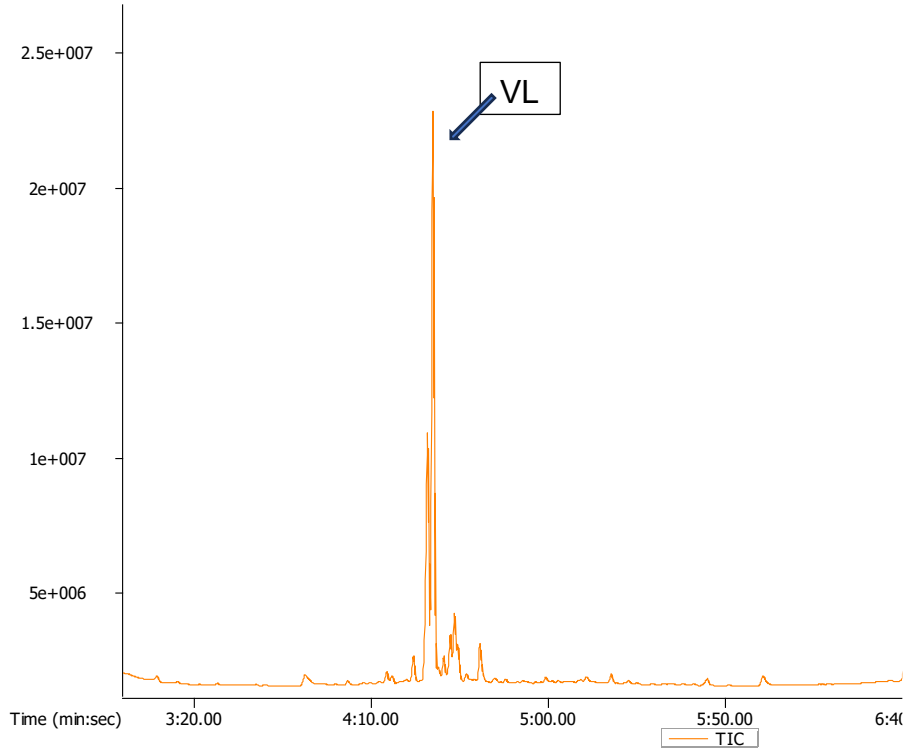

Figure 29: GC chromatogram of a reaction in the conversion of VL to NK using oleic acid on CYP450.

2.8 Laccase Enzyme Activity

We explored the use of Laccase enzyme for the biotransformation of VL. The method was extracted from a patent by *Hueng et al*. using laccase sourced from *Botrytis*

cinerea and *Trametes versicolor,* demonstrating successful production of NK with conversion of 59.13% with the use of ferulic acid as the mediator (59).

Inspired by this approach, the oxidation of VL to NK was conducted using laccase obtained from *Novoprime* Base 268. The reaction was performed in a citrate buffer with a pH 3.5, 100 mM to maintain the pH of the reaction. Ferulic acid was used as a mediator to enhance enzyme activity with a concentration of 5 mM, while tween-80 served as an emulsifier to prevent the separation of oil and water components. The reaction proceeded for 24 hours at room temperature (22 ± 3 °C) and in the presence of the oxygen source. This latter plays a vital role in oxidation reactions. To stop the reaction, the pH was increased to 9 using sodium carbonate (Na_2CO_3), followed by heating the mixture to 80 ˚C for 2 hours to attempt the degradation of valencene hydroperoxide to the desired product NK (59). The laccase enzyme's activity was evaluated further through different parameters:

2.8.1 Variation of mediators

Different mediators were assessed, including ferulic acid and salicylic acid. However, none exhibited any impact or enhancement on the oxidation of VL to NK, rendering the reaction unsuccessful.

2.8.2 Amounts of the buffer or enzyme

The amounts of the buffer or an enzyme were either halved or doubled independently to assess their effects on the formation of NK from VL.

2.8.3 Variation of terminal temperature

The post-reaction heating aimed to facilitate the degradation of valencene hydroperoxide into nootkatone. Temperatures of 80 ˚C and 90 ˚C were evaluated, both for 2 hours and, for comparison, 4 hours.

Despite exploring these parameters, the laccase-catalyzed oxidation of VL to NK was unsuccessful. Due to the absence of a GC peak in the GCMS results (**Figure 30**) and NK spot on the TLC plates indicated that the laccase enzyme could not oxidize VL to NK. However, we were able to break the emulsion by increasing the temperature of the reaction from 80 ˚C to 90 ˚C.

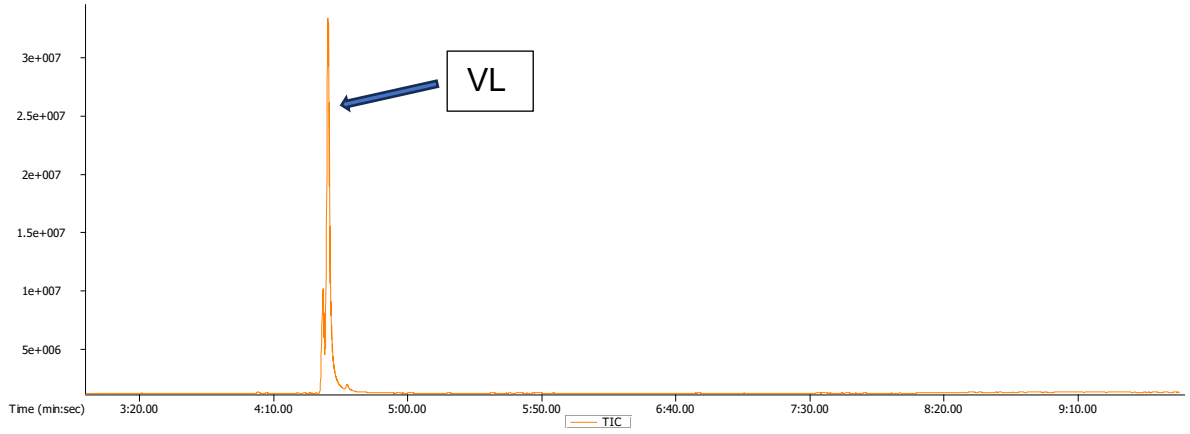

Figure 30: GC chromatogram for a reaction in the conversion of VL to NK using laccase.

CHAPTER 3

CONCLUSIONS AND RECOMMENDATIONS

This study focused on the biocatalysis-mediated oxidative conversion of valencene (VL) to nootkatone (NK) and evaluating factors affecting the activity of enzymes used to mediate the conversion.

Three catalytic options were explored for this conversion, each using an oxidative biocatalyst (lipoxygenase, cytochrome P450, and laccase)

Lipoxygenase (LOX):

The extraction method for LOX on both milled defatted soya beans (MDS) and ground soya beans (GSB) was successful and played an important role in the oxidation of VL to NK. This was because both extracts led to reasonable conversions ranging from 6.12 - 52.88 % conversions (mol/mol) at 60 ˚C with the addition of $FeSO_4.7H_2O$ and $MnSO_4$. after 7 days. However, GSB had some drawbacks such as the reactions formed a heavy emulsion that proved difficult to break; whereas MDS reactions formed an emulsion that was easily broken. Moreover, although GSB showed a higher conversion up to the 5^{th} day, it was then overtaken by the MDS reactions, probably due to the over-oxidation of NK in the GSB catalysed reactions to form nootkatone-11,12-epoxide.

Throughout our study, crude LOX was extracted by an overnight (18 hour) soak as the enzyme solution showed better results compared to when it was soaked over the weekend (60 hours) for both MDS and GSB. After the biocatalytic reaction, purification and characterisation of NK were performed and the structure of NK was unambiguously confirmed through techniques such as column chromatography, TLC, ^{1}H NMR, ^{13}C NMR, DEPT13, GCMS, and HPLC.

The investigation of factors affecting the activity of the soya bean LOX was revealed valuable information. The effects of metal ions on the reaction were assessed. Metal ions Fe^{2+} and Mn^{2+} were evaluated independently, however, their effects did not materialise as expected. As a result, combinations of the two metal ions were evaluated, as it was believed that the two metal ions may play two different roles. Fe^{2+} forms part of the soya bean LOX active site, as it is an iron-centred enzyme while Mn^{2+} is not part of the soya bean LOX active site. The two metal ions at concentrations of 2.64 mM enhanced the activity of the enzyme, but only in the presence of the sulphate counter ion.

When the reaction temperature was evaluated, it was found that there were low % conversions of 0.9 at 80 and 90 ˚C, probably due to enzyme thermal instability. Reactions performed at 70 ˚C exhibited slightly higher conversion rates than those at 60 ˚C ranging from 6.18 – 55.00 % conversions (mol/mol).

In assessing the effects of different fatty acids, oleic acid had the best results as compared to linoleic acid, vegetable oils (canola, olive, and sunflower oil), and anacardic acid. Even though polyunsaturated fatty acid (linoleic acid) was expected to have better results than monounsaturated fatty acid (oleic acid) due to a higher degree of unsaturation, our study indicated otherwise; however the linoleic rich sunflower oil outperformed both oleic acid rich canola and olive oil. On the other hand, anacardic acid did not mediate the reaction and may have inhibited MDS crude LOX. In conclusion, the soya bean crude LOX enzyme has successfully mediated the conversion of VL to NK which was one of the main aims of this study.

In addition, the terpene caryophyllene present in the crude valencene extract was oxidized to caryophyllene oxide. Lastly, the crude LOX proved that it could mediate the oxidation of styrene, resulting in benzoic acid and 1-phenylethane-1,2-diol, which further reacted through esterification to form 2-hydroxy-2-phenylethyl benzoate. This is to the best of our knowledge the first time that such results have been reported, and this indicates the broader potential of LOX to undertake other biotransformations.

Other oxidative enzymes:

In assessing whether CYP450 could facilitate the oxidation of VL to NK, mutants (D1 and D2) from the PRO-HT-P450-40x plate (sourced from Prozomix) showed activity. Mutants from the CoE-P450P plate (sourced from Codexis) performed poorly as compared to the mutants from the PRO-HT-P450-40x plate in the conversion of VL to NK. Monounsaturated fatty acid (oleic acid) was also assessed with the aim to enhance the activity of the CYP450 enzyme. However, the oleic acid unexpectedly showed some inhibitory effects towards the enzyme. In conclusion, some of the CYP450 variants sourced from Prozomix successfully mediated the conversion of VL to NK. Prozomix CYP450 variants D1 and D2 exhibited the highest activity at >16% conversion. Further improvements may be possible through reaction optimisation.

The laccase enzyme from Novoprime base 268 did not show any activity for the oxidation of VL to NK.

In conclusion, the overall objectives of the research project were achieved, and new scientific information was generated that could lead to other applications of LOX-mediated biocatalytic conversion of other terpenes. It is also evident from the oxidation of styrene we reported that LOX may have other applications in oxidative organic synthesis reactions.

Recommendation

In our study, sunflower oil served as a better mediator than other vegetable oils in combination with crude LOX. Therefore, more research should be undertaken to optimise this reaction due to its cost-effectiveness compared to oleic acid. Moreover, manganese-centred LOX should be assessed in the oxidation of VL to NK and compare its activity to the iron-centred LOX which was already assessed in this study.

The CYP450 variants from wells D1 and D2 in the PRO-HT-P450-40x plate sourced from Prozomix should be identified and the reactions optimised through evaluation of parameters such as temperature, pH (7.0 to 7.5), different buffer solutions, and others. The effects of metal ions such as Fe^{2+}, $Ca^{2+,}$ and Mn^{2+} enhanced the activity of metal-centred LOX. Therefore, the same metal ions should be used to assess their effects on the metal-centred CYP450 enzyme. Further optimisation of the enzyme itself would be possible through protein engineering. For laccase reactions, varying the the pH and/or mediator or their concentrations may have an effect. Laccase from *Cerrena unicolor* and *Trametes versicolor* should be assessed under the same conditions tested and be compared to laccase from *Novoprime Base 268*.

CHAPTER 4

METHODS AND MATERIALS

4.1 GENERAL PROCEDURES

The chemicals used were purchased from Sigma-Aldrich, or Merck (South Africa) unless stated otherwise.

4.2 CHEMICALS

Solvents used were ethyl acetate (EtOAc), dichloromethane (DCM), HPLC grade methanol (for GC-MS analysis), hexane, and deuterated chloroform (for NMR analysis). Hexane, dichloromethane, and ethyl acetate were distilled before use to remove unwanted materials, and others were used without further purification. Oleic acid (98% purity), linoleic acid, nootkatone (>98% purity), valencene (54.04% GC purity) v/v from Evolva (USA), tween-80, laccase (>98% purity) from *Novoprime* base 268, sunflower oil, canola oil, olive oil, styrene, and cytochrome p450 (PRO-HT-P450-40x plate were obtained from Prozomix and CoE-P450P plate from Codexis). Salts used were NaCl, NaOH, K_2CO_3, Na_2CO_3, $MgSO_4$, Na_2SO_4, KOH, calcium anarcaolate, citric acid monohydrate, trisodium citrate dihydrate, salicylic acid, ferulic acid, potassium dihydrogen phosphate, $FeSO_4.7H_2O$, $FeSO_4$, $MnSO_4$, $MnCl_2.4H_2O$, $CuSO_4.5H_2O$, $CuCl_2.2H_2O$, $CaCl_2.\ 2H_2O$ and boric acid. The milled defatted soya beans and ground soya beans were obtained from Seeds for Africa (South Africa).

4.3. SPECTROSCOPY AND PHYSICAL DATA

4.3.1. Nuclear Magnetic Resonance (NMR)

Nuclear magnetic resonance (NMR) spectra were recorded on either a Bruker AVANCE 300 MHz or a Bruker lll 500 MHz spectrometer. All spectra were recorded in chloroform-*d.* All chemical shift values are reported in parts per million referenced against trimethylsilane which is given an assignment of zero parts per million. Coupling constants (*J*-values) are given in Hertz (Hz)

4.4 CHROMATOGRAPHY

Normal chromatography was performed with silica gel 60 (Macherey-Nagel, particle size 0.063-0.200 mm) adsorbent, with both isocratic and gradient eluent systems being employed. Thin layer chromatography (TLC) of the compounds was executed on Macherey-Nagel Alugram Sil G/UV254 plates pre-coated with 0.25 mm silica gel 60 with a solvent system of 20% ethyl acetate and 80% hexane. The TLC plates were viewed under UV light (254 nm and 366 nm).

4.4.1 Gas chromatography (GC)

Gas chromatography (Agilent 7890B) with a GERSTEL MPS-2 auto-sampler and coupled to a Leco® Pegasus 4D time-of-flight mass spectrometry (ToF/MS) system was used to perform GC analysis. The 29.687 m × 0.25 mm × 0.25 µm Rxi-5Sil (Restek) primary column and 1 m × 0.25 mm × 0.25 µm Rxi-17Sil (Restek) secondary column made of 5% diphenyl/dimethyl polysiloxane was used to separate the compounds in the queued sample. The spectra acquisition rate, flow rate, and temperature program were adjusted to help optimise the analyte separation and detection methods. Due to the modification made above, the method below was followed:

A 1 µL splitless injection with carrier gas helium at 1.4 mL/min continuous flow rate whereby the GC primary oven was programmed at 50 ˚C (0.2 min), then 20 ˚C/min to 280 ˚C (1 min) which was the target temperature, and the secondary oven program was +5 ˚C offset with respect to the primary oven. The transfer line and front inlet temperatures were 280 ˚C and 200 ˚C respectively. The described method took 9 minutes and 29 seconds to complete the run. The temperature of the ion source was 200 ˚C while the modulator was off. The mass spectrometer acquisition rate was 10 spectra per second at a set mass range of 25-450 m/z. The Leco ChromaTOF software and NIST library were used for data processing and peak identification (55).

4.5 SAMPLE PREPARATION

4.5.1 NMR

For NMR analysis, each product isolated in the form of oil was dissolved in deuterated chloroform before analysis.

4.5.2 GC-MS

Every oil sample was dissolved in HPLC grade MeOH and the concentrations of 10-200 ppm, then diluted as needed. The standard curve of NK was prepared in a range of 25-200 ppm as displayed in **Appendix, Figure 34**.

4.6 Enzyme extraction method

Lipoxygenase enzyme (LOX) Extraction:

Ground soya bean (GSB) was prepared by being crushed into a coarse meal using a coffee grinder while milled defatted soya bean (MDS) was supplied in a defatted coarse meal texture by Seeds for Africa. Moreover, 20% (w/v) of the coarse meal or flour was then suspended in a sodium borate buffer (pH 8.5, 100 mM) and the soaked sample was placed on a magnetic stirrer at room temperature (22 ± 3 ˚C) for the sample to mix properly. The sample was left in a refrigerator (4 ˚C) with no form of agitation, overnight (18 hours) and some over the weekend (60 hours) depending on the type of study performed.

4.7 Biocatalytic reaction procedures

4.7.1 LOX enzyme activity

4.7.1.1 The standard reaction (MDS)

Method A

The preparation of sodium borate buffer (pH 8.5, 1 M) was through the addition of boric acid (61.83 g) and NaOH (10 g) to 800 ml of distilled water in a 1 L beaker then continued adding distilled water until the volume was 1 L. However, the crude LOX

enzyme works best at 100 mM buffer therefore 1 M was diluted to 100 mM via $C_1V_1=C_2V_2$.

A mixture containing (1.8 g, 45.003 mmol) of 10% (w/v) aqueous NaOH-solution, (5 g, 24.47 mmol) of valencene, and (2 g, 7.08 mmol) of monounsaturated fatty acid (oleic acid) was gently stirred in a round bottom flask which was placed inside an oil bath on a magnetic stirrer and an oxygen inlet (used balloon filled with oxygen). A solution of 100 ml crude LOX enzyme (MDS soaked in sodium borate buffer at pH 8.5, 100 mM overnight) was added, and the stirring was increased. The reaction temperature was maintained at 60 ˚C. The reaction took 7 days, and a small sample was taken every day to monitor the progression of the reaction which was worked up by extraction with ethyl acetate, then drying with dried with Na_2SO_4, and concentrated under a vacuum worked up using rotary evaporation at 60 ˚C (64).

WORK UP PROCEDURE

After 7 days, the reaction mixture was extracted using EtOAc (2 x 50 ml), then washed using 10% (w/v) aqueous NaOH-solution (2 x 50 ml) and neutralised with brine (2 x 50 ml) in a separatory funnel. The anhydrous $MgSO_4$ was used as a drying agent for the organic layer followed by concentration of the organic layer under a vacuum using rotary evaporation.

4.7.1.2 The study of salts

The same procedure as **method A** was adopted using a wide spread of salts such as $FeSO_4.7H_2O$, $FeSO_4$, $MnSO_4$, $MnCl_2.4H_2O$, $CuSO_4.5H_2O$, $CuCl_2.2H_2O$, and $CaCl_2.2H_2O$ were prepared as sources of Fe^{2+} and Cu^{2+}, $Ca^{2+,}$ or Mn^{2+} each at a mass of 0.05 g. As a result, we initially added $FeSO_4.7H_2O$ (0.05 g, 0.1798 mmol) alone, followed by its combination with $MnSO_4$ (0.05 g, 0.331 mmol) or $MnCl_2.4H_2O$ (0.05 g, 0.2605 mmol) or $CuCl_2.2H_2O$ (0.05 g, 0.2933 mmol) or $CuSO_4$. $5H_2O$ (0.05 g, 0.2602 mmol) or $CaCl_2.2H_2O$ (0.05g, 0.3401 mmol) and $FeSO_4$ (0.05 g, 0.3291 mmol) with $MnSO_4$ (0.05 g, 0.331 mmol).

Method B

A mixture containing (1.8 g, 45.003 mmol) of 10% (w/v) aqueous NaOH-solution, (5 g, 24.47 mmol) of valencene, (0.05 g, 0.1798 mmol) $FeSO_4.7H_2O$, (0.05 g, 0.331 mmol) $MnSO_4$, and (2 g, 7.08 mmol) of monounsaturated fatty acid were gently stirred in a round bottom flask which was placed inside an oil bath on a magnetic stirrer and an oxygen inlet (used balloon filled with oxygen). A solution of 100 ml crude LOX enzyme (MDS soaked in sodium borate buffer at pH 8.5, 100 mM overnight) was added, and the stirring was increased. The reaction temperature was maintained at 60 ˚C. The reaction took 7 days, and a small sample was taken every day to monitor the progression of the reaction which was worked up by extraction with ethyl acetate, then drying with dried with Na_2SO_4, and concentrated under a vacuum worked up using rotary evaporation.

WORK UP PROCEDURE

After 7 days, the reaction mixture was extracted using EtOAc (2 x 50 ml), then washed using 10% (w/v) aqueous NaOH-solution (2 x 50 ml) and neutralised with brine (2 x 50 ml) in a separatory funnel. The anhydrous $MgSO_4$ was used as a drying agent for the organic layer followed by concentration of the organic layer under a vacuum using rotary evaporation.

Reactions using **Method B** was adopted; however, $FeSO_4.7H_2O$ (0.05 g, 0.1798 mmol) and $MnSO_4$ (0.05 g, 0.331 mmol) were assessed separately, followed by the combination of $FeSO_4.7H_2O$ (0.05 g, 0.1798 mmol) with $MnCl_2.4H_2O$ (0.0655 g, 0.331 mmol), or $CaCl_2.2H_2O$ (0.0606 g, 0.331 mmol) and $FeSO_4$ (0.027 g, 0.1798 mmol) with $MnSO_4$ (0.05 g, 0.331 mmol).

4.7.1.3 Temperature study

The same procedure as **method A** was adopted and the reaction took 2 days; however, the reaction temperature was either kept at 60, 70, 80, or 90 ˚C. Similarly,

method B was adopted, but the reaction temperature was kept at 60 and 70 ˚C, as we then decided to carry out prolonged reactions at these two optimal temperatures.

4.7.1.4 Fatty acid study

The same procedure as **method B** was adopted; however, the reaction used different fatty acids such as linoleic acid, anacardic acid, and vegetable oils (olive oil, canola oil, and sunflower oil). The anacardic acid was liberated through the digestion of calcium anarcaedate, where 6 g of calcium anarcaedate was dissolved in 150 ml of 20% (v/v) aqueous HCL solution in a round bottom flask, which was placed inside an oil bath on a magnetic stirrer and 150 ml of ethyl acetate was introduced into the solution and left to stir overnight. In a separatory funnel, the solution was extracted using EtOAc (3 x 50 ml) and then washed using brine (3 x 50 ml). The $MgSO_4$ was used as a drying agent for the organic layer followed by concentration of the organic layer under a vacuum using rotary evaporation.

4.7.1.5 Different soya bean extractions

The same procedure as **methods A** and **B** was adopted; however, the reaction used LOX crude enzyme extracted from ground soya bean (GSB).

4.7.1.6 Enzyme soaking period

The same procedure as **method A** was adopted; however, the MDS and GSB were soaked over the weekend (60 hours).

4.7.1.7 Another related organic compound

The same procedure as **method B** was adopted; however, the valencene was replaced by styrene.

4.7.2 Cytochrome P450 enzyme

4.7.2.1 PRO-HT-P450-40x plate (Sourced from Prozomix)

Method C

A mixture containing (68 mg, 0.3327 mmol) of valencene, (26 mg, 0.0349 mmol) of NADPH, (5 mg) of CYP450, and 7 ml of potassium phosphate buffer at pH 7.2, 100 mM was gently stirred in a round bottom flask which was placed inside an oil bath on a magnetic stirrer and an oxygen inlet (used balloon filled with oxygen). The reaction temperature was kept at 37 ˚C throughout. The reaction took 5 days, and a small sample was taken every day to monitor the progression of the reaction (40,93,94).

WORK UP PROCEDURE

After 5 days, the crude reaction mixture was extracted using (2 x 25 ml) of EtOAc in a separatory funnel. The anhydrous $MgSO_4$ was used as a drying agent for the organic layer followed by concentration of the organic layer under a vacuum using rotary evaporation.

METHOD D

The progress of **Method C** proved that 2nd day exhibited higher conversion compared to the 5th day for several reactions, suggesting that the optimal period for CYP450 enzyme might be 2 days. Hence, **Method D** was implemented, following **Method C** where CYP450 reactions were run for 2 days going forward.

4.7.2.2 Fatty acid study (acts as a substrate).

The same procedure as **method D** was adopted; however, (28 mg, 0.099 mmol) of oleic acid was added to the reaction.

4.7.2.3 CoE-P450P plate (Sourced from Codexis)

The same procedure as **method D** was adopted; however, the reaction used 2 mg of CYP450 enzyme since each well of this plate contained 2 mg of the enzyme.

4.7.3 Laccase

Method E

REACTION SETUP

The preparation of citrate buffer (pH 3.5, 100 mM) was through the addition of citric acid monohydrate (12.61 g) and trisodium citrate dihydrate (14.70 g) to 600 ml of distilled water in 1 L beaker.

The mediator used in this reaction was ferulic acid which was prepared at a concentration of 5 mM according to the patent by Huang and colleagues (2001, patent No. US 6,200,786 B1). In this experiment, a reaction containing 112.5 ml of citrate buffer (pH 3.5, 100 mM), 1.25 ml of ferulic acid, 1.25 ml of tween-80, 1.25 ml of valencene (5.872 mmol), and 25 ml from 20% (w/v) of laccase was gently stirred in a round bottom flask which was placed inside an oil bath on a magnetic stirrer. This reaction proceeded at room temperature (22 ± 3 ˚C) for 2 days. There was a constant oxygen flow which was sparged into the reaction from the oxygen cylinder throughout.

After 2 days, the reaction was stopped by adding Na_2CO_3 to increase the pH of the reaction to 9.0, followed by heating of the solution at 80 ˚C for about 2 hours to degrade valencene hydroperoxide to nootkatone. The solution was then left to cool before the extraction method (59).

WORKUP PROCEDURE

In a separatory funnel, the reaction suspension was extracted using (3 x 50 ml) of DCM. The extraction method was repeated 3 times, to wash the organic solvent of

unwanted products and reagents. The anhydrous $MgSO_4$ was used as a drying agent for the organic layer followed by concentration of the organic layer under a vacuum using rotary evaporation.

4.7.3.1 Variation of mediators

The same procedure as **Method E** was adopted, however, using a different mediator, salicylic acid.

4.7.3.2 Amounts of the buffer or enzyme

The same procedure as **Method E** was adopted, however, the amount of citrate buffer and the amount of enzyme was first halved and then doubled.

4.7.3.3 Terminal heating temperature

The same procedure as **Method E** was adopted; however, the reaction was left at room temperature (22 ± 3 ˚C) (no heating took place), and another one of the reactions was heated at 80 and 90 ˚C both for 2 hours and, for comparison, 4 hours.

REFERENCES

1. Romero-Guido C, Belo I, Ta TMN, Cao-Hoang L, Alchihab M, Gomes N. Biochemistry of lactone formation in yeast and fungi and its utilisation for the production of flavour and fragrance compounds. Appl Microbiol Biotechnol. 2011;89(3):535–47.

2. Fraatz MA, Berger RG, Zorn H. Nootkatone-a biotechnological challenge. Appl Microbiol Biotechnol. 2009;83(1):35–41.

3. Byl SA. The essence and use of perfume in Egypt. Uni of SA. 2012;(February): 32-93.

4. Kaya SI, Cetinkaya A, Ozkan SA. Green analytical chemistry approaches on environmental analysis. Trends Environ Anal Chem. 2022;33(December 2021):e00157. https://doi.org/10.1016/j.teac.2022.e00157

5. Lenoir D, Schramm KW, Lalah JO. Green chemistry: Some important forerunners and current issues. Sustain Chem Pharm. 2020;18(March):100313. https://doi.org/10.1016/j.scp.2020.100313

6. Domínguez de María P. Biocatalysis, sustainability, and industrial applications. Curr Opin Green Sustain Chem. 2021;31:100514. https://doi.org/10.1016/j.cogsc.2021.100514

7. Tucker JL. The hidden power and competitive advantage of applying green chemistry metrics. Curr Opin Green Sustain Chem. 2022;35:100606. https://doi.org/10.1016/j.cogsc.2022.100606

8. Płotka-Wasylka J, Mohamed HM, Kurowska-Susdorf A, Dewani R, Fares MY, Andruch V. Green analytical chemistry as an integral part of sustainable education development. Curr Opin Green Sustain Chem. 2021;31.

9. Santos LB, Assis RS, Barreto JA, Bezerra MA, Novaes CG, Lemos VA. Deep eutectic solvents in liquid-phase microextraction: contribution to green chemistry. TrAC - Trends Anal Chem. 2022;146.

10. Fantoni T, Tolomelli A, Cabri W. A translation of the twelve principles of green chemistry to guide the development of cross-coupling reactions. Catal Today.

2022;397–399(April 2021):265–71. https://doi.org/10.1016/j.cattod.2021.09.022

11. Li B, Eilks I. A systematic review of the green and sustainable chemistry education research literature in mainland China. Sustain Chem Pharm. 2021;21(April):100446. https://doi.org/10.1016/j.scp.2021.100446

12. Becker M, Tickner JA. Driving safer products through collaborative innovation: Lessons learned from the green chemistry & commerce council's collaborative innovation challenge for safe and effective preservatives for consumer products. Sustain Chem Pharm. 2020;18(October):100330. https://doi.org/10.1016/j.scp.2020.100330

13. Betancor L, López-Gallego F. Heterogeneous biocatalysis for sustainable chemistry. Curr Opin Green Sustain Chem . 2022;35:100615. https://doi.org/10.1016/j.cogsc.2022.100615

14. Wackett LP, Ellis LBM. Biodegradation database and prediction, microbial. Encycl Microbiol. 2009;78–87.

15. Wohlgemuth R. Key enabling tools from biocatalytic one-step and multi-step reactions to biocatalytic total synthesis. N Biotechnol. 2021;60(August 2020):113–23. https://doi.org/10.1016/j.nbt.2020.08.006

16. Bommarius AS, Riebel BR. Fundamentals and applications of biocatalysis. 2004;45: 157-169. ISBN:3-527-30344-8

17. Robinson PK. Principles and biotechnological applications. Essays Biochem. 2015;59:1–41.

18. Baysal T, Demirdöven A. Lipoxygenase in fruits and vegetables. Enzyme Microb Technol. 2007;40(4):491–6.

19. Liburdi K, Esti M, Petroselli V, Mendler-Drienyovszki N, Radicetti E, Mancinelli R. Catalytic properties of lipoxygenase extracted from different varieties of Pisum sativum and Lens culinaris. J Food Biochem. 2021;45(2):1–8.

20. Wennman A, Oliw EH, Karkehabadi S, Chen Y. Crystal structure of manganese lipoxygenase of the rice blast fungus magnaporthe oryzae. J Biol

Chem. 2016;291(15):8130–9. http://dx.doi.org/10.1074/jbc.M115.70738021.

21. Li DC, Lui ZW, Lu J. Purification and characterization of lipoxygenase from the thermophilic fungus *Thermomyces lanuginosus*. Mycol Res. 2001;105(2):190–4.

22. Wennman A, Hamberg M, Oliw EH. Catalytic convergence of manganese and iron lipoxygenases by replacement of a single amino acid. 2012;287(38):31757–65.

23. Cristea M, Oliw EH. A G316A mutation of manganese lipoxygenase augments hydroperoxide isomerase activity. J Biol Chem. 2006;281(26):17612–23. http://dx.doi.org/10.1074/jbc.M510311200

24. Su C, Oliw EH. Manganese lipoxygenase. J Biol Chem . 1998;273(21):13072–9. http://dx.doi.org/10.1074/jbc.273.21.13072

25. Urlacher VB, Girhard M. Cytochrome P450 monooxygenases in biotechnology and synthetic biology. Vol. 37, Trends Biotechnol. Elsevier Ltd; 2019. p. 882–97.

26. Zhang H, Wang C, Guo F, Jin L, Song R, Yang F. In silico simulation of cytochrome P450-mediated metabolism of aromatic amines: A case study of N-hydroxylation. Ecotoxicol Environ Saf. 2022;237(April).

27. Nam W. Metalloporphyrins as models for cytochrome P450. Ewha Womans Uni, Seoul, Korea. 1985;(2):281-304.

28. Urban P, Mignotte C, Kazmaier M, Delorme F, Pompon D. Cloning, yeast expression, and characterization of the coupling of two distantly related Arabidopsis thaliana NADPH-cytochrome P450 reductases with P450 CYP73A5. J Biol Chem. 1997 Aug 1;272(31):19176–86.

29. Urlacher VB, Eiben S. Cytochrome P450 monooxygenases: perspectives for synthetic application. Trends Biotechnol. 2006;24(7):324–30.

30. Gao S, Liu K, Liu H, Yin S, Guo X, Zhang Y. Functional analysis of a cytochrome P450 gene CYP9Z6 responding to terpinen-4-ol in the red flour beetle, *Tribolium castaneum*. Pestic Biochem Physiol. 2022;183(October

2021):105065. https://doi.org/10.1016/j.pestbp.2022.105065

31. Girvan HM, Munro AW. Applications of microbial cytochrome P450 enzymes in biotechnology and synthetic biology. Curr Opin Chem Biol. 2016;31:136–45. http://dx.doi.org/10.1016/j.cbpa.2016.02.018

32. Cao Y, Ge J. Hybrid enzyme catalysts synthesized by a de novo approach for expanding biocatalysis. Chinese J Catal. 2021;42(10):1625–33. http://dx.doi.org/10.1016/S1872-2067(21)63798-1

33. Madhavi V, Lele SS. Laccase: properties and applications. Review and Article. 2009;4(Thurston 1994):1694–717.

34. Lin S, Wei J, Yang B, Zhang M, Zhuo R. Bioremediation of organic pollutants by white rot fungal cytochrome P450: The role and mechanism of CYP450 in biodegradation. Chemosphere. 2022;301(April):134776. https://doi.org/10.1016/j.chemosphere.2022.134776

35. Vipotnik Z, Michelin M, Tavares T. Biodegradation of chrysene and benzo[a]pyrene and removal of metals from naturally contaminated soil by isolated *Trametes versicolor* strain and laccase produced thereof. Environ Technol Innov. 2022;28:102737. https://doi.org/10.1016/j.eti.2022.102737

36. Alokpa K, Lafortune F, Cabana H. Application of laccase and hydrolases for trace organic contaminants removal from contaminated water. Environ Adv. 2022;8(April):100243. https://doi.org/10.1016/j.envadv.2022.100243

37. Krings U, Berger RG. Natural product communications. Terpene Bioconversion. 2010;1(4):9–12.

38. Isabirye M, Raju DV., Kitutu M, Yemeline V, Deckers J. P. Advanced biometric technologies and liveness detection in biometrics. Terpenes and terpernoids. Intech. 2012;13. http://dx.doi.org/10.1016/j.colsurfa.2011.12.014

39. Frohwitter J, Heider SAE, Peters-Wendisch P, Beekwilder J, Wendisch VF. Production of the sesquiterpene (+)-valencene by metabolically engineered *Corynebacterium glutamicum*. J Biotechnol. 2014;191:205–13.

http://dx.doi.org/10.1016/j.jbiotec.2014.05.032

40. Sowden RJ, Yasmin S, Rees NH, Bell SG, Wong LL. Biotransformation of the sesquiterpene (+)-valencene by cytochrome P450cam and P450BM-3. Org Biomol Chem. 2005 Jan 7;3(1):57–64.

41. Faraldos JA, González V, Senske M, Allemann RK. Templating effects in aristolochene synthase catalysis: Elimination versus cyclisation. Org Biomol Chem. 2011;9(20):6920–3.

42. Palmerín-Carreño DM, Rutiaga-Quiñones OM, Verde-Calvo JR, Prado-Barragán A, Huerta-Ochoa S. Screening of microorganisms for bioconversion of (+)-valencene to (+)-nootkatone. LWT - Food Sci Technol. 2015;64(2):788–93.

43. Li X, An Q, Qu S, Ren J, Fan G, Zhang L. Biological macromolecules differential proteomic analysis of citrus flavor (+) -valencene biotransformation to (+) -nootkatone by *Yarrowia lipolytica*. International Journal. 2022;220(August):1031–48.

44. Ghasemy-Piranloo F, Kavousi F, Dadashian S. Comparison for the production of essential oil by conventional, novel and biotechnology methods. Authorea . 2020;1(1):1–34. https://doi.org/10.22541/au.160315281.12110663/v1

45. Ambrož M, Boušová I, Skarka A, Hanušová V, Králová V, Matoušková P. The influence of sesquiterpenes from *Myrica rubra* on the antiproliferative and pro-oxidative effects of doxorubicin and its accumulation in cancer cells. Molecules. 2015;20(8):15343–58.

46. Li X, Ren JN, Fan G, Zhang LL, Pan SY. Advances on (+)-nootkatone microbial biosynthesis and its related enzymes. J Ind Microbiol Biotechnol. 2021;48(7–8).

47. Wilson CW, Shaw PE, McDonald RE, Greany PD, Yokoyama H. Effect of gibberellic acid and 2-(3,4-dichlorophenoxy)triethylamine on nootkatone in grapefruit peel oil and total peel oil content. J Agric Food Chem. 1990;38(3):656–9.

48. Wen J, Li X, Liu W, Fang Y, Xie J, Xu Y. Photocatalysis fundamentals and

surface modification of TiO_2 nanomaterials. Cuihua Xuebao/Chinese J Catal. 2015;36(12):2049–70. http://dx.doi.org/10.1016/S1872-2067(15)60999-8.

49. Fan J, Liu Z, Xu S, Yan X, Cheng W, Yang R. Non-food bioactive product (+)-nootkatone: chemistry and biological activities. Ind Crops Prod. 2022;177(December 2021):114490.

50. Hong B, Lebeuf R, Delbaere S, Alsters PL, Nardello-Rataj V. One-pot synthesis of (+)-nootkatone via dark singlet oxygenation of valencene: The triple role of the amphiphilic molybdate catalyst. Catalysts. 2016;6(12):1–11.

51. Gavira C, Höfer R, Lesot A, Lambert F, Zucca J, Werck-Reichhart D. Challenges and pitfalls of P450-dependent (+)-valencene bioconversion by *Saccharomyces cerevisiae*. Metab Eng. 2013 Jul 1;18:25–35.

52. Castillo-Araiza CO, Palmerín-Carreño D, Prado-Barragán A, Huerta-Ochoa S. On the conceptual design of a partitioning technology for the bioconversion of (+)-valencene to (+)-nootkatone on whole cells: Experimentation and modelling. Chem Eng Process Process Intensif. 2017 Dec 1;122:493–507.

53. Gigot C, Ongena M, Fauconnier ML, Wathelet JP, du Jardin P, Thonart P. The lipoxygenase metabolic pathway in plants: Potential for industrial production of natural green leaf volatiles. Biotechnol Agron Soc Environ. 2010;14(3):451–60.

54. Machate DJ, Melo ESP, Oliveira LCS, Bogo D, Michels FS, Pott A. Oxidative stability and elemental analysis of sunflower (*Helianthus annuus*) edible oil produced in Brazil using a domestic extraction machine. Front Nutr. 2022;9.

55. Makhubela IM. The conversion of various terpenes by oxidative biocatalysis. Uni of Wits. 2022;(March): 89-60.

56. Marti VG, Coenen A, Schörken U. Synthesis of linoleic acid 13-hydroperoxides from safflower oil utilizing lipoxygenase in a coupled enzyme system with in-situ oxygen generation. Catalysts. 2021;11(9).

57. Collazo L, Klinman JP. Control of the position of oxygen delivery in soybean lipoxygenase-1 by amino acid side chains within a gas migration channel . J Biol Chem. 2016;291(17):9052–9. http://dx.doi.org/10.1074/jbc.

58. Kokorin A, Urlacher VB. Artificial fusions between P450 BM3 and an alcohol dehydrogenase for efficient (+) -nootkatone production. J Biol Chem. 2022;202200065.

59. Huang R, Chester W, Christensen PA, Labuda IM. US006200786B1: Process for the preparation of nootkatone by laccase catalysis. United State Patents. 2001;1(12).

60. Ivanov I, Heydeck D, Hofheinz K, Roffeis J, O'Donnell VB, Kuhn H. Molecular enzymology of lipoxygenases. Arch Biochem Biophys. 2010;503(2):161–74. http://dx.doi.org/10.1016/j.abb.2010.08.016

61. Wang B, Zhang Q, Zhang N, Bak KH, Soladoye OP, Aluko RE. Insights into formation, detection and removal of the beany flavor in soybean protein. Trends Food Sci Technol. 2021;112(January):336–47.

62. Yuvaraj M, Sathya Priya R, Jagathjothi N, Saranya M, Suganthi N, Sharmila R. Silicon nanoparticles (SiNPs): Challenges and perspectives for sustainable agriculture. Physiol Mol Plant Pathol. 2023;128(August):102161. https://doi.org/10.1016/j.pmpp.2023.102161

63. Scalliet R. US006214236B1: Process for breaking an emulsion. United States Patent. 2001;1(12):4–10.

64. Muller B, Dean C, Schmidt C, Kuhn JC. US5847226A: Process for the preparation of nootkatone. 1996;(19). https://patents.google.com/patent/US5847226A/en

65. Xie J, Sun B, Wang S, Ito Y. Isolation and purification of nootkatone from the essential oil of fruits of *Alpinia oxyphylla* by high-speed counter-current chromatography. Food Chem. 2009;117(2): 375–80. http://dx.doi.org/10.1016/j.foodchem.2009.04.011

66. Yong Z, Zibao H, Zhi Z, Ning M, Ruiqi W, Mimi C. Nootkatone, a sesquiterpene ketone from *Alpiniae oxyphyllae fructus*, ameliorates metabolic-associated fatty liver by regulating AMPK and MAPK signaling. Front Pharmacol. 2022;13(July):14–1.

67. Koch RB, Brumfiel BL, Brumfiel MN. Calcium requirement for lipoxygenase

catalyzed linoleate. Food Chem. 1970;(20).

68. Eek P, Järving R, Järving I, Gilbert NC, Newcomer ME, Samel N. Structure of a calcium-dependent 11R-lipoxygenase suggests a mechanism for Ca2+ regulation. J Biol Chem. 2012;287(26):22377–86.

69. Mohammad A, Alireza K, Abdolrahim N, Mohammad M, Mohammad A. The inhibitory effect of KCN, NaN_3 and some bivalent Ions on lipoxygenase activity of the puriied human placental. J Biol Chem. 2013;9(1): 45-39.

70. Marvian-hosseini Z, Asoodeh A. Biochemical characterization of purified lipoxygenase from sesame (*Sesamum indicum*). Int J Food Prop. 2017;20(1):948–58. https://doi.org/10.1080/10942912.2017.1318291

71. Andrade C. Understanding the difference between standard deviation and standard error of the mean. Indian J Psychol Med. 2020;42(4):409–10

72. Akkaya MR. Fatty acid compositions of sunflowers (*helianthus annuus L*.) grown in east mediterranean region. Riv Ital delle Sostanze Grasse. 2018;95(4):239–47.

73. Farahmandfar R, Asnaashari M, Sayyad R. Comparison antioxidant activity of Tarom Mahali rice bran extracted from different extraction methods and its effect on canola oil stabilization. J Food Sci Technol. 2015;52(10):6385–94.

74. Hernández ML, Sicardo MD, Belaj A, Martínez-Rivas JM. The Oleic/linoleic acid ratio in olive (*Olea europaea* L.) fruit mesocarp is mainly controlled by OeFAD2-2 and OeFAD2-5 genes together with the different specificity of extraplastidial acyltransferase enzymes. Front plant Sci. 2021;12(March):10–1.

75. Rigo E, Ninow JL, Di Luccio M, Vladimir Oliveira J, Polloni AE, Remonatto D. Lipase production by solid fermentation of soybean meal with different supplements. Lwt. 2010;43(7):1132–7.

76. Prabakaran M, Lee KJ, An Y, Kwon C, Kim S, Yang Y. Changes in soybean flour fatty-acid content based on storage temperature and duration. Molecules. 2018;23(10).

77. Pignitter M, Zaunschirm M, Lach J, Unterberger L, Kopic A, Keßler C.

Regioisomeric distribution of 9- and 13-hydroperoxy linoleic acid in vegetable oils during storage and heating. J Sci Food Agric. 2018;98(3):1240–7.

78. Halvorsen BL, Blomhoff R. Determination of lipid oxidation products in vegetable oils and marine omega-3 supplements. Food Nutr Res. 2011;55.

79. Kubo I, Joung T, Tsujimoto K, Tocoli FE. Evaluation of lipoxygenase inhibitory activity of anacardic acids. Environ Sci. 2008; 2-8.

80. Tsujimoto K, Hayashi A, Ha TJ, Kubo I. Anacardic acids and ferric ion chelation. J Adv Inst Sci Technol. 2018;(September); 9-1. http://hdl.handle.net/10119/4873

81. Kubo I, Ha TJ, Shimizu K. Lipoxygenase inhibitory activity of 6-pentadecanylsalicylic acid without prooxidant effect. Natural Product Communications. 2010;9–4.

82. Mazumder AR, Brinto HA, Chakrabortty P, Begum A. Processing and nutrient quality evaluation of defatted soy meat. Integr Food, Nutr Metab. 2018;5(4):1–6.

83. Khetarpaul N, Grewal RB, Goyal R, Garg R. Development of partially defatted soy flour and dhal. Food Chem. 2004;87(3):355–9.

84. Fidyt K, Fiedorowicz A, Strządała L, Szumny A. β-caryophyllene and β-caryophyllene Oxide—natural compounds of anticancer and analgesic properties. Cancer Med. 2016;5(10): 3007–17.

85. Karakaya S, Yilmaz SV, Özdemir Ö, Koca M, Pınar NM, Demirci B. A caryophyllene oxide and other potential anticholinesterase and anticancer agent in Salvia verticillata subsp. J Essent Oil Res. 2020;32(6):512–25. https://doi.org/10.1080/10412905.2020.1813212

86. Lee HY, Ko MJ. Thermal decomposition and oxidation of β-caryophyllene in black pepper during subcritical water extraction. Food Sci Biotechnol. 2021;30(12):1527–33. https://doi.org/10.1007/s10068-021-00983-z

87. Yang D, Michel L, Chaumont JP, Millet-Clerc J. Use of caryophyllene oxide as an antifungal agent in an in vitro experimental model of onychomycosis.

Mycopathologia. 2000;148(2):79–82.

88. Nickerson DP, Harford-Cross CF, Fulcher SR, Wong LL. The catalytic activity of cytochrome P450(cam) towards styrene oxidation is increased by site-specific mutagenesis. FEBS Lett. 1997;405(2):153–6. http://dx.doi.org/10.1016/S0014-5793(97)00174-9

89. Zhang L, Zhang Z, He X, Zhang F, Zhang Z. Regulation of the products of styrene oxidation. Chem Eng Res Des. 2017;120:171–8. http://dx.doi.org/10.1016/j.cherd.2017.02.012

90. Andrade MA, Martins LMDRS. Selective styrene oxidation to benzaldehyde over recently developed heterogeneous catalysts. Molecules. 2021;26(6).

91. Gazu Q, Shozi M, Mpungose P. Oxidation of styrene to benzaldehyde and styrene oxide over nickel and copper ceria solution combustion catalysts. MATEC Web Conf. 2023;374:01004.

92. Sowden RJ, Yasmin S, Rees NH, Bell SG, Wong LL. Biotransformation of the sesquiterpene (+)-valencene by cytochrome P450cam and P450BM-3. Org Biomol Chem. 2005;3(1):57–64.

93. Cankar K, Houwelingen AV, Bosch D, Sonke T, Bouwmeester H, Beekwilder J. A chicory cytochrome P450 mono-oxygenase CYP71AV8 for the oxidation of (+)-valencene. FEBS Lett. 2011 Jan 3;585(1):178–82.

94. Gavira C, Höfer R, Lesot A, Lambert F, Zucca J, Werck-Reichhart D. Challenges and pitfalls of P450-dependent (+)-valencene bioconversion by *Saccharomyces cerevisiae*. Metab Eng. 2013;18: 25–35. http://dx.doi.org/10.1016/j.ymben.2013.02.003

95. Girhard M, Machida K, Itoh M, Schmid RD, Arisawa A, Urlacher VB. Regioselective biooxidation of (+)-valencene by recombinant *E. coli* expressing CYP109B1 from *Bacillus subtilis* in a two-liquid-phase system. Microb Cell Fact. 2009;8:1–12.

96. Wriessnegger T, Augustin P, Engleder M, Leitner E, Müller M, Kaluzna I. Production of the sesquiterpenoid (+)-nootkatone by metabolic engineering of Pichia pastoris. Metab Eng. 2014;24: 29-18.

http://dx.doi.org/10.1016/j.ymben.2014.04.001

97. Van BI, Groeneboer S, Saerens K, Soetaert W. The role of cytochrome P450 monooxygenases in microbial fatty acid metabolism. FEBS J. 2011;278(2):206–21.

98. Konkel A, Schunck WH. Role of cytochrome P450 enzymes in the bioactivation of polyunsaturated fatty acids. Biochim Biophys Acta. 2011;1814(1): 210–22. http://dx.doi.org/10.1016/j.bbapap.2010.09.009

APPENDIX

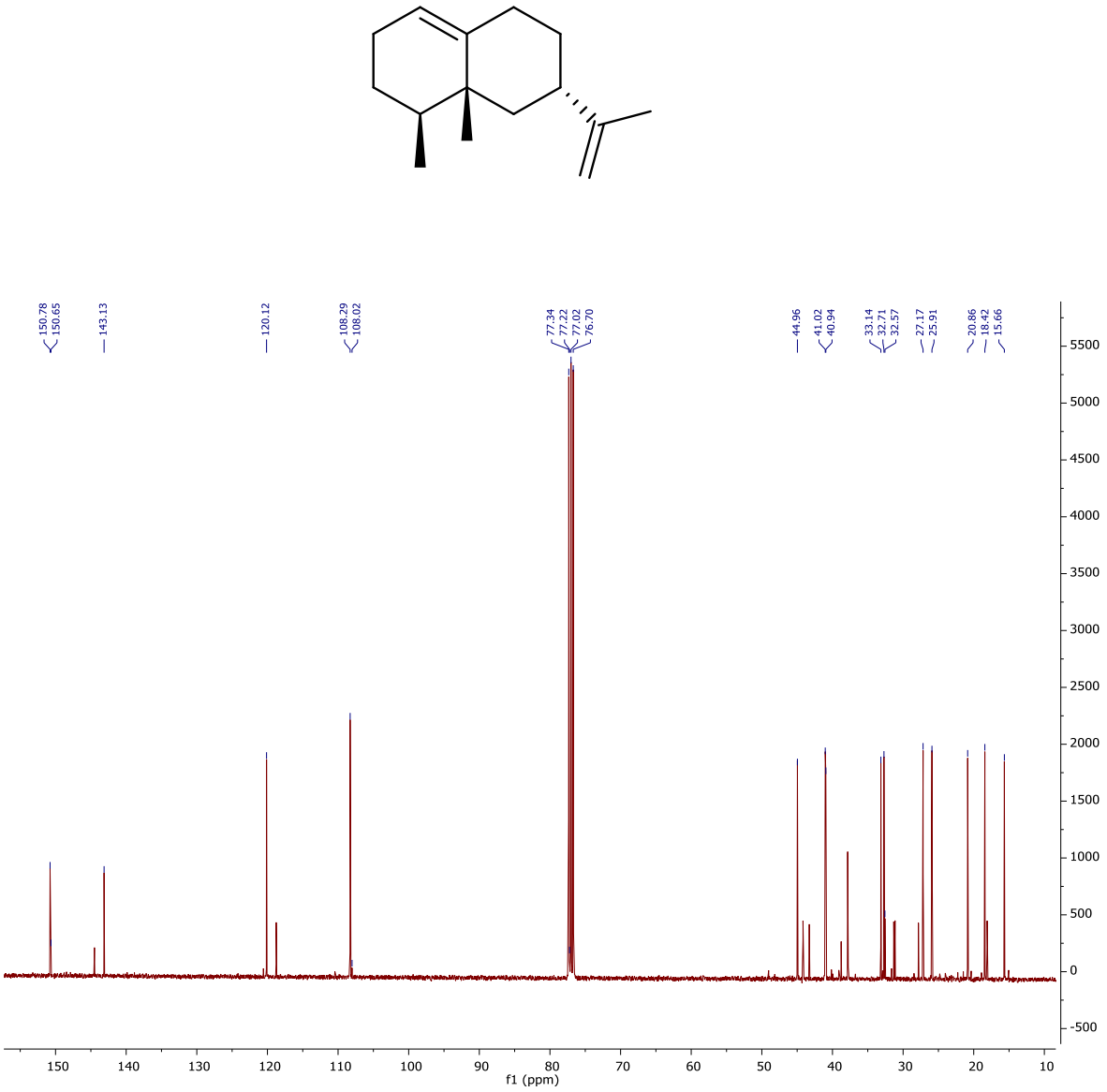

Figure 31: ^{13}C NMR spectrum of valencene.

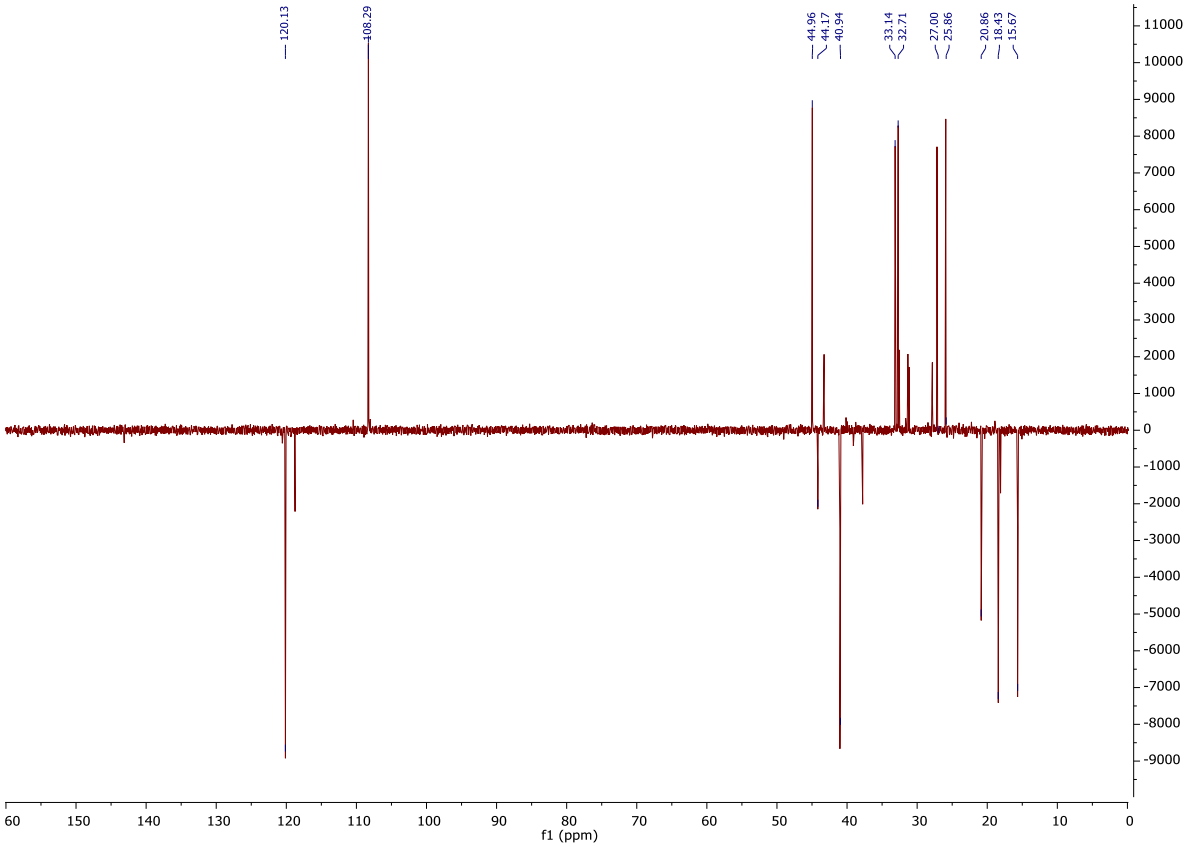

Figure 32: DEPT135 NMR spectrum of valencene.

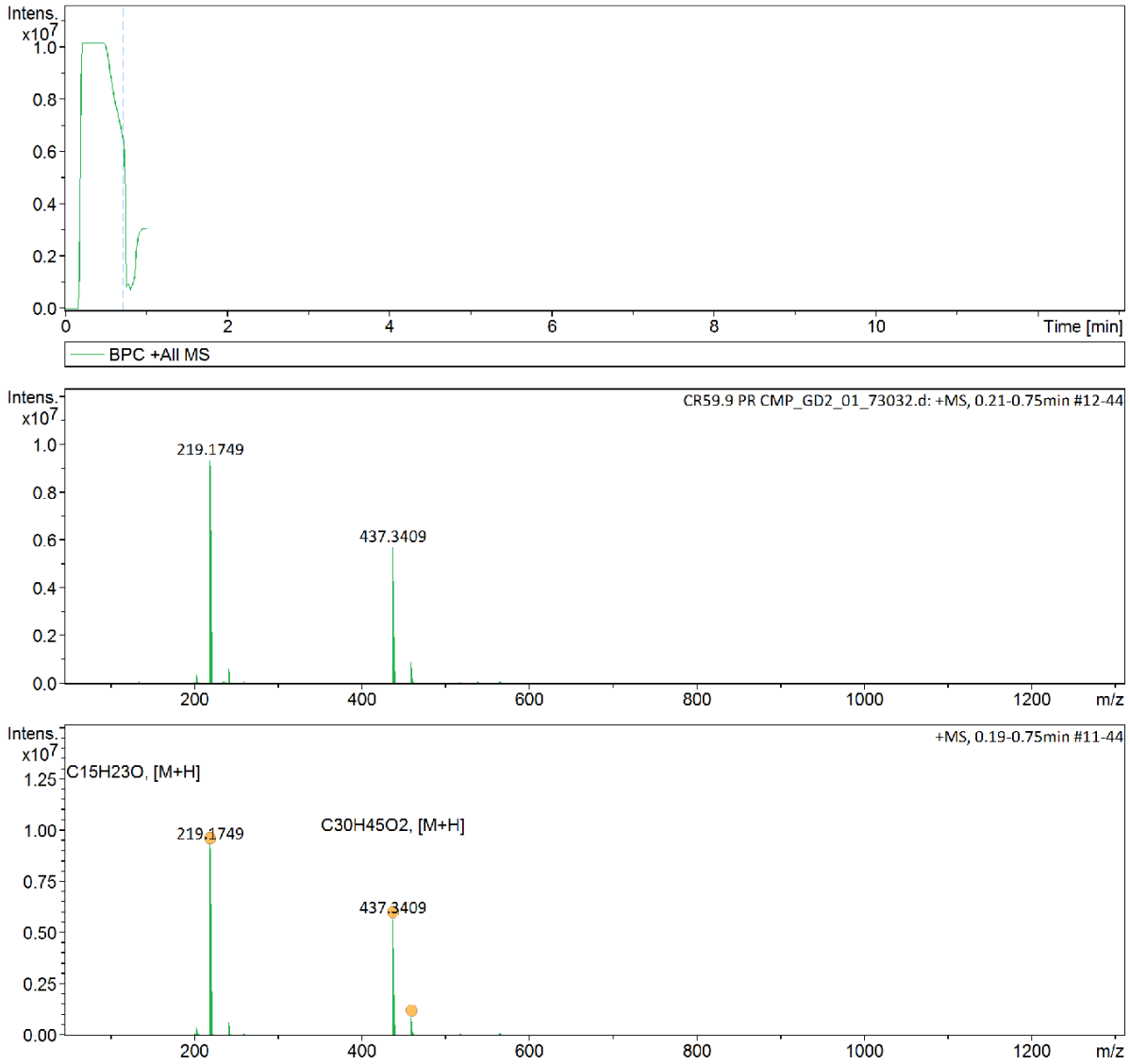

Figure 33: HPLC spectra for NK isolated from a crude mixture resulted from the conversion of VL. The peak at 219.1749 represents NK while at 437.3409 represents its dimerisation.

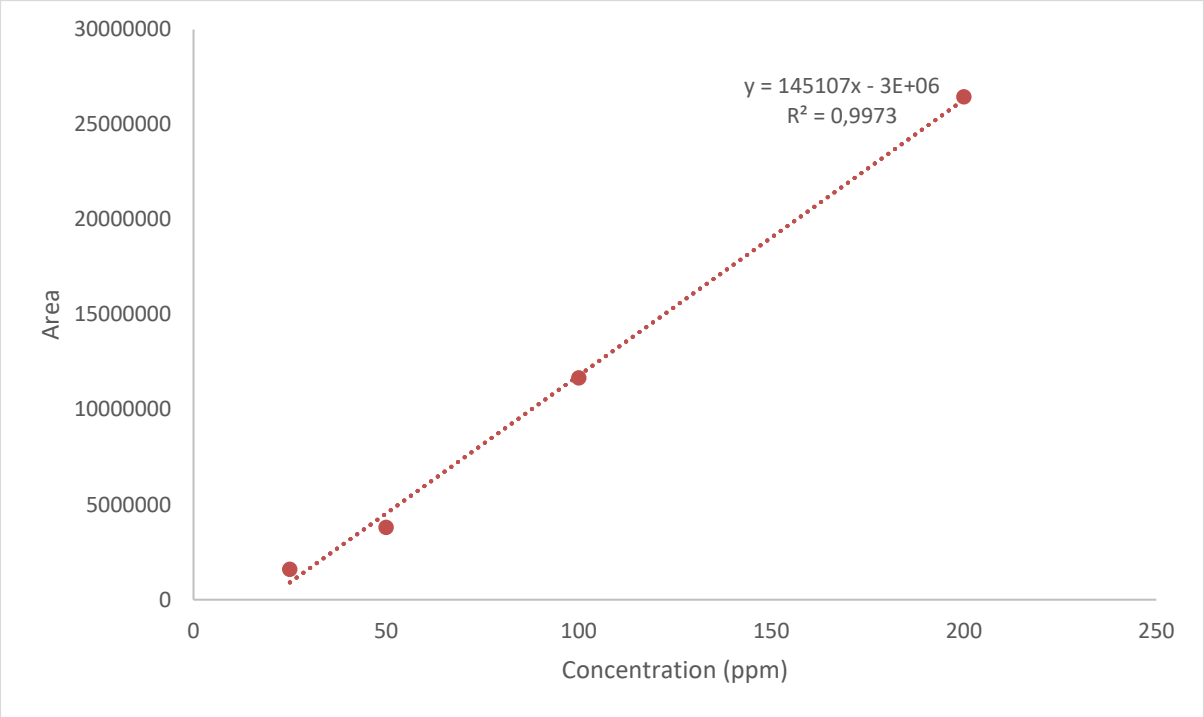

Figure 34: Calibration curve of NK.

Table 16: The mol % of NK formed with the addition of $FeSO_4.7H_2O$ and $MnSO_4$ using a concentration of 2.64 mM respectively on MDS LOX.

$FeSO_4.7H_2O$ and $MnSO_4$							
Days	Nootkatone concentration (ppm)	Mass of Nootkatone (mg)	moles of Nootkatone (µmol)	Valencene concentration (ppm)	Mass of valencene (mg)	moles of valencene (µmol)	Nootkatone (Mol %)
0	0	0	0	691.21	0.691	3.383	0
1	27.28	0.0273	0.125	478.49	0.478	2.342	5.07
2	25.43	0.0254	0.116	350.42	0.350	1.715	6.34
3	54.59	0.0546	0.250	275.32	0.275	1.347	15.65
4	70.32	0.0703	0.322	419.92	0.420	2.055	13.54
5	86.20	0.0862	0.395	242.21	0.242	1.185	25.00
6	86.01	0.0860	0.394	179.57	0.179	0.878	30.97
7	107.31	0.1073	0.491	154.92	0.155	0.758	39.31
8	74.91	0.0749	0.344	99.89	0.0998	0.488	41.34
9	86.17	0.0862	0.395	99.43	0.0994	0.487	44.78

ppm = mg/L

Number of moles = $\frac{mass}{molecular\ weight}$

Molecular weight for nootkatone is 218, 340 g/mol.

Molecular weight for valencene is 204.35 g/mol.

NK Mol % = $\frac{moles\ for\ NK}{\text{moles for NK+moles for VL}}$

Table 17: All the runs and average conversions of salts in 1:1 mole ratio

Conversion (%)																								
DAYS	Without Salts				$FeSO_4.H_2O$ and $MnSO_4$				$FeSO_4.H_2O$ and $MnCl_2.4H_2O$			$FeSO_4.H_2O$ and $CaCl_2.2H_2O$			$FeSO_4$ and $MnSO_4$			$MnSO_4$				$FeSO_4.H_2O$		
	1st Run	2nd Run	3rd Run	Avg	1st Run	2nd Run	3rd Run	Avg	1st Run	2nd Run	Avg	1st Run	2nd Run	Avg	1st Run	2nd Run	Avg	1st Run	2nd Run	3rd Run	Avg	1st Run	2nd Run	Avg
1	----	3.21	11.00	7.11	1.91	6.30	10.33	6.18	33.03	0.82	16.93	25.83	7.07	16.45	10.60	10.00	10.30	9.98	3.40	0.63	4.67	10.00	11.40	10.70
2	2.63	6.09	16.56	8.43	1.78	13.05	18.45	11.09	40.58	3.55	22.06	30.83	11.21	21.02	19.59	21.18	20.39	12.40	4.27	2.00	6.22	14.52	17.76	16.14
3	----	7.79	17.23	12.51	16.28	14.06	25.04	18.46	42.09	4.45	23.27	31.96	17.34	24.65	25.71	25.83	25.77	13.45	6.00	3.75	7.73	14.91	19.41	17.16
4	----	10.26	20.94	15.60	19.32	15.39	30.10	21.60	43.00	4.72	23.86	42.52	22.32	32.42	33.07	27.45	30.26	18.04	8.37	3.34	9.92	17.66	19.64	18.65
5	8.90	12.85	22.10	14.62	29.09	19.57	32.59	27.08	45.87	5.40	25.64	48.07	28.00	38.04	40.37	30.83	35.60	19.82	9.75	4.49	11.35	20.32	20.34	20.33
6	----	16.69	27.44	22.07	43.67	22.58	36.95	34.40	46.35	6.02	26.19	59.01	19.02	39.02	43.96	36.10	40.03	18.12	10.24	6.15	11.50	23.98	28.54	26.26
7	29.87	18.38	32.83	27.03	59.60	22.88	46.16	42.88	49.49	5.84	27.67	60.53	20.65	40.59	52.33	40.00	46.17	21.16	8.44	7.66	12.42	24.21	29.09	26.65
8	----	24.33	36.90	30.62	54.66	27.14	41.48	41.09	48.93	----	----	----	----	----	56.51	----	----	----	----	----	----			
9	----	27.36	31.60	29.48	75.46	30.29	59.25	55.00	51.94	----	----	----	----	----	58.57	----	----	----	----	----	----			